NATIONAL ADVISORY COMMITTEE FOR AERONAUTICS

NACA CONFERENCE ON FUELS

A COMPILATION OF THE PAPERS PRESENTED

BY NACA STAFF MEMBERS

Flight Propulsion Research Laboratory
Cleveland, Ohio

May 26, 1948

NACA

CONFIDENTIAL

NACA CONFERENCE ON FUELS

A COMPILATION OF THE PAPERS PRESENTED

BY NACA STAFF MEMBERS

Flight Propulsion Research Laboratory
Cleveland, Ohio

May 26, 1948

CONTENTS

The authors are members of the staff of
the NACA laboratory at Cleveland, Ohio.

INTRODUCTION

The conference on Fuels was organized by the NACA to convey the latest programs in progress in this field to those involved in the development and evaluation of fuels for aircraft propulsion systems.

The technical discussions are reproduced herewith in the same form in which they were presented at the conference in the interest of effecting prompt distribution. The presentations in this record are considered as complementary to, rather than substitutes for, the Committee's system of complete and formal reports.

A list of the conferees is included.

NATIONAL ADVISORY COMMITTEE
FOR AERONAUTICS

CONFIDENTIAL

LIST OF CONFEREES

The following conferees were registered at the NACA conference on Fuels, Flight Propulsion Research Laboratory, Cleveland, Ohio, May 26, 1948:

*Adams, Comdr. S. M.	Bureau of Aeronautics, Dept. of Navy
Alfrey, Dr. Turner	Polytechnic Institute of Brooklyn
Alquist, H. E.	NACA
Arden, Frederick	Office of Domestic Commerce, Dept. of Commerce
Bailey, B. S.	Texas
*Barnard, Dr. D. P.	Standard Oil of Indiana
Barnett, Henry C.	NACA
Bates, Dr. J. R.	Sun Oil
Beal, Dr. John L.	Cornell University
Beighley, C. M.	Ohio State University
Best, Robert	Fredric Flader
*Blackwood, A. J.	Esso Laboratories - Research Div., Standard Oil Development
Boll, R.	University of Michigan
Bollo, Frank G.	Shell Oil, Shell Development
Bower, William E.	Wright Aeronautical
*Brooks, D. B.	National Bureau of Standards
Brown, Edmund D.	Pratt & Whitney Aircraft Div., United Aircraft
Buttner, H. J.	Purdue University
Campbell, M. H.	E. I. DuPont De Nemours
Clayden, A. L.	Sun Oil
Clegg, John W.	Battelle Memorial Institute
*Cullom, K. S.	Civil Aeronautics Administration
Damon, Glenn H.	Bureau of Mines
deGanahl, Carl	Kaiser Fleetwings
Dembrow, D. E.	Johns Hopkins University
Dorsey, Lt. Col. E. T.	Naval Operations, Guided Missiles, Dept. of Navy
Dougherty, Floyd G.	Allison Div., General Motors
Ebersole, Earl R.	NACA
Echols, Dr. L. S.	Shell Oil
Edse, Rudolph	Ohio State University

*Member of NACA Subcommittee on Aircraft Fuels.

vii

CONFIDENTIAL

Fox, Comdr. C.   Armed Services Petroleum Board
Fricke, Dr. Edwin   Republic Aviation

Gerstein, Melvin   NACA
*Gibbons, Dr. Louis C.   NACA
Grey, Dr. J. T.   Cornell University

Hardin, Max   Allison Div., General Motors
Hart, D. K.   Bureau of Ordnance, Dept. of Navy
*Heron, S. D.   Ethyl, Research Laboratory
Hibbard, Robert R.   NACA
Hiersch, F. A.   Continental Aviation & Engineering
*Hill, Dr. J. Bennett   Sun Oil
Hill, P. R.   NACA
*Holaday, W. M.   Socony-Vacuum Oil
Huff, Vearl N.   NACA
Hundere, A.   California Research

Jackson, C. B.   Mine Safety Appliances
*Johnson, C. R.   Shell Oil
Johnson, Dr. W. C.   Westinghouse Electric
Jonash, Edmund R.   NACA

Keller, George H.   Wright Aeronautical
Kemper, Carlton   NACA
Kerley, Robert V.   Ethyl
Klein, E. L.   Bureau of Aeronautics, Dept. of Navy
Koffer, G. W.   Westinghouse Electric
Kuhback, C. M.   Texas

Lawson, W. E.   E. I. DuPont De Nemours
Littell, R. E.   NACA
Long, K. E.   Harshaw Chemical
Lott, M. A.   Aircraft Engine Laboratory, Naval
                                    Air Materiel Center
Luecht, John   University of Michigan
Lovell, Wheeler G.   Ethyl
Lowry, C. D., Jr.   Research and Development Board

Malick, E. A.   Phillips Petroleum
Miller, Cearcy D.   Battelle Memorial Institute
Moore, Robert A.   Socony-Vacuum Oil
Morris, Brooks T.   General Tire & Rubber

*Member of NACA Subcommittee on Aircraft Fuels.

*Nerad, A. J.   General Electric
Nutt, Harold V.   U. S. Naval Engineering, Experi-
                                         ment Sta.

Ordin, Paul M.   NACA

Patton, James R., Jr.   Office Naval Research, Dept. of
                                         Navy
Perlow, Dr. Mina-Rea   Office of Domestic Commerce, Dept. of
                                         Commerce
Pigford, Thomas H.   Massachusetts Institute of Technology
Pinkel, Benjamin   NACA
Pinkston, J. T.   Harshaw Chemical
Pomeroy, A. L.   Thompson Products

Rall, Harry T.   Bureau of Mines, Petroleum Experi-
                                         ment Sta.
Reese, Bruce   Purdue University
Reinhardt, T. F.   Bell Aircraft
Reissner, Dr. Hans   Polytechnic Institute of Brooklyn
Rethman, Major V. C.   AMC, Liaison Office, Cleveland
Reynolds, Thaine W.   NACA
Ritch, Lt. Comdr. J. B.   U. S. Naval Engineering, Experi-
                                         ment Sta.
Rogers, M.   Bureau of Ordnance, Dept. of Navy
Rubert, Dr. Kennedy F.   NACA
Ruegg, Fillmer W.   National Bureau of Standards

Saitta, Lieut. V. F.   Bureau of Ships, Dept. of Navy
Sarto, J. O.   Chrysler
Schluderberg, Donald C.   DeLaval Steam Turbine
Schulman, Fred   Office Naval Research, Dept. of Navy
Scott, Charles   Goodyear Aircraft
Sforzini, Robert A.   Packard Aircraft Engine Div.,   '
                                         Packard Motor Car
Sharp, Edward R.   NACA
Shayeson, M. W.   AMC, U. S. Air Force
Sheets, Dr. H. E.   Goodyear Aircraft
Sloop, John L.   NACA
Staub, C. H.   Mine Safety Appliances
Stetson, G. L.   Shell Oil

*Member of NACA Subcommittee on Aircraft Fuels.

Tanczos, F. I.   Bureau of Ordnance, Dept. of Navy
Tower, Leonard K.   NACA

Van Sweringen, R. A.   Standard Oil of Indiana
Vogt, C. J.   University of California

Wade, Gustav   Bureau of Mines, Petroleum Experi-
                                    ment Sta.
Wallet, Capt. H. J.   AMC, Liaison Office, Cleveland
Wear, Jerrold D.   NACA
Weissenberger, Lt. Col. G. J.   Naval Operations, Guided Missiles,
                                    Dept. of Navy
Whitney, E. G.   Ranger Aircraft Engines
Wilhoyte, H. J.   Westinghouse Electric
Wilkinson, C. A.   Boeing Aircraft
Williams, Glenn C.   Massachusetts Institute of Tech-
                                    nology
Winternitz, Dr. P. F.   Reaction Motors
Wise, Paul H.   NACA

CORRELATION OF ENGINE CONDITIONS AT INCIPIENT KNOCK

By Leonard K. Tower and Louis C. Gibbons

Flight Propulsion Research Laboratory

INTRODUCTION

Evaluation of the knock-limited performance of fuels in reciprocating engines has been complicated by the fact that engine operating variables influence both the relative and absolute performance of fuels. Three important operating variables are fuel-air ratio, inlet-air temperature, and compression ratio. The well-known effects of these three variables are shown in figure 1:

At the top of the figure, knock-limited indicated mean effective pressure is plotted against fuel-air ratio for 28-R fuel. With other variables held constant, the knock-limited indicated mean effective pressure increases with increasing fuel-air ratio at richer than stoichiometric fuel-air ratios.

The middle part of the figure shows a plot of knock-limited indicated mean effective pressure against inlet-air temperature with compression ratio and fuel-air ratio constant. Increasing the inlet-air temperature decreases the knock-limited indicated mean effective pressure.

At the bottom of figure 1, indicated mean effective pressure is plotted against compression ratio with inlet-air temperature and fuel-air ratio held constant. Increasing compression ratio decreases knock-limited indicated mean effective pressure.

Thus, in order to obtain a thorough evaluation of a fuel, it has been necessary to obtain knock-limited performance over a wide fuel-air-ratio range at several compression ratios and inlet-air temperatures.

Previous investigations (references 1 and 2) have shown that the effects of compression ratio and inlet-air temperature on knock-limited performance can be correlated so that a fuel can be investigated at several inlet-air temperatures at a constant compression ratio and its performance can be satisfactorily predicted at other compression ratios. These previous studies gave separate correlations for each fuel-air ratio. It is the purpose of this paper to present a method whereby fuel-air ratio can be

included with inlet-air temperature and compression ratio in a
single correlation. By the use of this correlation, it is possible
to predict the influence of these three variables on the knock-
limited performance of a fuel from a minimum of test data.

RESULTS AND DISCUSSION

The correlation method is based on the hypothesis that the
charge of fuel and air entering the cylinder is compressed adia-
batically by the piston motion and combustion occurs as illustrated
in figure 2. The charge is ignited by the spark and the flame
front progresses across the cylinder. Under knocking conditions,
it is assumed that a small amount of unburned charge (designated
end gas) reaches a critical density and temperature, and causes
knock by exploding before the normal flame has traversed the entire
cylinder. For a given end-gas density there is one temperature at
which knock will occur. This theory served as a basis for
developing the correlation of compression ratio with inlet-air
temperature and was used in the extension of the method to fuel-
air ratio.

If the temperature and pressure of the charge entering the
cylinder and the compression ratio of the engine are known, it is
possible to calculate by the usual thermodynamic equations the
temperature and density of the charge after compression by the
piston.

In accordance with the above assumptions, it is also possible
to calculate the temperature and density that the end gas will
attain by burning of the charge. The equations involved in the
calculations for end-gas temperature and end-gas density are as
follows:

The density of the charge after compression by the piston is.

$$\rho_c = W/V_c \tag{1}$$

where

ρ density

W weight of fuel and air inducted per cycle

V volume

and the subscript c indicates condition of the gas after compres-
sion due to the piston.

The temperature of the gas after compression by the piston is

$$T_c = T_o \, r^{\gamma-1} \tag{2}$$

where

T   temperature

r   compression ratio

γ ratio of specific heats

and the subscript o indicates initial condition.

The end-gas temperature can then be calculated as

$$T_k = T_c \left(1 + \frac{\Delta T}{T_c}\right)^{\frac{\gamma-1}{\gamma}} \tag{3}$$

where

ΔT temperature rise due to combustion process

and the subscript k indicates end gas at knocking condition.

The end-gas density can be calculated as

$$\rho_k = \rho_c \left(\frac{T_k}{T_c}\right)^{\frac{1}{\gamma-1}} = F_1(T_k) \tag{4}$$

The previous assumption with regard to the end-gas conditions for knock stated that ρ_k is a function of T_k as is shown in equation (4).

The term $(T_k)^{\frac{1}{\gamma-1}}$ removed from the left-hand side of equation (4) results in the expression $\dfrac{F_1(T_k)}{(T_k)^{\frac{1}{\gamma-1}}}$. This expression resolves into the second function of T_k, which is $F_2(T_k)$. If the value of T_k from equation (3) is substituted in equation (4),

$$\frac{\rho_c}{(T_c)^{\frac{1}{\gamma-1}}} = F_2(T_k) = F_2\left[T_c\left(1 + \frac{\Delta T}{T_c}\right)^{\frac{\gamma-1}{\gamma}}\right] \tag{5}$$

The evaluation of ΔT, the temperature rise due to burning of the charge, is dependent upon the heat of combustion of the fuel, the fuel-air ratio, and the specific heat of the gas at constant volume. For purposes of this analysis, ΔT was considered to be a function of fuel-air ratio $F_3(f)$. A reference fuel-air ratio of 0.08 was arbitrarily chosen and the temperature rise of 4040° F due to constant volume combustion was determined from thermodynamic charts. The term ΔT then becomes $4040\, F_3(f)$. For a fuel-air ratio of 0.08, this function of fuel-air ratio is 1 and departs from 1 as the fuel-air ratio is varied from 0.08.

In equation (5), $4040\, F_3(f)$ may be substituted for ΔT and equation (6) is obtained

$$\frac{\rho_c}{(T_c)^{\frac{1}{\gamma-1}}} = F_2\left[T_c\left(1 + \frac{4040\, F_3(f)}{T_c}\right)^{\frac{\gamma-1}{\gamma}}\right] \tag{6}$$

It is emphasized that the function of fuel-air ratio $F_3(f)$ is the key to this method of analysis. Function of fuel-air ratio is evaluated from knock data rather than thermodynamic data and consequently, incorporates the discrepancies between the idealized cycle that has been postulated and the actual cycle that occurs in the engine. If the difference between the ideal and actual cycles does not change markedly with varying operating conditions, a useful tool has been developed. If knock test data taken under varying operating conditions are satisfactorily correlated, it would indicate that the difference between the cycles does not change to an appreciable extent.

The method for evaluating $F_3(f)$ from knock test data is shown in figure 3. A plot of $\frac{\rho_c}{T_c^{2.5}}$ against T_c for knock-limited data was obtained with 28-R fuel on a CFR engine operated

over a range of fuel-air ratios at six different inlet-air temper-
atures, at constant compression ratio, and at five compression
ratios from 5 to 10 at one inlet-air temperature. A separate curve
was obtained for each fuel-air ratio.

In reconsidering the equation at the top of figure 3 if the
term $\dfrac{\rho_c}{T_c^{2.5}}$ is held constant, then the quantity inside the brackets
must be constant. If the fuel-air ratio is varied, the entire
expression must still remain constant. For a selected constant
value of 4 for $\dfrac{\rho_c}{T_c^{2.5}}$, at each point where the dashed line
crosses a fuel-air ratio line the value of the bracketed term is
the same. This bracketed quantity can be evaluated at a fuel-air
ratio of 0.08 because $F_3(f)$ at 0.08 is 1 and the value of T_c
can be read from the curve. As shown in the lower equation, a
numerical value for the right side of the equation can be obtained
for the 0.08 fuel-air ratio by introducing T_c . Then for other
fuel-air ratios, the proper value for T_c can be selected for
$F_3(f)$ because the term on the right has a numerical value.

This function was determined for eight fuels. In each case
the constant value of $\dfrac{\rho_c}{T_c^{2.5}}$ was selected so that about the same
number of data points fell on either side of the line. Figure 4
shows a plot of $F_3(f)$ against fuel-air ratio for the eight fuels
listed on the figure. All of the data fall near a mean curve but
it is to be expected that $F_3(f)$ will vary somewhat with dif-
ferent fuels, and if data are available for a fuel, its individual
function should be used in the correlation. However, when the
curve of function of fuel-air ratio is not available for a fuel,
the mean curve can be used in the correlation with satisfactory
results.

The individual fuel-air-ratio functions $F_3(f)$ were used to
plot the end-gas density against the end-gas temperature for the
eight fuels. Figure 5 shows the end-gas density plotted against
the end-gas temperature for 28-R fuel. The data points were
obtained from knock-limited mixture-response curves on a CFR engine
at an inlet-air temperature of 250° F and compression ratios of
5, 6, 7.3, 8.7, and 10. Mixture-response curves were also obtained
at a compression ratio of 8.0 and inlet-air temperatures of 100°,
150°, 200°, 250°, 300°, and 350° F.

The data can be put into the equations and the end-gas density and temperature can be calculated. As indicated from the equations shown in figure 5, the data required for the end-gas temperature calculation are the inlet-air temperature T_o, the compression ratio r, and the function of fuel-air ratio $F_3(f)$. For the end-gas density calculation, the data required are the charge weight W, the total volume V_t, the inlet-air temperature T_o, and the end-gas temperature T_k. When calculated on this basis, knock-limited performance data obtained at variable inlet-air temperature, compression ratio, and fuel-air ratio fell on a single line.

Figures 6 through 12 show the correlations obtained with aviation alkylate, S-reference fuel, 2,3-dimethylbutane, triptane, cyclohexane, cyclopentane, and triptene. All of the fuels contained 4.0 ml of tetraethyl lead per gallon except 28-R, which contained 4.6 ml per gallon. The correlations on the basis of end-gas density and end-gas temperature were good for all of the fuels with the exception of triptane, where the correlation is good at high end-gas temperatures but there is considerable scatter of the data at the low end-gas temperatures. These points represent knock-limited performance at very high power levels where the engine frequently goes into preignition and under such conditions it is difficult to obtain reproducible knock data. This may possibly be the explanation for the scatter of the data.

It was of interest to know whether a correlation could be obtained on another cylinder because all of the data presented herein were obtained on a CFR engine. Unpublished data from the Pratt & Whitney Aircraft Division of United Aircraft Corporation were available for the performance of 28-R fuel on an R-1830 single cylinder at three compression ratios, four inlet-air temperatures, and over a range of fuel-air ratios. Figure 13 shows the correlation on the basis of end-gas density and temperature. The dashed line shows the correlation obtained on the CFR engine. Reasonable agreement was obtained when the differences in cylinder size, cooling, and valve overlap are considered.

The faired curves for the eight fuels tested in the CFR engine are shown in figure 14. This plot illustrates that at mild operating conditions fuels give very large differences in knock-limited performance whereas at severe operating conditions the differences are small but significant. In this plot are shown the effects of compression ratio, inlet-air temperature, and fuel-air ratio. It also illustrates the fact that all fuels do not respond in the same way to increasing severity of operating conditions. For

temperature, compression ratio, and fuel-air ratio on knock-limited performance have been correlated on the basis of the density and temperature of the end gas during knocking combustion. No attempt has been made as yet to include the influences of other engine operating variables such as spark advance and engine speed in the correlation.

The use of the method described will allow the prediction of the knock-limited performance of the fuel types investigated over wide ranges of inlet-air temperature, compression ratio, and fuel-air ratio from a minimum of knock test data.

REFERENCES

1. Rothrock, A. M., and Biermann, Arnold E.: The Knocking Char-
   acteristics of Fuels in Relation to Maximum Permissible
   Performance of Aircraft Engines. NACA Rep. No. 655, 1939.

2. Evvard, John C., and Branstetter, J. Robert: A Correlation of
   the Effects of Compression Ratio and Inlet-Air Temperature
   on the Knock Limits of Aviation Fuels in a CFR Engine - I.
   NACA ACR No. E5D20, 1945.

example, 28-R fuel at low end-gas temperatures has the lowest end-gas density, but at high end-gas temperatures its end-gas density is above three of the fuels.

In order to illustrate how end-gas conditions are related to performance and operating conditions of the engine, three fuels are compared on the basis of charge flow in figure 15. The curves for triptane, 2,3-dimethylbutane, and 28-R are taken from figure 14 and plotted on the basis of end-gas density against end-gas temperature. Then from the first equation on figure 15 it is shown again that end-gas temperature is a function of inlet-air temperature, compression ratio, and fuel-air ratio. On the figure are plotted values for $T_o r^{0.4}$ and also lines of constant fuel-air ratio determined from the mean curve for function of fuel-air ratio.

Then considering the end-gas density ρ_k, which is a function of charge flow, cylinder volume, and inlet-air temperature, the expression $\dfrac{W_c}{V_t(T_o)^{2.5}}$ can be held constant and ρ_k can be plotted against values of T_k. Lines of constant $\dfrac{W_c}{V_t(T_o)^{2.5}}$ are superimposed on the plot. In order to use the chart, a given inlet-air temperature and compression ratio are selected. The point where the dashed line starts on figure 15 corresponds to a compression ratio of 8.7 and an inlet-air temperature of 250° F, which give a value of approximately 1700° R. By following the dashed line to the desired fuel-air ratio, in this case 0.11, and then by proceeding vertically, a comparison of the knock-limited charge flow of the three fuels can be obtained when the compression ratio and inlet-air temperature are held constant. The charge flow is directly proportional to the knock-limited manifold pressure. The knock-limited indicated mean effective pressure can be calculated if the indicated specific fuel consumption is known. It is apparent that under the operating conditions selected the knock-limited manifold pressure of triptane is four times that of 28-R fuel. If the operating conditions are more severe as indicated by a higher inlet-air temperature, a higher compression ratio, or a leaner fuel-air ratio, the differences between the knock-limited performance of the fuels are smaller.

SUMMARY

In summary it may be stated that for the fuels investigated the influences of three engine operating variables, inlet-air
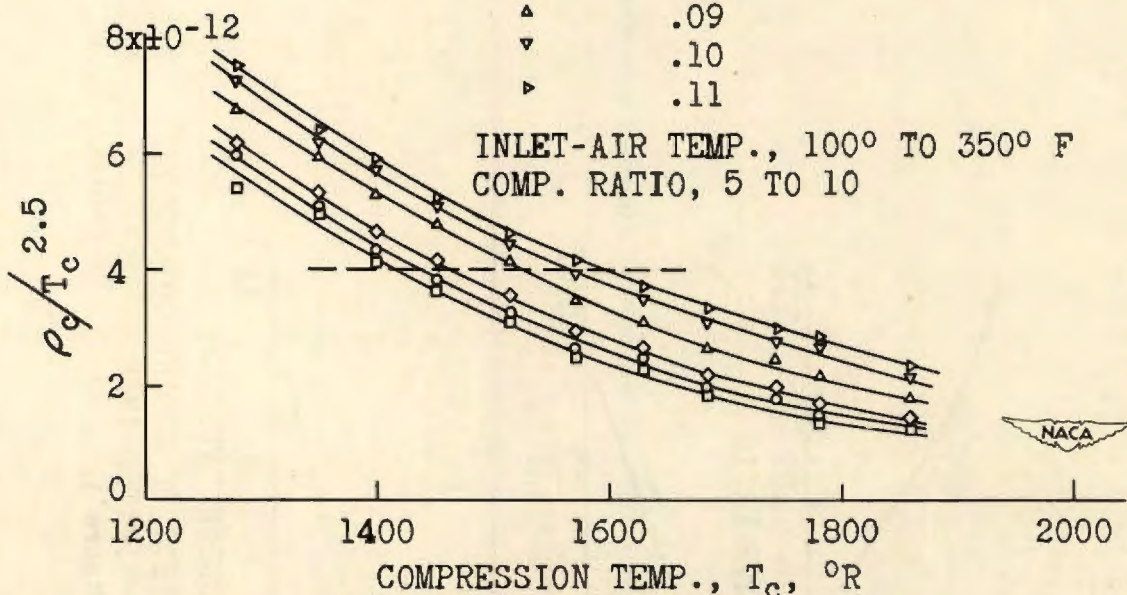
28-R FUEL

$$\rho_c \Big/ T_c^{2.5} = F_2\left[T_c\left(1 + \frac{4040 \quad F_3(f)}{T_c}\right)^{0.286}\right]$$

$$T_c\left(1 + \frac{4040 \ F_3(f)}{T_c}\right)^{0.286} = T_{c_{0.08}}\left(1 + \frac{4040}{T_{c_{0.08}}}\right)^{0.286}$$

FUEL-AIR RATIO

○	0.06
□	.07
◇	.08
△	.09
▽	.10
▷	.11

INLET-AIR TEMP., 100° TO 350° F
COMP. RATIO, 5 TO 10

PLOT FOR DETERMINING FUNCTION OF FUEL-AIR RATIO, $F_3(f)$
Figure 3.

986-A

EXAMPLES OF THE EFFECT OF ENGINE CONDITIONS
ON KNOCK-LIMITED IMEP
Figure 1.

SCHEMATIC DIAGRAM OF TRAVEL OF FLAME
FRONT ACROSS CYLINDER
Figure 2.
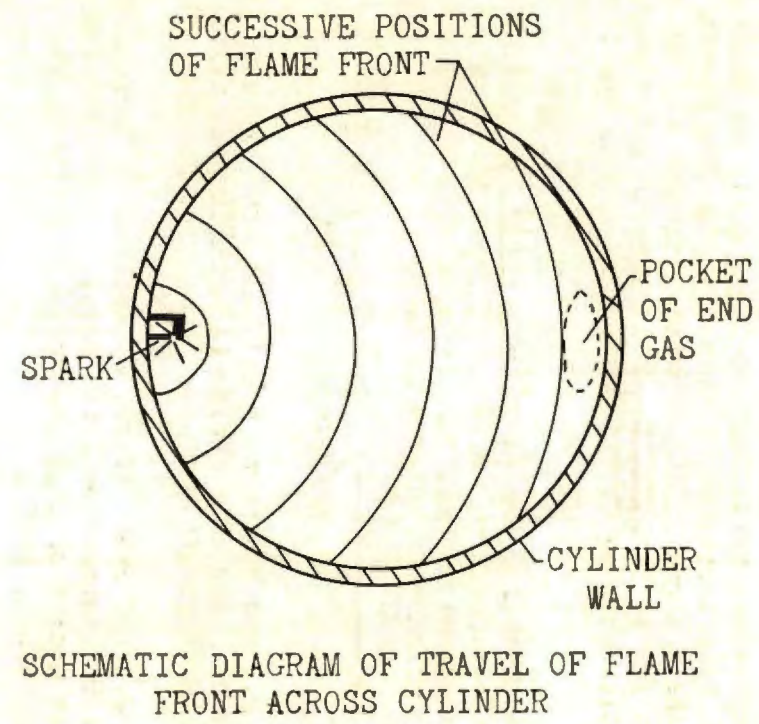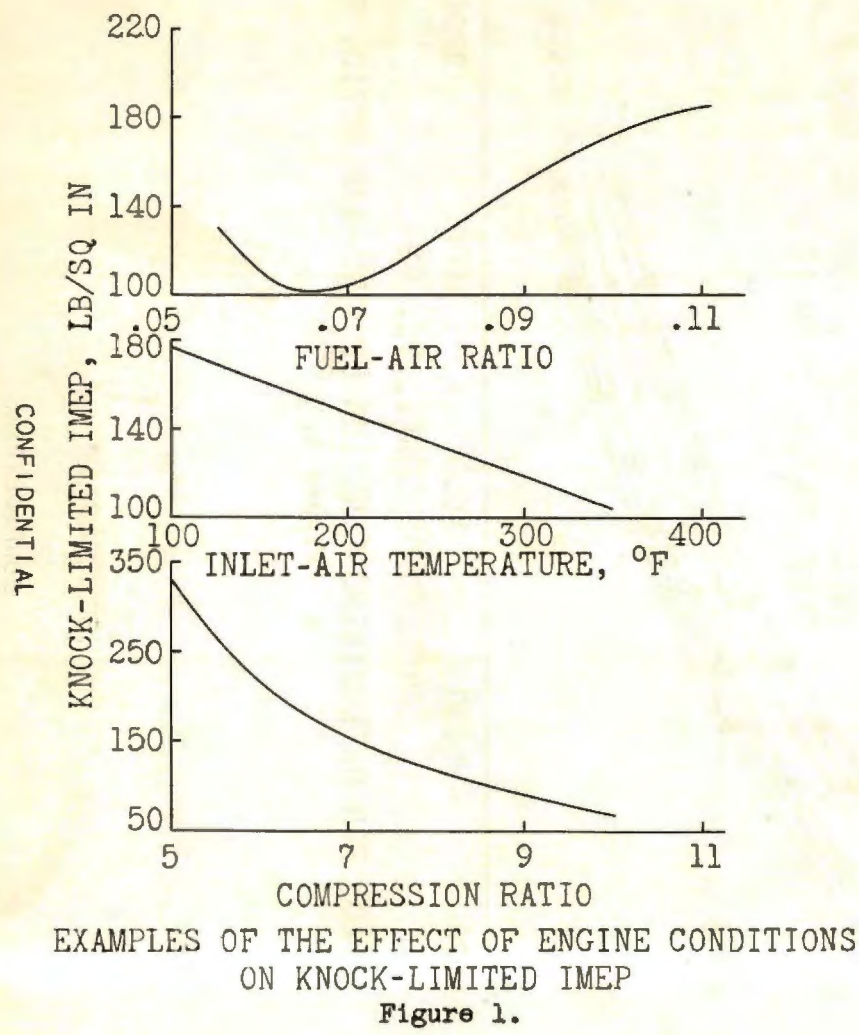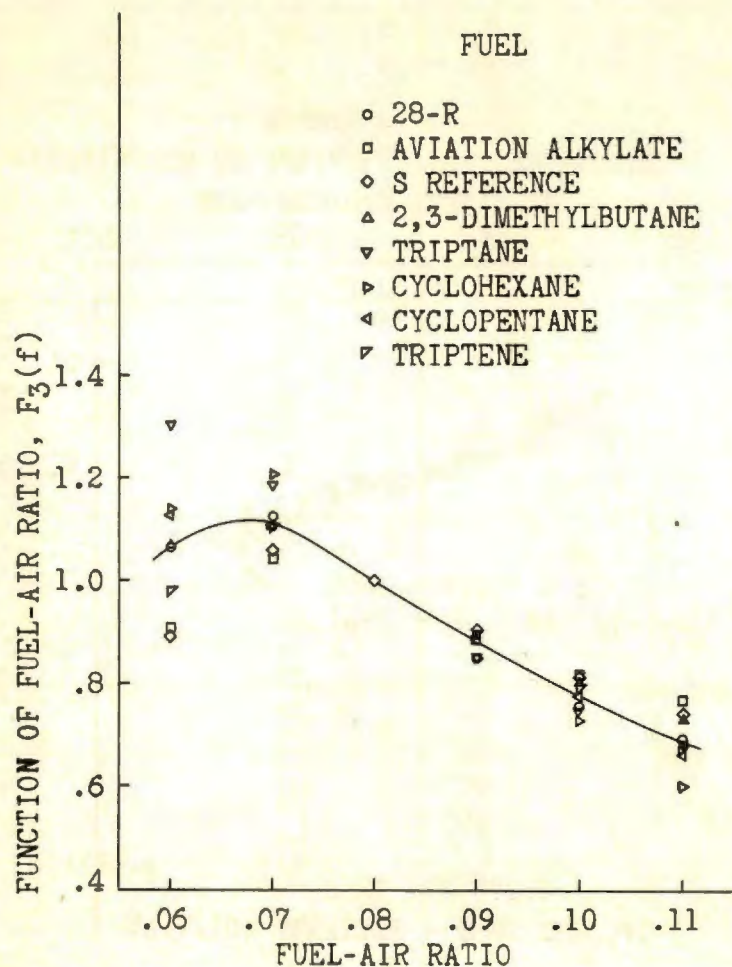
VARIATION OF FUNCTION OF FUEL-AIR RATIO WITH
FUEL-AIR RATIO FOR EIGHT FUELS IN CFR ENGINE.

Figure 4.

CORRELATION OF VARIABLES FOR CFR ENGINE

Figure 5.

AVIATION ALKYLATE + 4 ml TEL/GAL

FUEL-AIR RATIO

o	0.06
□	.07
◇	.08
△	.09
▽	.10
▷	.11

INLET-AIR TEMP., 100° TO 350° F
COMP. RATIO, 5 TO 10

CONFIDENTIAL

EFF. END-GAS DENSITY, LB/CU IN

EFF. END-GAS TEMP., °R
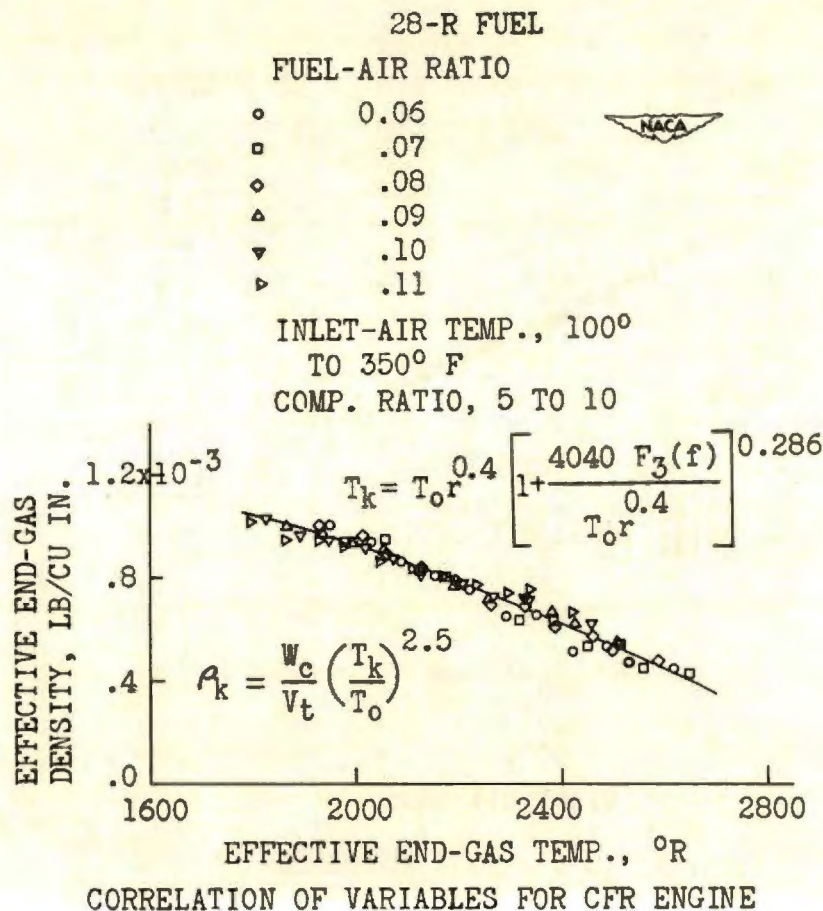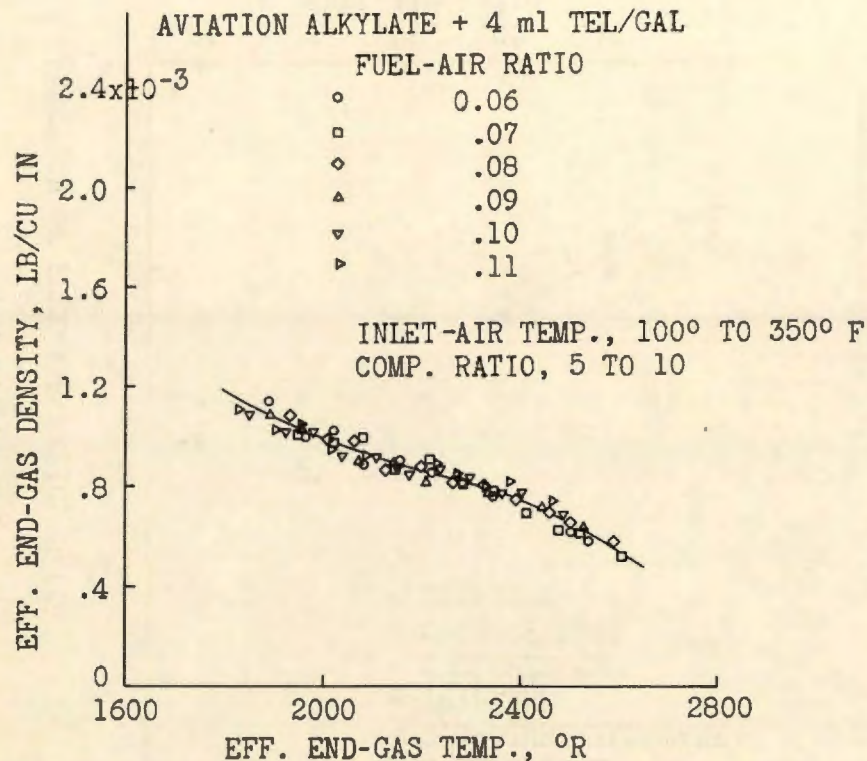
CORRELATION OF VARIABLES FOR CFR ENGINE
Figure 6.

S REFERENCE FUEL + 4 ml TEL/GAL
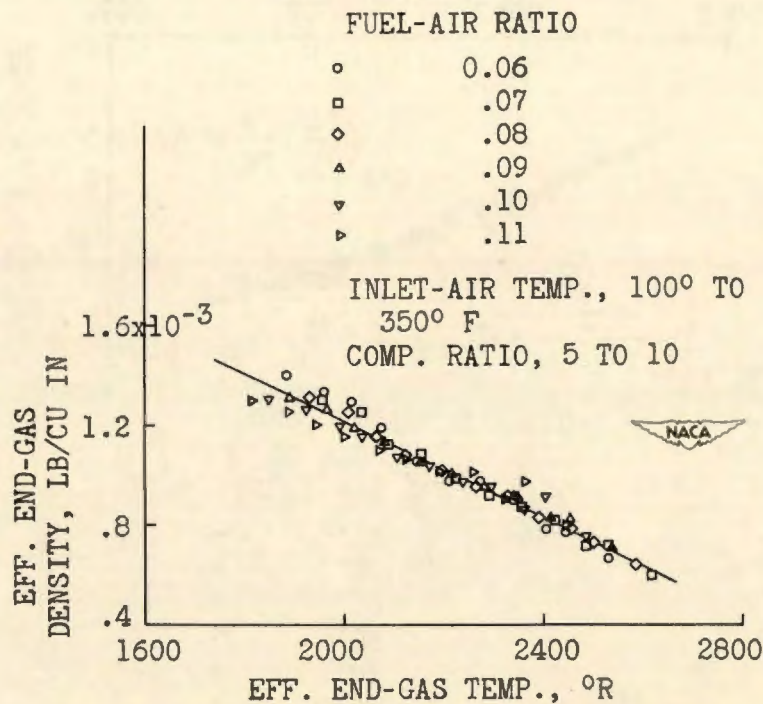
FUEL-AIR RATIO

o	0.06
□	.07
◇	.08
△	.09
▽	.10
▷	.11

INLET-AIR TEMP., 100° TO
350° F
COMP. RATIO, 5 TO 10

NACA

CONFIDENTIAL

EFF. END-GAS
DENSITY, LB/CU IN

EFF. END-GAS TEMP., °R

CORRELATION OF VARIABLES FOR CFR ENGINE
Figure 7.

2,3-DIMETHYLBUTANE + 4 ml TEL/GAL

FUEL-AIR RATIO
○ 0.06
□ .07
◇ .08
△ .09
▽ .10
▷ .11

INLET-AIR TEMP., 100° TO 350° F
COMP. RATIO, 5 TO 10

EFF. END-GAS DENSITY, LB/CU IN.
EFF. END-GAS TEMP., °R

CORRELATION OF VARIABLES FOR CFR ENGINE
Figure 8.

TRIPTANE + 4 ml TEL/GAL

FUEL-AIR RATIO
○ 0.06
□ .07
◇ .08
△ .09
▽ .10
▷ .11

INLET-AIR TEMP., 100° TO 350° F
COMP. RATIO, 5 TO 10

EFF. END-GAS DENSITY, LB/CU IN
EFF. END-GAS TEMP., °R
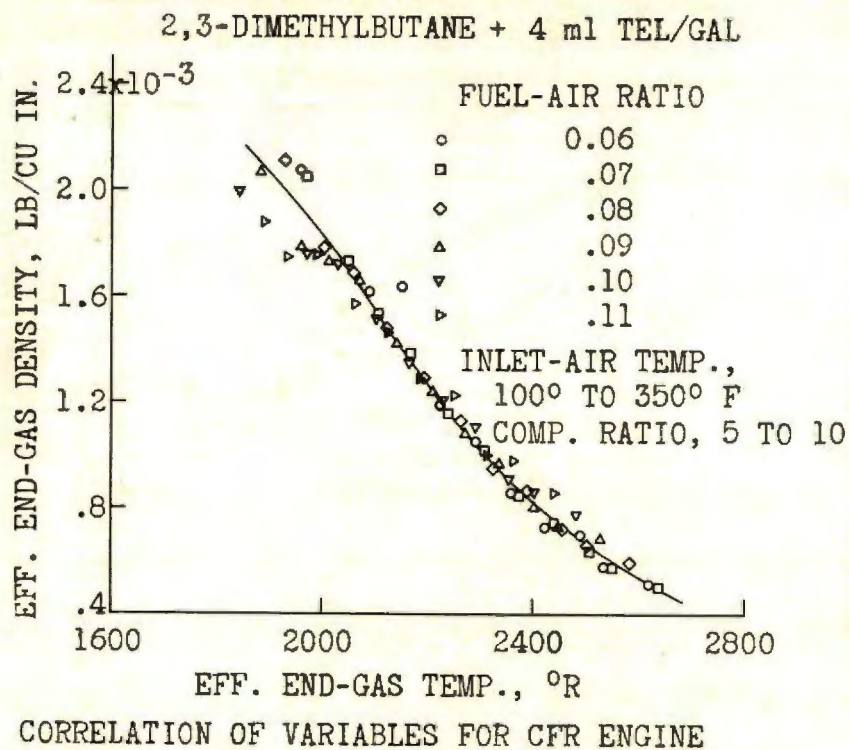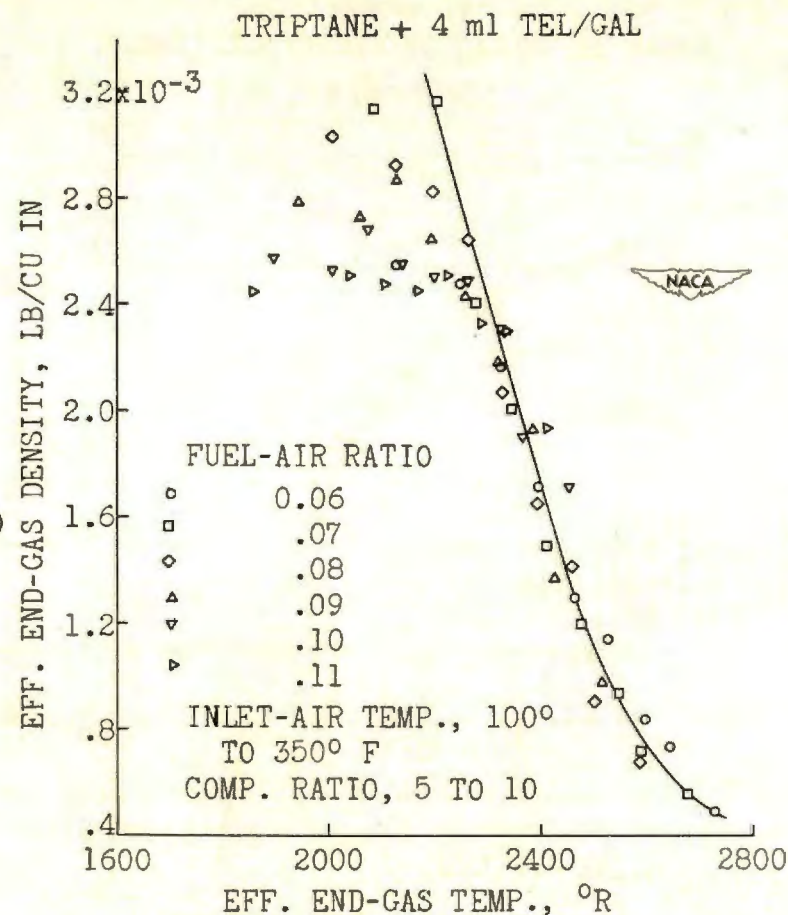
CORRELATION OF VARIABLES FOR CFR ENGINE
Figure 9.

CYCLOHEXANE + 4 ml TEL/GAL

FUEL-AIR RATIO

○	0.06
□	.07
◇	.08
△	.09
▽	.10
▷	.11

INLET-AIR TEMP., 100° TO 350° F

COMP. RATIO, 5 TO 10

EFF. END-GAS DENSITY, LB/CU IN

EFF. END-GAS TEMP., °R
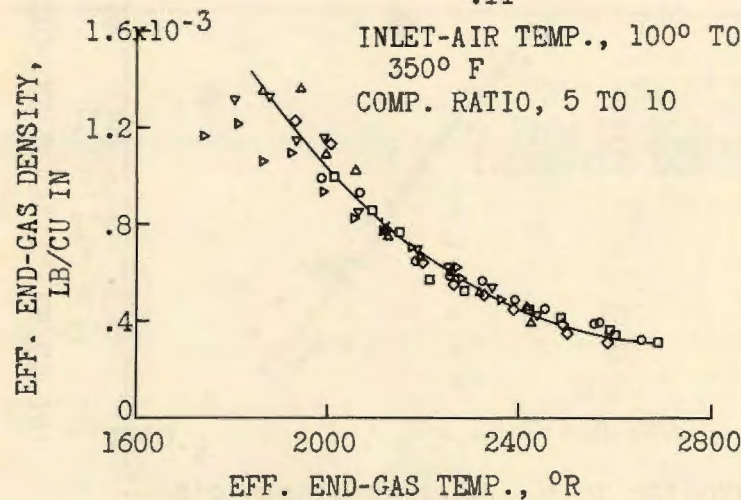
CORRELATION OF VARIABLES FOR CFR ENGINE

Figure 10.

CYCLOPENTANE + 4 ml TEL/GAL

FUEL-AIR RATIO
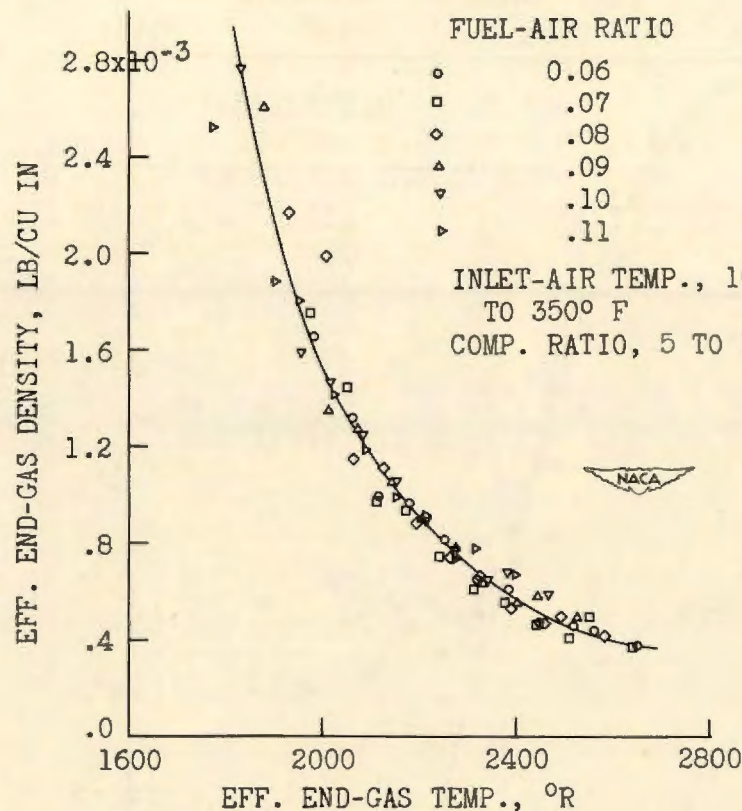
○	0.06
□	.07
◇	.08
△	.09
▽	.10
▷	.11

INLET-AIR TEMP., 100° TO 350° F

COMP. RATIO, 5 TO 10

EFF. END-GAS DENSITY, LB/CU IN

EFF. END-GAS TEMP., °R

CORRELATION OF VARIABLES FOR CFR ENGINE

Figure 11.

V-986

TRIPTENE + 4 ml TEL/GAL

FUEL-AIR RATIO

○	0.06
□	.07
◇	.08
△	.09
▽	.10
▷	.11

INLET-AIR TEMP., 100°
TO 350° F
COMP. RATIO, 5 TO 10

CONFIDENTIAL

EFF. END-GAS DENSITY, LB/CU IN
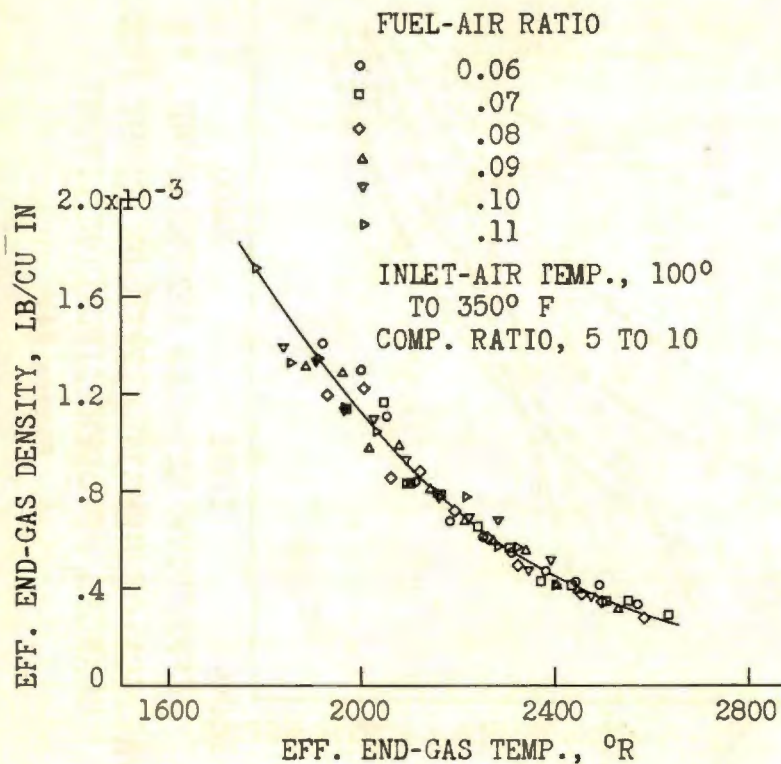
CORRELATION OF VARIABLES FOR CFR ENGINE

Figure 12.

28-R FUEL

FUEL-AIR RATIO

○	0.06
□	.07
◇	.08
△	.09
▽	.10

INLET-AIR TEMP., 150° TO 300° F
COMP. RATIO, 6.7, 7.4 AND 8.0

CONFIDENTIAL

EFF. END-GAS DENSITY, LB/CU IN

R-1830

CFR

EFF. END-GAS TEMP., °R
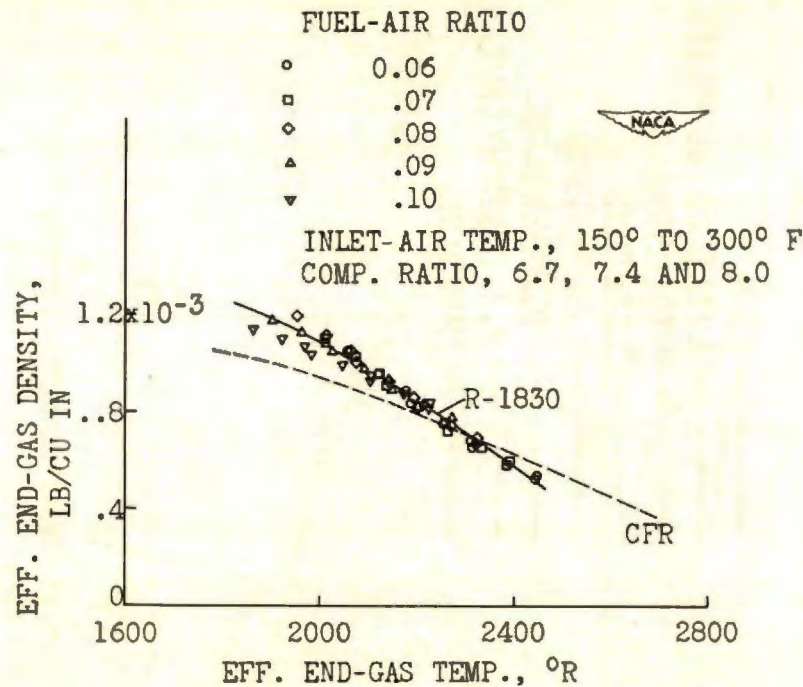
CORRELATION OF VARIABLES FOR R-1830 CYLINDER

Figure 13.

EFF. END-GAS TEMP., °R

FUEL

——————— 28-R
— — — — — AVIATION ALKYLATE
——— — —— CYCLOHEXANE
——— — · — TRIPTENE
——— — · · —S REFERENCE
——— · — · — CYCLOPENTANE
— · — · — · 2,3-DIMETHYLBUTANE
——— · · · — TRIPTANE

COMPARISON OF SENSITIVITIES OF EIGHT FUELS TO
CHANGES OF OPERATING CONDITIONS
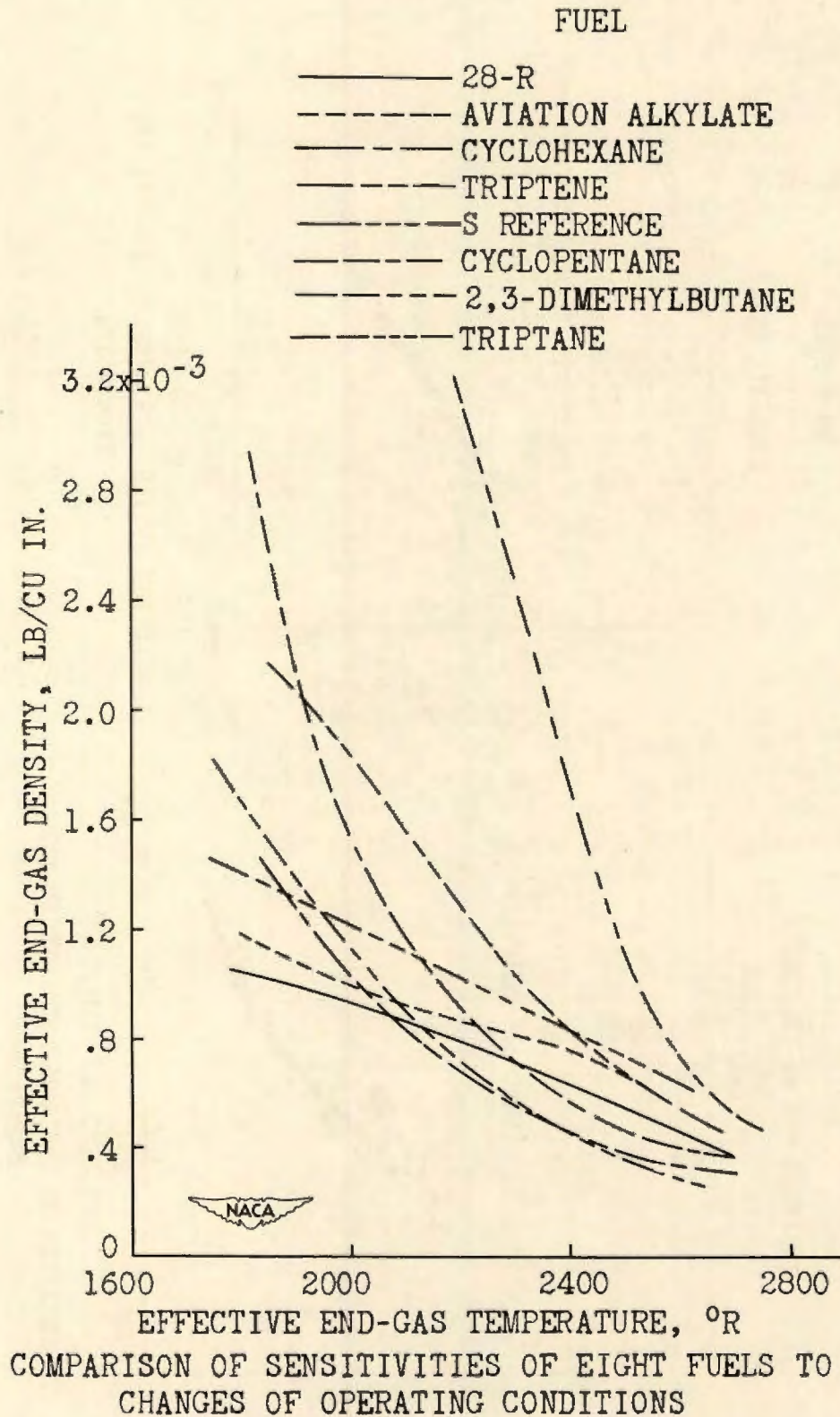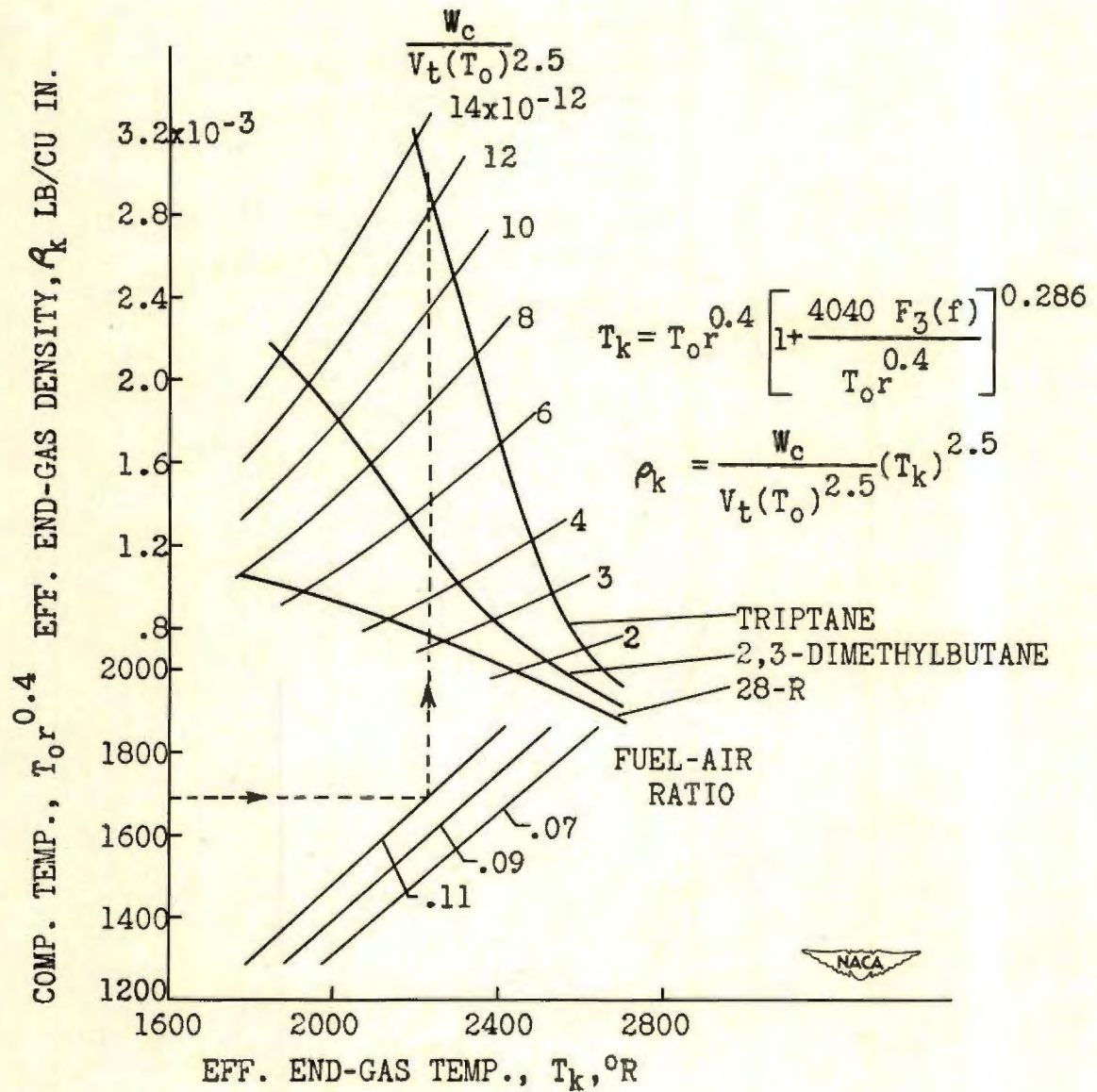
Figure 14.

KNOCK-LIMITED AIR FLOW FROM INLET CONDITIONS.

Figure 15.

EFFECT OF MOLECULAR STRUCTURE OF AROMATIC HYDROCARBONS

AND ETHERS ON KNOCK-LIMITED ENGINE PERFORMANCE

By Henry C. Barnett

Flight Propulsion Research Laboratory

INTRODUCTION

In 1937 the NACA initiated an investigation to evaluate the antiknock characteristics of several classes of organic compounds. The over-all program included the synthesis and purification of the compounds, which were not available commercially, as well as the engine evaluation. The portion of the program involving engine tests was planned in such a manner as to provide data on the following factors:

(1) Relation between molecular structure and antiknock ratings

(2) Blending characteristics

(3) Temperature sensitivity

(4) Lead response

The compounds investigated (reference 1) included 27 aromatics, 23 ethers, and 18 branched paraffins and olefins. The present paper, however, will be confined largely to a discussion of results obtained on the aromatics and brief mention of the ethers.

APPARATUS AND FUELS

Engines and Operating Conditions

The engines and operating conditions used in the program are listed in table I. The first two engines, F-3 and F-4, are standard engines used to evaluate the performance numbers of conventional aviation fuels. These engines are always, for the purpose of determining antiknock ratings, operated at specified conditions. The F-3 engine is a nonsupercharged engine in which the compression ratio is varied to determine the knock limit of a given fuel at a lean fuel-air ratio. All conditions other than compression ratio are reasonably constant for the duration of a test.

The F-4 engine is a supercharged engine in which all conditions except manifold pressure and fuel-air ratio are held constant. The knock limits are determined by varying the manifold pressure until knocking occurs. Although the fuel-air ratios can be varied for this engine, the antiknock rating is reported only for a rich fuel-air ratio, usually about 0.11. Thus, the F-3 method may be indicative of fuel performance at cruise conditions whereas the F-4 method may be indicative of take-off performance.

Two sets of operating conditions are shown in table I for the 17.6 engine. All variables for these two sets of conditions are the same except inlet-air temperature. The temperatures of 100° and 250° F were used to permit a consideration of the sensitivities of the various aromatics to temperature change. The 17.6 designation refers to the engine displacement of 17.6 cubic inches. This displacement is about half that of the F-3 or F-4 engines.

At the beginning of the program, tests were made in a full-scale aircraft-engine cylinder. The first set of full-scale conditions (table I) is considered comparable to cruise operation and the second set is comparable to take-off operation. Full-scale engine tests were later abandoned inasmuch as resluts in the small-scale engines appeared to be adequate.

Base Fuels

Inasmuch as limited quantities of the aromatics were available, all tests were conducted on blends rather than on the pure aromatic. By this procedure considerable information could be determined for a relatively small quantity of aromatic. For these blends, two base fuels were used. The first was isooctane and the second was a blend of $87\frac{1}{2}$-percent isooctane and $12\frac{1}{2}$-percent n-heptane leaded to 4 ml TEL per gallon.

RESULTS AND DISCUSSION

Relation Between Molecular Structure and

Knock-Limited Performance

Aromatics. - As mentioned previously, one of the factors considered in the present investigation is the relation between molecular structure and knock-limited performance. Such relations vary

with engines and operating conditions but, in general, may be considered satisfactory guides in the selection of components for conventional aviation fuels. It is emphasized, however, that for the purposes of this paper the desirability of any particular compound for use in a conventional fuel is based solely on knock-limited performance considerations.

In regard to aromatic hydrocarbons, it is believed that a concentration of 25 percent is a practical maximum limit to assume for a conventional fuel; consequently, the discussion in this paper is based primarily on final blends containing 25-percent aromatic and 75 percent of the isooctane - n-heptane base fuel. In all cases the final blends contained 4 ml TEL per gallon.

The relation between molecular structure and knock-limited performance for a series of alkylbenzenes at a lean fuel-air ratio is shown in figure 1. On the left ordinate, the knock-limited imep ratio is shown as the measure of performance. This ratio is simply the knock-limited indicated mean effective pressure of the 25-percent aromatic blend divided by the knock-limited indicated mean effective pressure of the base fuel. On the right ordinate, a performance number scale is shown for the F-3 engine data. The use of the performance number scale is necessitated by the fact that imep measurements are not made on the F-3 engine.

For all three engines, the performance of the aromatics increases up to the point where the molecule contains nine carbon atoms and then decreases if a tenth carbon atom is added.

At full-scale cruise conditions, it is seen that a 25-percent benzene blend has a knock limit 20 percent higher than the base fuel; toluene is 28 percent higher; ethylbenzene, 35 percent higher; n-propylbenzene, 47 percent higher; whereas, butylbenzene is only 11 percent better than the base fuel. At the other conditions shown the trends are the same but the magnitude of the improvement is less. In fact, under simulated full-scale take-off conditions the benzene blend is lower in performance than the base fuel, which is represented by the ratio 1.0. In the F-3 engine the base fuel has a performance number of 120 and with the exception of n-propylbenzene all the aromatic blends have performance numbers lower than 120. This depreciation in performance is characteristic of aromatics at conditions as severe as those encountered in the F-3 engine.

In several of the full-scale engine tests, the operating conditions were changed from those shown in table I. Data points obtained at these altered conditions are connected by broken

lines in figure 1 and succeeding figures and are not directly comparable to data points connected by solid lines. Such points are included merely to complete the picture and indicate the performance trends with molecular structure.

Figure 2 is similar to figure 1 except that the fuel-air ratio is rich and the F-4 rich rating method has replaced the F-3 lean rating method. The trends shown are somewhat different than those in figure 1, but the similarity between the F-4 engine data and the full-scale data is apparent. In all these cases, the first addition of a carbon atom to the benzene ring produces a sharp improvement in performance; the next addition results in a decrease except for the F-4 data, which are unchanged; the next addition slightly increases the performance; and the addition of the tenth carbon atom results in a very sharp drop in knock-limited indicated mean effective pressure as found at the lean conditions.

The change in performance arising from changes in molecular weight in an homologous series has been illustrated in figures 1 and 2. Figure 3 shows the effect of different isomeric structures on performance when the molecular weight is unchanged. For this example the four butylbenzenes, n-butylbenzene, isobutylbenzene, sec-butylbenzene, and tert-butylbenzene have been chosen. In addition to the F-3 engine data and full-scale engine data, 17.6 engine data at inlet-air temperatures of 100° and 250° F are included in this figure.

At the two 17.6 conditions and the F-3 condition, changing from the normal to the iso, the secondary, and the tertiary structures progressively improves the performance. In the case of the full-scale take-off conditions, the data points connected by the broken line may not be comparable to the points joined by the solid lines inasmuch as the operating conditions were somewhat different.

Data for the four butylbenzenes at a rich fuel-air ratio is presented in figure 4. Except for the full-scale take-off data, the trends shown are similar to those found at lean conditions in figure 3. The 17.6 data show a more uniform increase in performance than do the other data.

Generally speaking, in figures 1, 2, 3, and 4, the trends in performance of the aromatic blends in the standard F-3 and F-4 engines were similar to those in the other engines. For simplicity the remaining portion of this discussion is therefore confined largely to data obtained in the F-3 and F-4 engines.

The knock-limited performance of dimethylbenzenes (xylenes) is illustrated in figure 5. In both the F-3 and F-4 engines, the 1,3-dimethylbenzene blend gave higher performance than either 1,2- or 1,4-dimethylbenzene. The 1,4-dimethylbenzene had a knock limit only slightly less than 1,3-dimethylbenzene but still was considerably higher than 1,2-dimethylbenzene.

The trends shown in figure 5 for dimethylbenzenes are the same as those shown in figure 6 for methylethylbenzenes; that is, 1-methyl-3-ethylbenzene is appreciably better than 1-methyl-2-ethylbenzene and slightly better than the 1-methyl-4-ethylbenzene. The same trend is also true for the diethylbenzenes in figure 7.

Compounds such as these in which additions have been made at two positions on the benzene ring are known as di-substituted compounds. Figure 8 illustrates antiknock trends for tri-substituted compounds. The 1,2,4-trimethylbenzene blend has a slightly higher knock limit than the 1,2,3-trimethylbenzene blend in the F-4 engine but has a slightly lower knock limit in the F-3 engine. The 1,3,5-trimethylbenzene is considerably better than either of the other trimethylbenzenes.

A few of the trends indicated by studies of relations between molecular structure and knock-limited performance have been presented in figures 1 to 8. An idea of the relative antiknock characteristics of all the aromatic hydrocarbons can be obtained from an examination of the F-3 data in figure 9. The base fuel has a performance number of 120 as indicated by the broken line. About 17 aromatics fall above this line indicating an improvement in knock-limited performance of the base fuel. These aromatics fall within a range of about 7 performance numbers above the performance of the base fuel. From these data taken at F-3 lean conditions, 1,3,5-trimethylbenzene and tert-butylbenzene appear to be the most desirable aromatics based on the 25-percent blends examined, but it is emphasized that even these two aromatics increased the rating of the base fuel by only 7 performance numbers.

A point is indicated in figure 9 for the paraffinic fuel, 2,2,3-trimethylbutane (triptane). This point was obtained, as in the case of the aromatics, by blending 25-percent triptane and 75 percent of the isooctane - n-heptane base fuel. The triptane blend shown here has a performance number of 135 as compared to about 127 for the best aromatic blend.

The same type of plot is shown in figure 10 for F-4 engine data. As contrasted to the F-3 data (fig. 9), the 25-percent

additions of aromatic in the base fuel have caused considerable improvement in F-4 performance - from 110 performance number for the base fuel to about 175 for the best aromatic blend. This result confirms the well-known fact that aromatics in fuel blends offer considerable advantage at rich fuel-air ratios but only moderate improvement at lean fuel-air ratios under severe conditions. The 1,3,5-trimethylbenzene blend is still one of the highest performance blends but the tert-butylbenzene blend, which showed up well in the F-3 tests, is exceeded in knock-limited performance by a number of other aromatic blends. Other than 1,3,5-trimethylbenzene, the best aromatic shown is 1-methyl-4-tert-butylbenzene.

The triptane blend, as before, is included in figure 10 for comparison and it is obvious that many of the aromatic compounds are superior at F-4 conditions.

Ethers. - A summary plot of F-3 engine data for ether blends is presented in figure 11. Both aliphatic and aromatic ethers were examined. Of the blends shown, the isopropyl tert-butyl ether blend gave the highest performance at the F-3 lean conditions. Ethyl tert-butyl and methyl tert-butyl ether were next in order, about five performance numbers lower. None of the aromatic ethers improved the performance of the base fuel.

It is seen in figure 11 that for F-3 conditions the best ether blend is about 30 performance numbers better than the base fuel, whereas in figure 9 it was shown that the best aromatic blend was only 7 performance numbers better than the base fuel.

Again, for comparison, a point for the triptane blend is included. The three ethers mentioned in the preceding paragraph were a few performance numbers better than triptane.

The same ether blends at F-4 conditions are presented in figure 12. A blend of methyl tert-butyl ether has the highest performance number at these conditions and shows about the same improvement over the base fuel that was obtained with the best aromatic, 1,3,5-trimethylbenzene. It is shown in figure 12 that a number of the aromatic ethers have improved the rating of the base fuel and that the triptane blend is about 30 performance numbers lower than methyl tert-butyl ether blend.

Blending Characteristics

It is emphasized that to this point most of the discussion has been based upon antiknock studies of 25-percent blends with a

base fuel. This concentration of aromatic was chosen because other factors would restrict the use of blends containing aromatics in excess of 25 percent. Despite this limitation, higher concentrations of aromatics are important to a clearer understanding of antiknock performance as is illustrated in figure 13. The five aromatics shown in this figure were chosen merely to illustrate differences in blending characteristics.

This analysis has been confined to 25-percent blends and it is seen (fig. 13) that the m-diethylbenzene blend produced the greatest knock-limited performance with 1-ethyl-4-methylbenzene second. At a concentration of 50 percent, however, these two aromatics are exceeded in performance by toluene and isopropylbenzene. Thus, the relative order of rating based on investigations of one particular blend concentration can be different from the order obtained at another concentration.

This fact is further illustrated in figure 14 for 17 aromatics examined in the F-4 engine. Although the 50-percent blends in this figure are arranged in order of decreasing performance, it is apparent that the 25-percent blends do not follow the same trend. For example, m-diethylbenzene is eighth in this list based on performance of 50-percent blends but is one of the two best aromatics in 25-percent blends.

A similar result is obtained in the F-3 engine as shown in figure 15. Although data for the 50-percent blends are incomplete, it is apparent in the F-3 engine that increasing percentages of aromatic in the blend tend to decrease the antiknock value. For example, 25-percent blend of 1-isopropyl-4-methylbenzene has a performance number of 121, whereas the 50-percent blend has a rating of about 114; also, in the case of benzene, the rating drops from 118 to 100 when the concentration is increased from 25 to 50 percent.

Temperature Sensitivity

The next factor considered in the investigation of aromatic fuels is temperature sensitivity. The tests made to evaluate this factor were conducted in the 17.6 engine. In this instance, 20-percent blends of aromatic and isooctane were examined at inlet-air temperatures of 100° and 250° F while all other conditions were identical. Figure 16 presents the results of these tests.

On the abscissa of figure 16 is plotted a ratio, which for the purpose of this paper, is designated temperature sensitivity. This ratio is simply the knock-limited indicated mean effective pressure

of the blend at 100° F divided by the knock-limited indicated mean
effective pressure at 250° F. For comparison, data for triptane
are included on this plot. The compounds, except for triptane, are
arranged in order of decreasing sensitivity at a lean fuel-air
ratio. The order of temperature sensitivity is not the same at rich
mixtures as it is at lean mixtures.

The 1,3,5-trimethylbenzene, which has the highest F-3 and
F-4 ratings (figs. 9 and 10) of all the aromatics examined, appears
to be the most sensitive aromatic at lean and rich mixtures.
However, 1-ethyl-4-methylbenzene and p-xylene appear to be com-
parable in sensitivity at rich mixtures to 1,3,5-trimethylbenzene.
It is interesting to note that for rich mixtures the temperature
sensitivity of triptane is less than that of all the aromatics
with the possible exception of 1-ethyl-2-methylbenzene. At lean
mixtures, all the aromatics below ethylbenzene are less sensitive
than triptane.

Lead Response

The last factor of importance in this evaluation of aromatics
is the lead response. Figure 17 persents data for the same blends
used in the temperature sensitivity studies. Triptane is also
included in this figure. Lead response, shown on the abscissa of
this figure, is defined as the knock-limited indicated mean effective
pressure of the leaded blend divided by the indicated mean effective
pressure of the unleaded blend. Leaded blends contained 4 ml TEL per
gallon.

It is seen in figure 17 that tert-butylbenzene blend has the
highest lead response at lean mixtures and is exceeded at rich
mixtures only by 1-isopropyl-4-methylbenzene. The triptane blend
has a lead response comparable to that of benzene as indicated
by these data.

CONCLUSIONS

In summarizing the conclusions that may be drawn from the
data presented, it is emphasized that such conclusions must neces-
sarily apply only for the 25-percent blends. The conclusions,
thus qualified, are as follows:

1. The best aromatics at F-3 conditions are 1,3,5-trimethylbenzene and <u>tert</u>-butylbenzene. At these same conditions, however, both of these aromatic blends were exceeded in performance by a comparable blend of triptane.

2. At F-4 conditions the best aromatics were 1,3,5-trimethylbenzene and 1-methyl-4-<u>tert</u>-butylbenzene and the performance of both exceeded that of triptane.

3. At F-3 conditions the best ether was isopropyl <u>tert</u>-butyl ether and its performance exceeded that of triptane and the best aromatic.

4. At F-4 conditions the best ether was methyl <u>tert</u>-butyl ether and its performance exceeded that of triptane but did not exceed the best aromatic.

REFERENCE

1. Barnett, Henry C., Drell, I. L., and Branstetter, J. Robert: NACA Evaluation of Pure Organic Compounds as Components of High-Antiknock Aviation-Fuel Blends. NACA Rep.(to be pub.).

986-B

TABLE I

ENGINES AND OPERATING CONDITIONS

ENGINE	SPARK ADVANCE °BTC	COMP. RATIO	COOLANT TEMP. °F	SPEED RPM	INLET-AIR TEMP. °F	FUEL-AIR RATIO
F-3	35	VARIABLE	374	1200	220 (MIXTURE)	--------
F-4	45	7.0	375	1800	225	VARIABLE
17.6	30	7.0	212	1800	100	VARIABLE
	30	7.0	212	1800	250	VARIABLE
FULL-SCALE SINGLE	20	7.3	a365	2000	210	VARIABLE
	20	7.3	a365	2500	250	VARIABLE

aREAR-SPARK-PLUG-BUSHING TEMPERATURE.
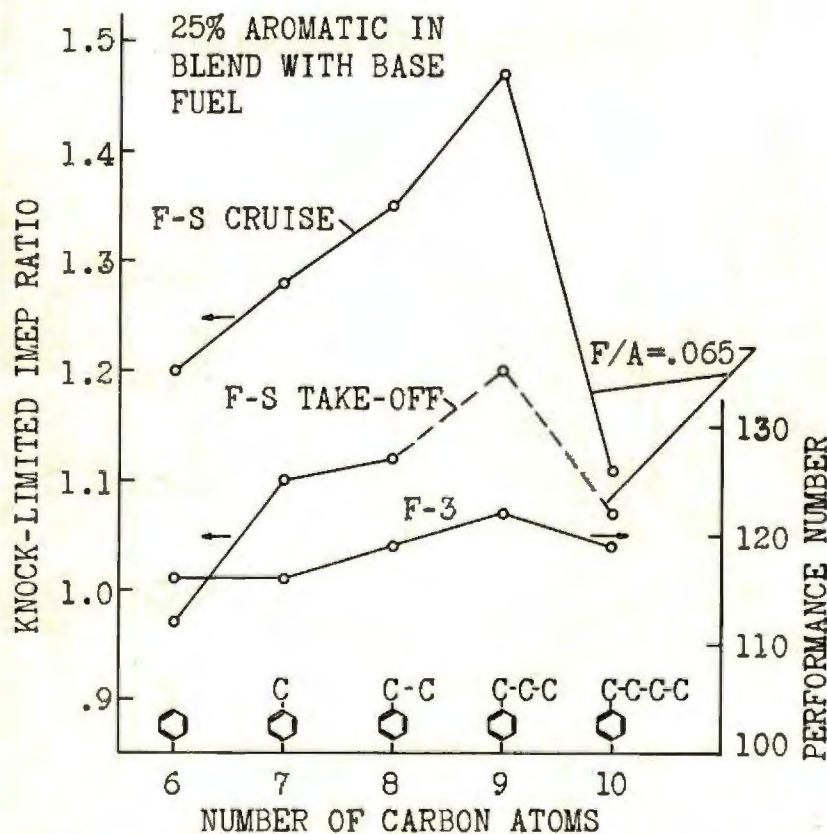
KNOCK-LIMITED PERFORMANCE OF ALKYLBENZENES.

Figure 1
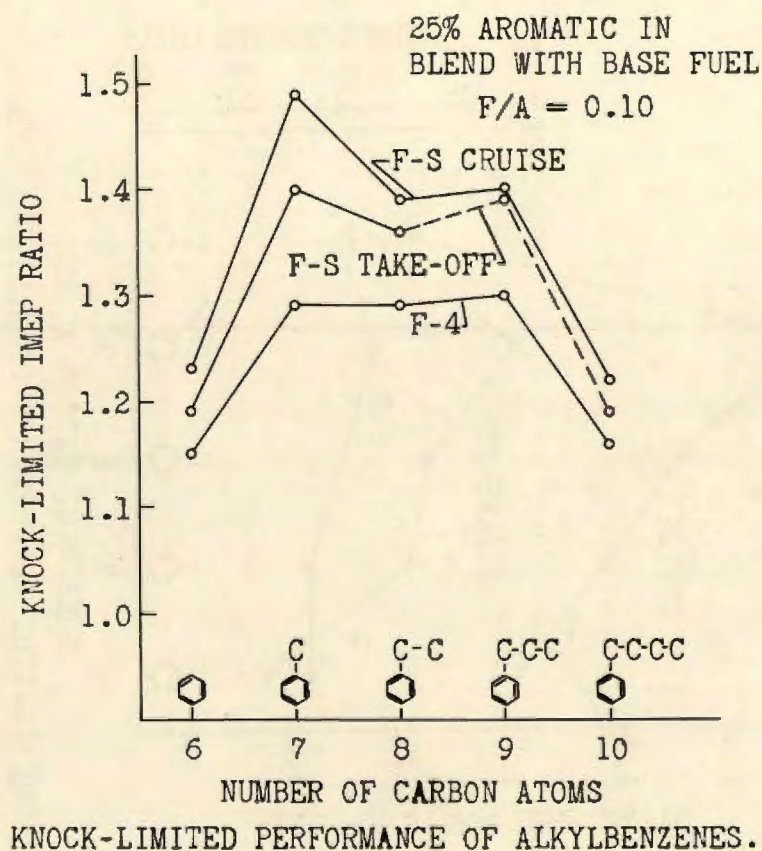
KNOCK-LIMITED PERFORMANCE OF ALKYLBENZENES.

Figure 2

KNOCK-LIMITED PERFORMANCE OF BUTYLBENZENES.

Figure 3

KNOCK-LIMITED PERFORMANCE OF
BUTYLBENZENES.
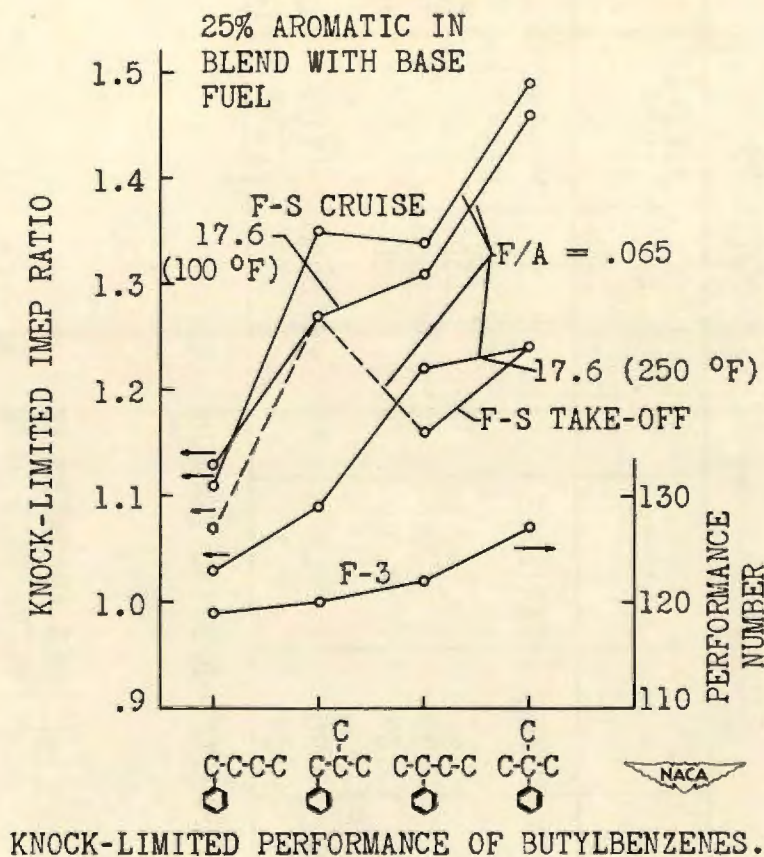
Figure 4

KNOCK-LIMITED PERFORMANCE OF
DIMETHYLBENZENES.
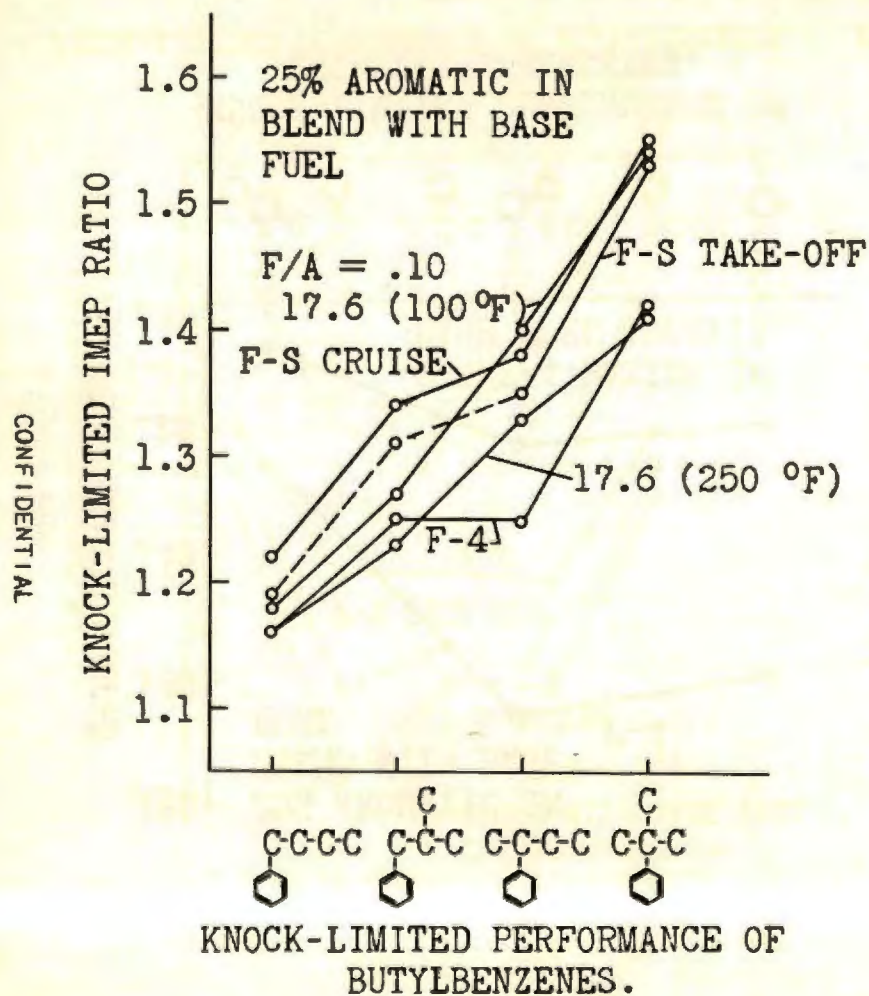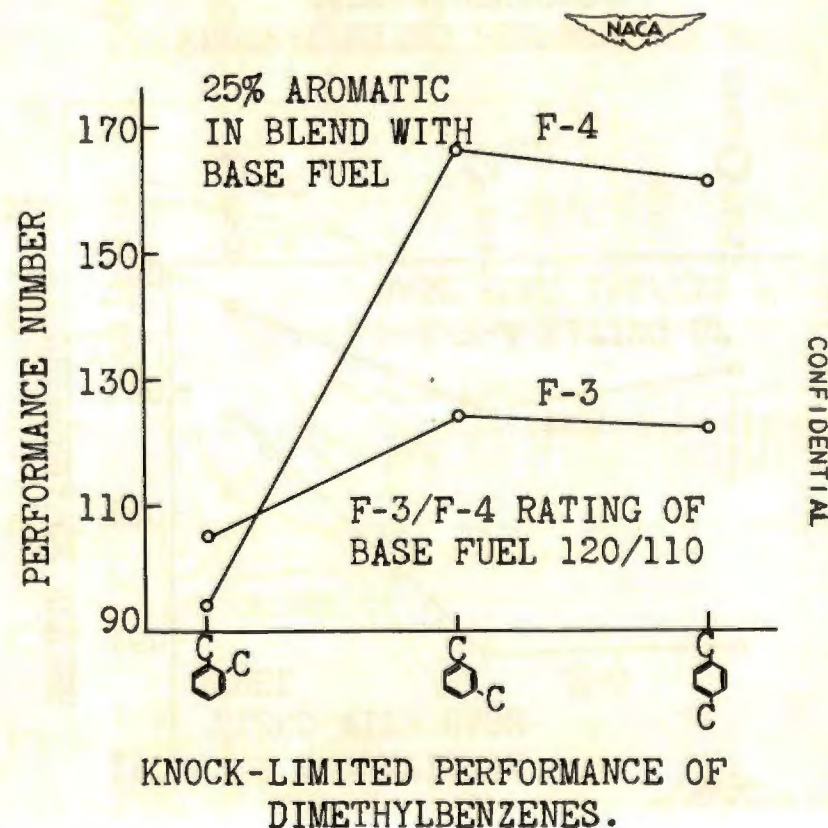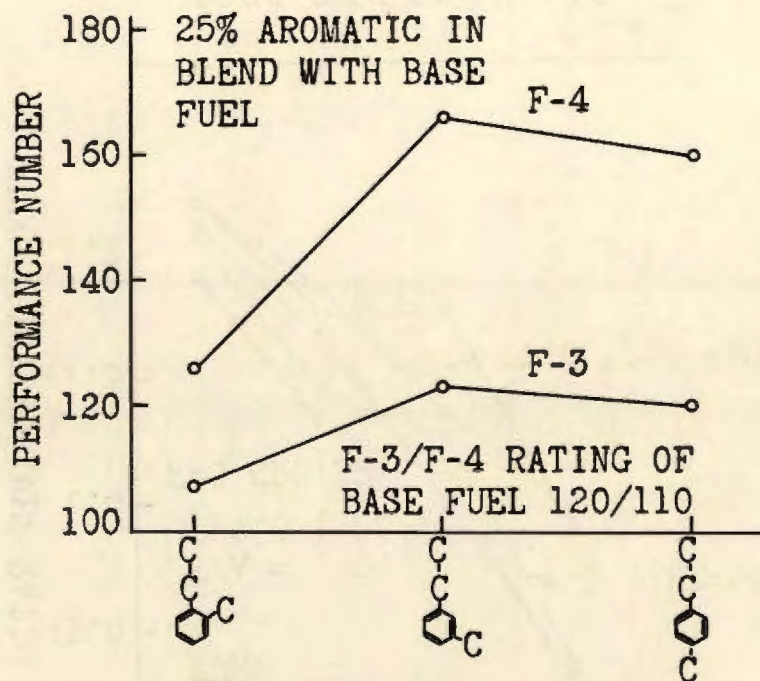
Figure 5

KNOCK-LIMITED PERFORMANCE OF
METHYLETHYLBENZENES.

Figure 6
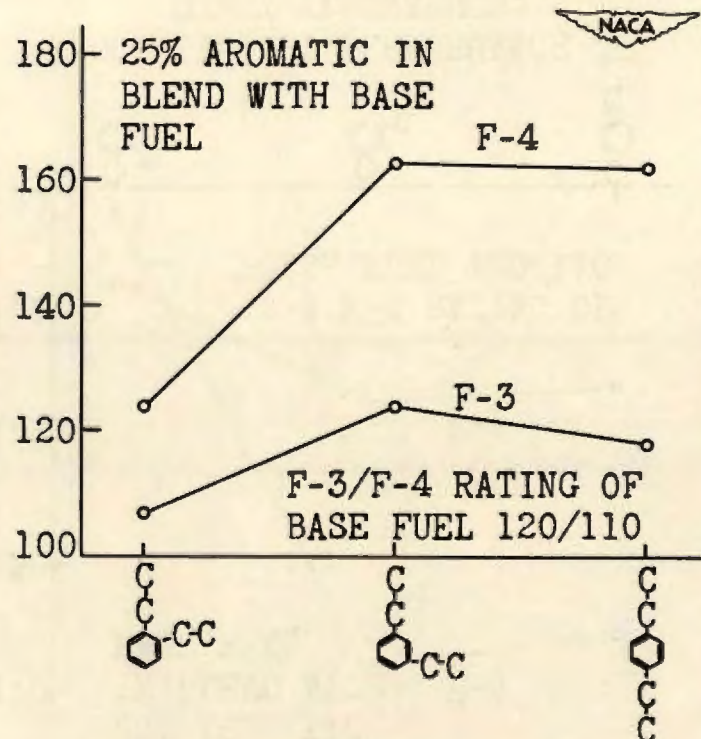
KNOCK-LIMITED PERFORMANCE OF
DIETHYLBENZENES.

Figure 7
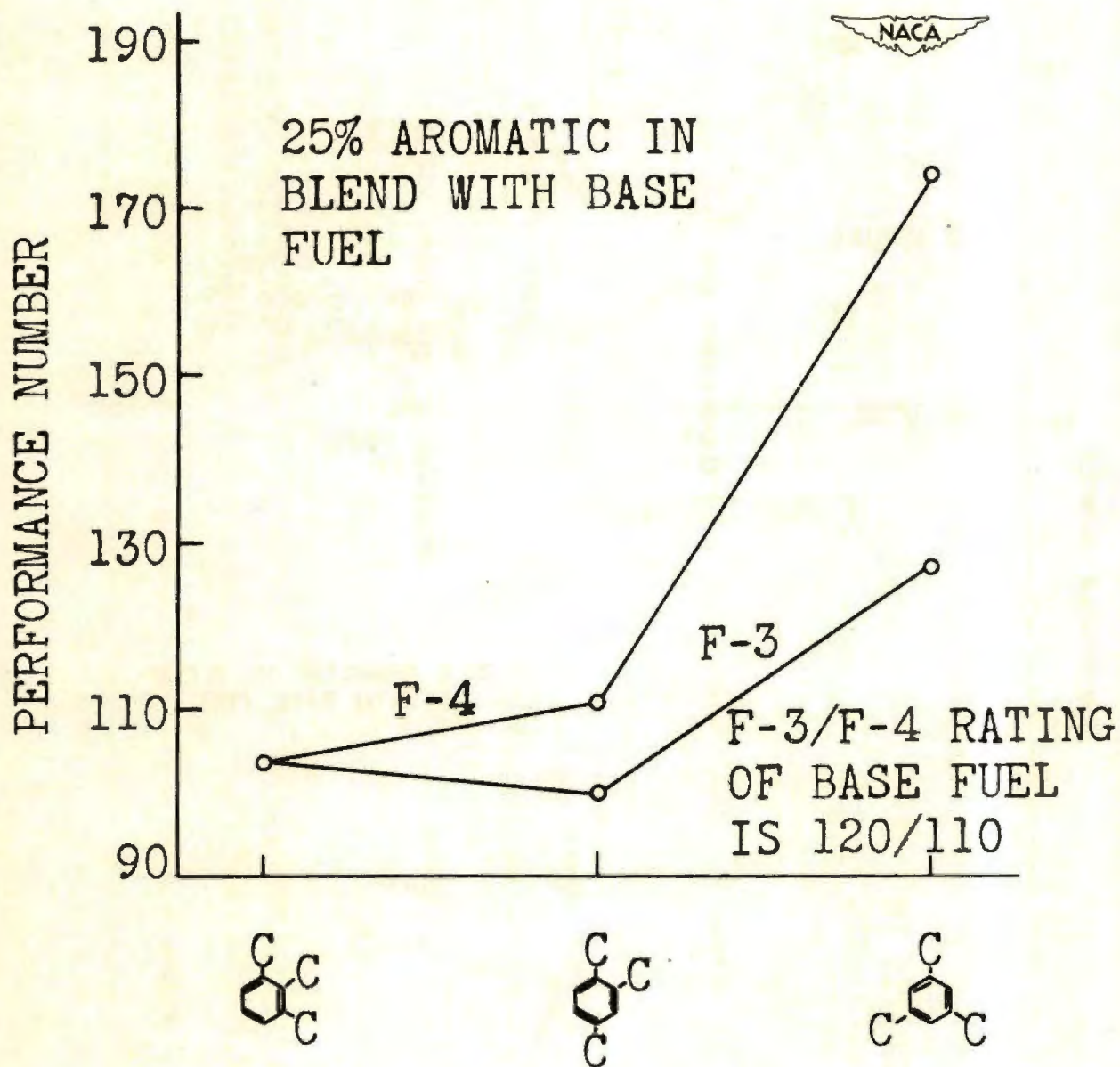
KNOCK-LIMITED PERFORMANCE OF
TRIMETHYLBENZENES.

Figure 8
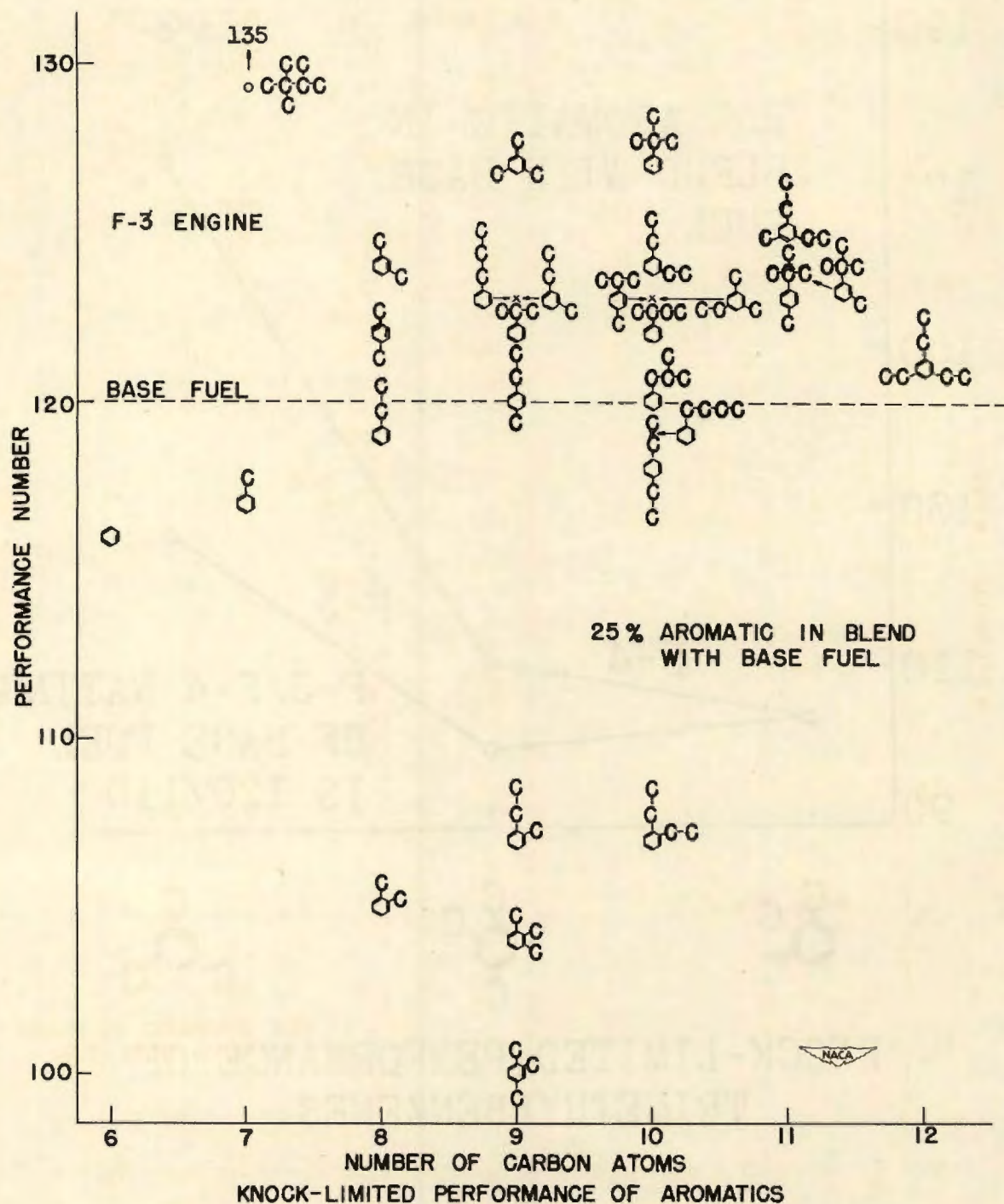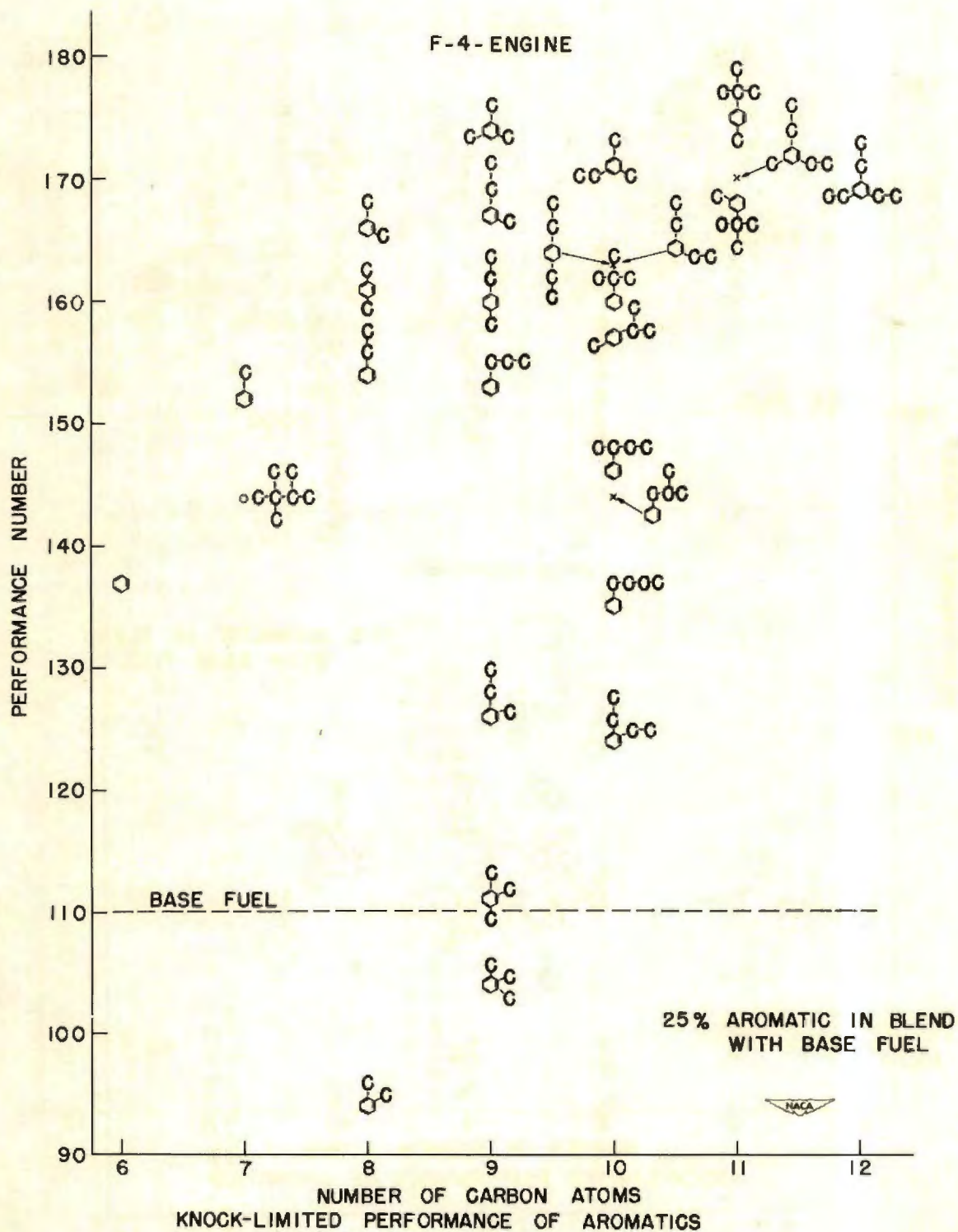
Figure 9

Figure 10

Figure 11.

Figure 12

986-B

KNOCK-LIMITED PERFORMANCE OF AROMATIC BLENDS.
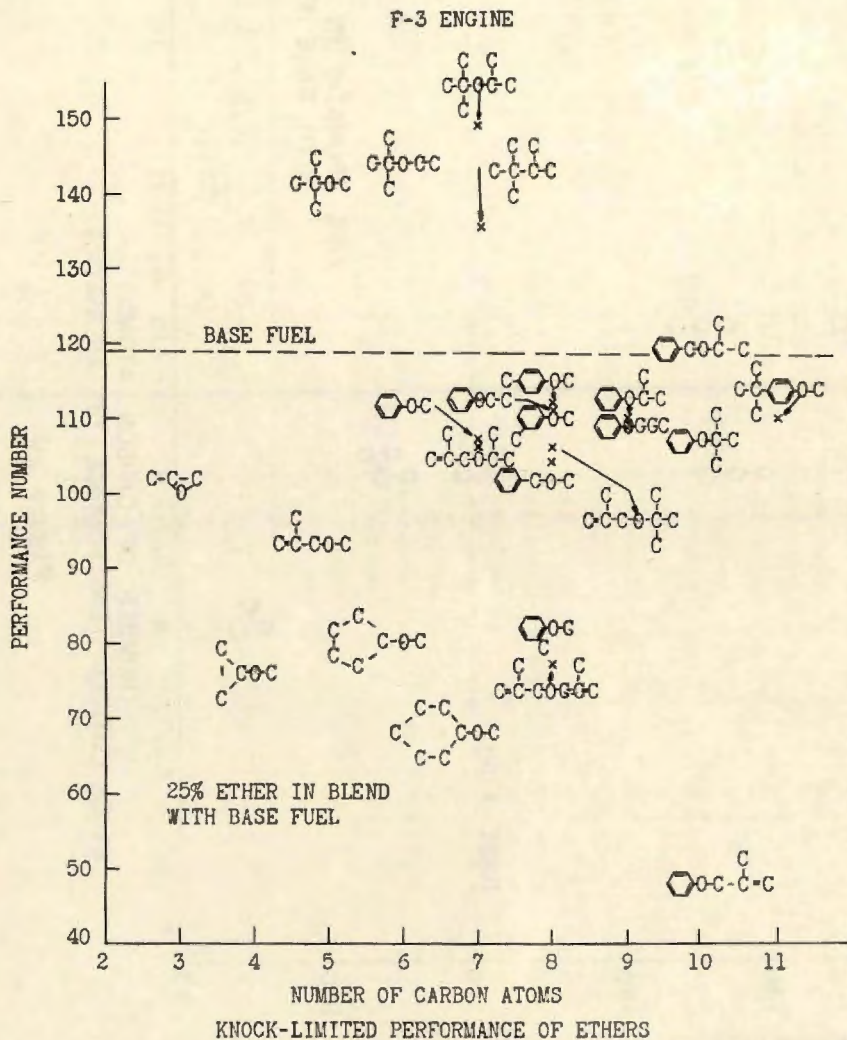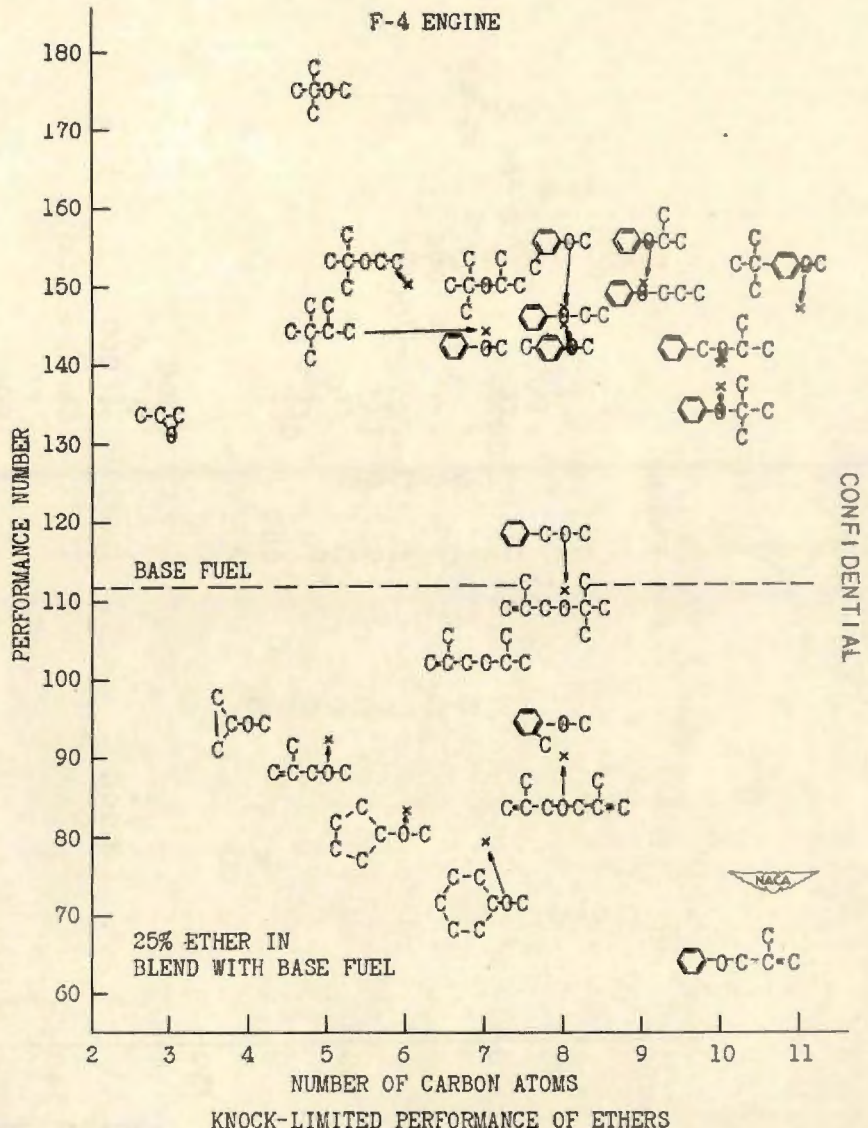
Figure 13.

KNOCK-LIMITED PERFORMANCE OF AROMATIC BLENDS
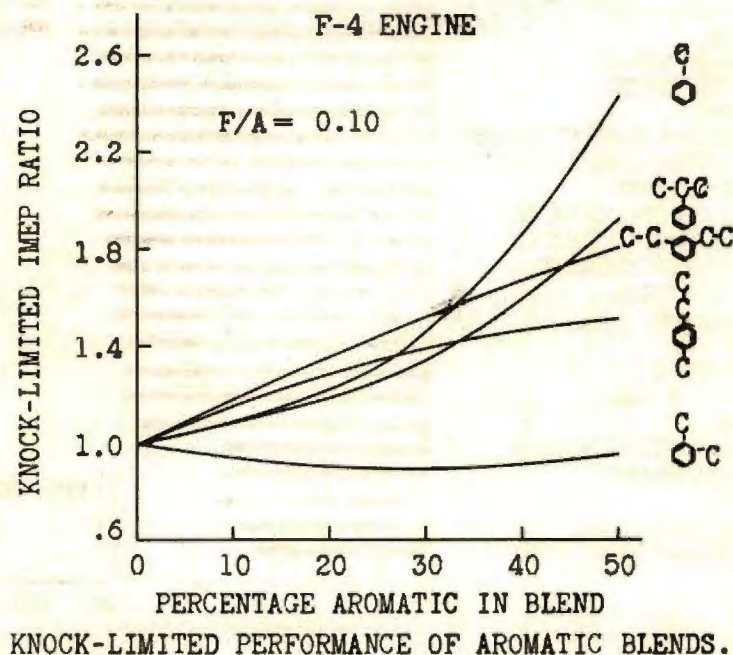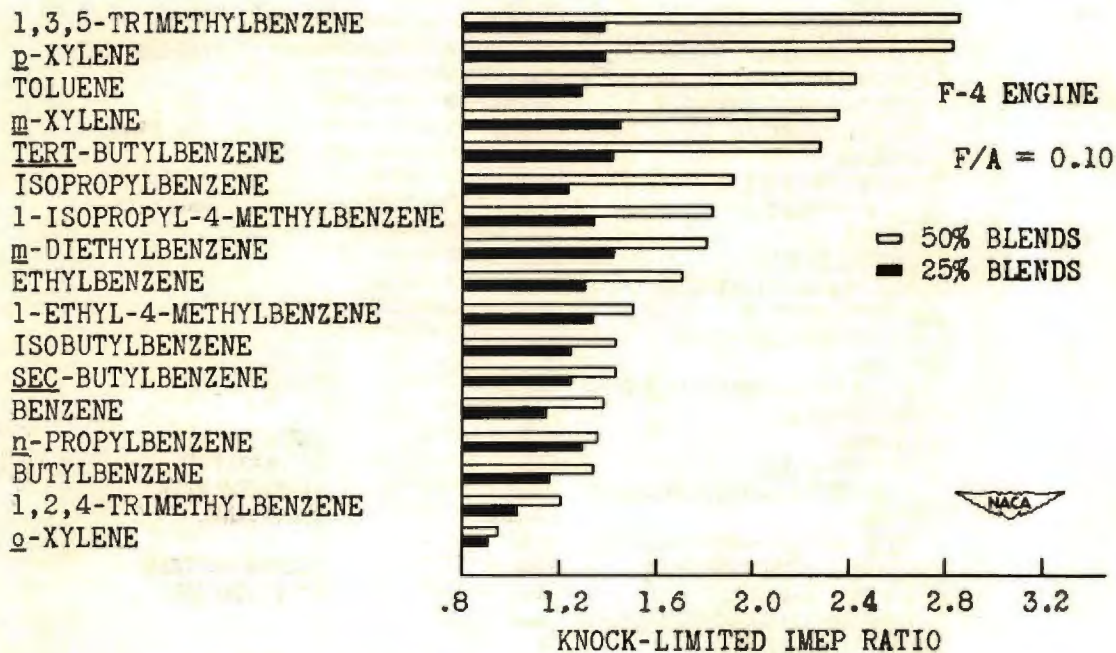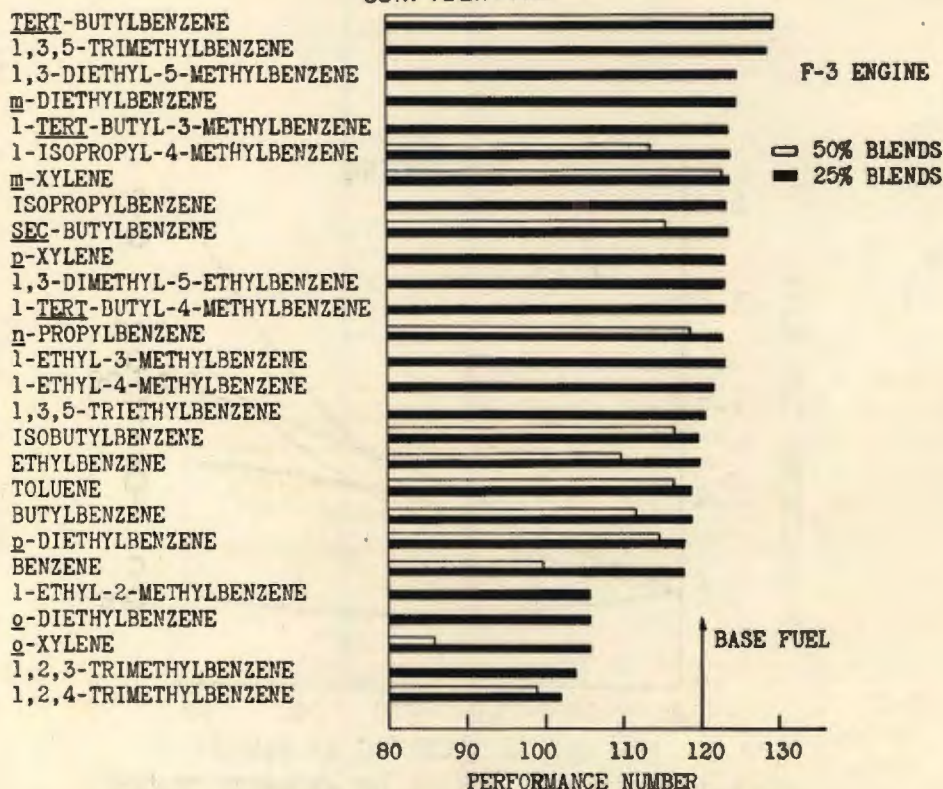
Figure 14.

Knock-Limited Performance of Aromatic Blends.
Figure 15.
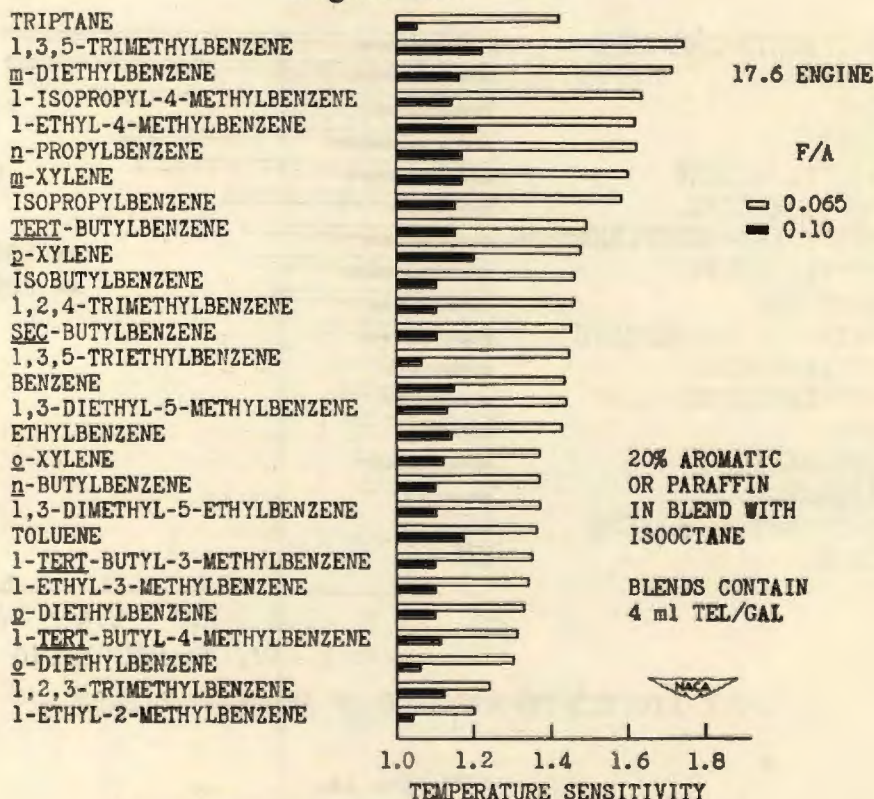
Temperature Sensitivity of Aromatics.
Figure 16.

986-B
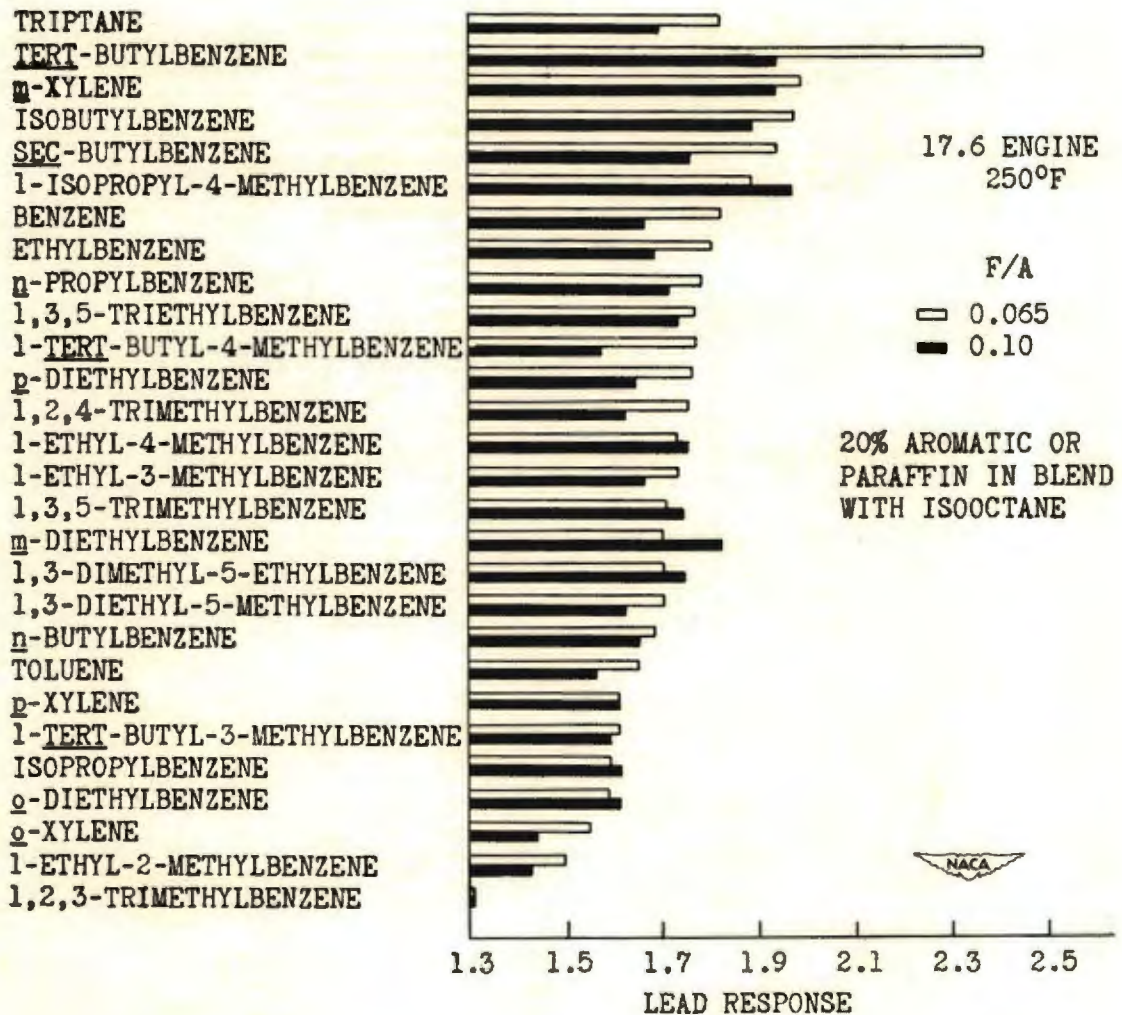
Lead Response of Aromatics.

Figure 17.

CORRELATION OF FUEL PROPERTIES WITH MOLECULAR STRUCTURE

FOR HYDROCARBONS OF HIGH ENERGY PER UNIT VOLUME

By Paul H. Wise

Flight Propulsion Research Laboratory

INTRODUCTION

The change in aircraft power plants from reciprocating to jet engines shifted the emphasis to different parameters for evaluating the fuels used. Fuels that would be unsatisfactory in reciprocating engines show performances equal or superior to high octane gasoline when burned in a jet-engine combustor.

One of the important properties to be considered in evaluating a fuel for jet engines is the thermal energy per unit volume. High speed aircraft are volume-limited because of their design requirements of thin wings and fuselages, and the fuel storage space is restricted. A fuel with high thermal energy per unit volume would be valuable to give aircraft of this type increased flight range.

The first step in finding fuels with higher values of thermal energy per unit volume was a search of literature for data on known hydrocarbons. Such data were obtained (references 1 to 3) on several homologous series of different types and these are shown in figure 1. The net heat of combustion per cubic foot of each compound is plotted as the abscissa and the corresponding boiling point as the ordinate. It is apparent that the alkyl-cyclohexane and alkylbenzene series are superior to aviation gasoline and AN-F-32 with respect to thermal energy per unit volume.

There are also data (references 1 to 3) that indicate that dicyclic aromatic hydrocarbons such as naphthalene and biphenyl and their derivatives should be placed on this graph in the area corresponding to about 1,000,000 to 1,100,000 Btu per cubic foot and 450° to 500° F. These values represent a substantial gain in thermal energy per cubic foot over aviation gasoline. This gain in thermal energy per cubic foot could be utilized to extend flight range. However, because these data are inadequate and in many cases unreliable, they cannot be used as a basis for analyzing the value of dicyclic aromatic hydrocarbons as engine fuels.

It was decided that the NACA Cleveland laboratory undertake a
research program which includes the preparation and purification of
selected hydrocarbons and the accurate determination of their physical
properties (reference 4). It was believed that, when sufficient
reliable data were available, it would be possible to indicate
certain types of structure that would be most promising for combus-
tion tests and further development.

The hydrocarbons chosen for investigation are outlined in fig-
ures 2 and 3. In figure 2 is shown naphthalene and its hydrogenated
derivatives, tetralin and decalin. Each derivative may be considered
to be the parent hydrocarbon of a series and will be substituted
with the various alkyl groups (designated as R) shown in the upper
right-hand corner of the figure. Each parent hydrocarbon has more
than one position in which the alkyl groups can be substituted as
indicated by the position of the R group over the brackets.

The structure in the lower part of figure 2 is one example of
a series of alkylbenzenes that is being investigated. The alkyl
groups have six, seven, or eight carbon atoms, which can be arranged
in various branched structures. The related saturated hydrocarbons
are also to be prepared

The hydrocarbons outlined in figure 3 are related to biphenyl.
Those to the right of the parent hydrocarbon are the various alkyl
biphenyls, and different derivatives are obtained by placing sub-
stituents in the three positions shown.

Diphenylmethane can be varied in three different ways. The
first is to introduce the various alkyl groups R outlined in
figure 2 in the 2, 3, and 4 positions as in the case of biphenyl.

The other variations can be achieved either by adding alkyl
groups as a side chain attached to the carbon atom between the
phenyl groups to give the 1,1-dicyclic alkanes or by lengthening
the chain of carbon atoms between the two rings to form the
α,ω-dicyclic alkanes.

The illustrated saturated derivatives, which can be prepared
by hydrogenating the aromatic hydrocarbons, have been included in
this program. It is known that the saturated compounds have lower
melting points and burn more easily than the corresponding aromatic
hydrocarbons. On the other hand they have higher viscosities and
lower net heats of combustion per unit volume than their aromatic
counterparts. Inasmuch as many properties must be considered in

selecting a fuel, it seemed advisable to study the saturated compounds to determine accurately the extent of the changes produced by hydrogenation.

The parameters, which are considered to be important in evaluating these compounds with respect to use as fuels, are Btu per cubic foot, Btu per pound, melting point, boiling point, viscosity, and density.

The values of Btu per cubic foot and Btu per pound are both important in considering a prospective fuel. For jet fuels the value of Btu per cubic foot is more important because of the limited fuel storage space.

The melting point must be considered because the fuel must be a fluid at operating temperatures, and a maximum value for the melting point is required in fuel specifications (reference 5). Four points of blends of the pure hydrocarbons are also to be determined.

The boiling point is important because it affects ease of ignition and vaporization as well as handling problems connected with the fuel.

The viscosities are determined over a range of temperatures in order to know that the fuel can be pumped through fuel lines and nozzles under operating conditions. The viscosities of blends of the hydrocarbons will be determined.

Density is important in relating Btu per pound and Btu per cubic foot so a high density value is desired.

In the investigation, the compounds will be compared first with respect to these parameters, and those which appear to be most likely to be valuable as experimental fuels will be examined with respect to the following combustion characteristics: ease of ignition, inflammability limits, flame speed, and carbon formation.

In discussing the data obtained, the hydrocarbons are presented as homologous series. The values of net heats of combustion are presented as the ratio of the absolute value to the corresponding absolute value of high octane aviation gasoline (reference 6). This ratio permits an evaluation within a series and at the same time compares each compound with a fuel now in use. The ratio of net heat per unit volume is used as one coordinate in comparing the other properties of the compounds.

Most of the compounds were synthesized and purified and their
physical constants were determined by the Fuel Synthesis and Analyt-
ical Chemistry Sections of this laboratory. Some of the data were
obtained by purifying commercially available compounds.

2-n-ALKYL BIPHENYL HYDROCARBONS

The alkyl biphenyl hydrocarbons with the substituent in the
two position make up the first series. The change in Btu per cubic
foot with respect to the change in Btu per pound is illustrated in
figure 4. The parent hydrocarbon, biphenyl, has a Btu-per-pound
value about 90 percent of that of aviation gasoline, but at the
same time it is 34 percent higher in Btu per cubic foot. A drop
of about 2 percent in relative Btu per cubic foot accompanies the
addition of the first carbon atom. Subsequent lengthening of the
chain causes less change in this value, and the 2-n-butylbiphenyl
is still 28 percent superior to aviation gasoline with respect to
Btu per cubic foot. On the same basis of comparison, AN-F-32, with
a ratio of 1.12, is 12 percent higher than aviation gasoline.

The effect of the various substituents on the melting and
boiling point is shown in figure 5. The melting point of biphenyl
is 156.6° F. The melting point of the 2-n-alkyl biphenyl hydrocarbons
is lowered by each carbon atom that is added to the chain; 2-n-
butylbiphenyl melts at 7.3° F.

The curve representing the boiling point shows that the addi-
tion of the four-carbon-atom side chain to biphenyl raises the boil-
ing point from 491° to 556° F.

A comparison of the changes in viscosity with respect to chain
length and temperature is presented in figure 6. At 210° F there
is a 45 percent increase in kinematic viscosity from biphenyl to
2-n-butylbiphenyl. At 32° F, where the viscosity of biphenyl can-
not be determined because the compound is a solid, the effect of
the longer chain is more pronounced. The increase in viscosity
from 2-methylbiphenyl to 2-n-butylbiphenyl is 85 percent.

1,1-DICYCLIC ALKANE HYDROCARBONS

The changes in relative heats of combustion for the 1,1-dicyclic
alkanes are shown in figure 7. In the aromatic series the relative
Btu-per-cubic-foot value decreases as the chain is built up to four
carbon atoms in 1,1-diphenylbutane; this compound, however, has a
relative Btu-per-cubic-foot value almost 30 percent higher than
aviation gasoline.

The cyclohexyl compounds are about 6 percent lower in relative Btu-per-cubic-foot values and 8 percent higher in relative Btu-per-pound values than the aromatic series. Hydrogenation appreciably lowers the density, which accounts for the lower values of net heat of combustion per cubic foot even though the net heat on the weight basis is increased. The cyclohexyl compounds average about 25 percent higher in Btu per cubic foot than aviation gasoline; the aromatic compounds average about 32 percent higher in Btu per cubic foot than aviation gasoline.

In the aromatic series of the 1,1-dicyclic alkanes the boiling point is increased from 491° to 564° F by adding four carbon atoms (fig. 8). In the cyclohexyl series the first compound, bicyclohexyl, boils at 462° F and the four-carbon-atom chain raises the boiling point to 559° F. The compounds in the cyclohexyl series boil at lower temperatures than the corresponding aromatic hydrocarbons, but the differences are small when more than one carbon atom has been added in the side chain.

The melting points of the compounds in the aromatic and cyclohexyl series are illustrated in figure 9. The aromatic series shows a spread of 170° F from biphenyl at 156° F to 1,1-diphenylbutane at -14° F. In the cyclohexyl series, bicyclohexyl melts about 120° F below the corresponding aromatic hydrocarbon. The other members of the cyclohexyl series are also lower melting compounds than their aromatic counterparts except 1,1-dicyclohexylbutane, which melts at a temperature 26° F higher than 1,1-dephenylbutane.

The viscosity data for the two series of 1,1-dicyclic alkanes are shown in figure 10. In order to compare the aromatic series at 32°, 100°, and 210° F, it is necessary to start with 1,1-diphenylethane because the biphenyl and diphenylmethane are solids at 32° F. The increase in viscosity from 1,1-diphenylethane to 1,1-diphenylbutane is 35 percent at 210° F, 65 percent at 100° F, and 200 percent at 32° F.

In the cyclohexyl series at 210° F, the individual hydrocarbons have values of kinematic viscosity that are about 50 percent higher than those of the corresponding aromatic compounds. At 100° F the difference averages about 95 percent, and at 32° F the difference is as high as 250 percent in the case of 1,1-dicyclohexylbutane where the combination of the long chain and the two cyclohexyl rings gives the compound the high viscosity of 75.5 centistokes.

α, ω -DICYCLIC ALKANES

Figure 11 shows the relative heats of combustion of the α,ω-dicyclic alkanes, which are so designated because the two rings are at the ends of a straight chain of carbon atoms. In the aromatic series the addition of each carbon atom between the two rings produces a slight decrease in heat of combustion per cubic foot from the high value of biphenyl; 1,3-diphenylpropane, however, has a 29 percent higher heat of combustion than aviation gasoline.

The cyclohexyl derivatives have values about 8 percent higher in relative Btu per pound, but 6 to 9 percent lower in Btu per volume than the aromatic hydrocarbons. The values of net heat of combustion per cubic foot for cyclohexyl derivatives are still about 24 percent higher than gasoline.

The melting points of the α,ω-dicyclic alkane series are shown in figure 12. The aromatic hydrocarbons alternate between high and low melting points, and the last compound, 1,3-diphenylpropane, melts at -5.6° F, which compares favorably with the values of 7.3° F for 2-n-butylbiphenyl and -14° F for 1,1-diphenylbutane.

The cyclohexyl series follows a similar alternate high and low pattern. The melting points of this series are all lower than the corresponding aromatic compounds except 1,3-dicyclohexylpropane, which melts at a temperature 11° F higher than 1,3-diphenylpropane.

The changes in boiling point that are produced by introducing carbon atoms between the two rings are shown in figure 13. The boiling points of the aromatic series increase from 491° to 569° F when three carbon atoms are added, which is a greater increase than that obtained in the 2-n-alkyl biphenyl series and the 1,1-dicyclic alkane series. The boiling points of the cyclohexyl compounds are consistently lower than those of the aromatic hydrocarbons.

The viscosity data of the α,ω-dicyclic alkane series are shown in figure 14. 1,3-diphenylpropane is the only aromatic compound in this series on which measurements could be made at 32° F. At 210° F the viscosity of the aromatic series increases 40 percent from biphenyl to 1,3-diphenylpropane.

In the cyclohexyl series the corresponding transition, bicyclohexyl to 1,3-dicyclohexylpropane, produces an increase of 60 percent in viscosity. As the temperature is lowered, the viscosity increase becomes 110 percent at 100° F and at 32° F, where bicyclohexyl is a solid and cannot be compared, the increase from dicyclohexylmethane to 1,3-dicyclohexylpropane is 90 percent.

SUMMARY

In introducing this discussion it was stated that the chief object of the program was to try to alter the physical properties of certain high melting hydrocarbons by introducing various substituent groups and at the same time to preserve the high net heat of combustion per unit volume. In order to summarize what has been accomplished, the properties of the compounds in the three aromatic series related to biphenyl have been plotted on the same set of coordinates so that they may be compared more easily in figure 15.

The parent hydrocarbon, biphenyl, melts at 156° F. The derivative, 1,1-diphenlybutane, has the lowest melting point (-14° F), which is 170° F lower than the melting point of biphenyl. It is known that at some point in the process of lengthening the side chain the melting point curve will start to rise, but it is not established that this point has been reached in any of these series at this time. Perhaps some of the compounds which would be obtained by further addition of carbon atoms to the side chains would have lower melting points than any given herein.

The loss in relative Btu per cubic foot from biphenyl to 1,1-diphenylbutane is only about 4 percent, which is still almost 30 percent above the Btu-per-cubic-foot value for aviation gasoline. It is reasonable to accept a small additional loss in this value if the melting point can be lowered by adding one or two more carbon atoms. The melting points of these hydrocarbons are too high because the present maximum requirement for the melting point of jet fuel is -76° F (reference 5).

In figure 16, the viscosity changes produced by these structural alterations are illustrated. The viscosity of 1,1-diphenylbutane is high, and the other low melting hydrocarbons fall in the same range so that the work is not complete with respect to this property.

The series that have been discussed will be extended by lengthening the side chains, and the synthesis of the other series that were outlined in the introduction are in progress. The data on all the physical properties will be analyzed and the compounds which are selected as the most promising will be evaluated with respect to the combustion characteristics.

REFERENCES

1. Anon.: Selected Values of Properties of Hydrocarbons. Circular C461, Nat. Bur. Standards, Nov. 1947.

2. Doss, M. P.: Physical Constants of the Principal Hydrocarbons.
   The Texas Co., 4th ed., 1943.

3. Egloff, Gustav: Physical Constants of Hydrocarbons. Vols. I,
   II, and III. Reinhold Pub. Corp., 1946.

4. Wise, Paul H., Serijan, Kasper T., and Goodman, Irving A.:
   Physical Properties of Substituted Dicyclic Hydrocarbons.
   NACA TN (to be pub.).

5. Army-Navy Aeronautical Specification Fuel; Aircraft Turbine and
   Jet Engine; AN-F-58, Dec. 12, 1947.

6. Army-Navy Aeronautical Specification Fuel; Aircraft Reciprocating
   Engine; AN-F-48, Oct. 21, 1946.

VARIATION OF HEAT OF COMBUSTION WITH BOILING POINT
OF HYDROCARBONS.

Figure 1.

BENZENE WITH BRANCHED SIDE CHAIN
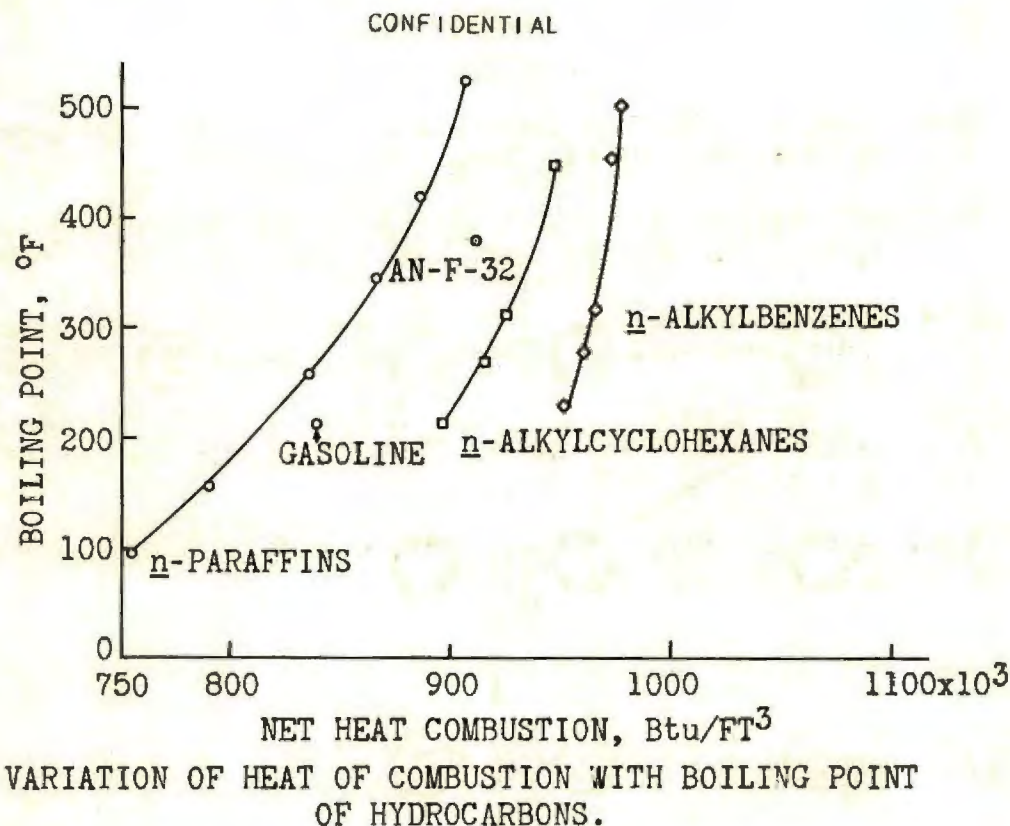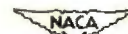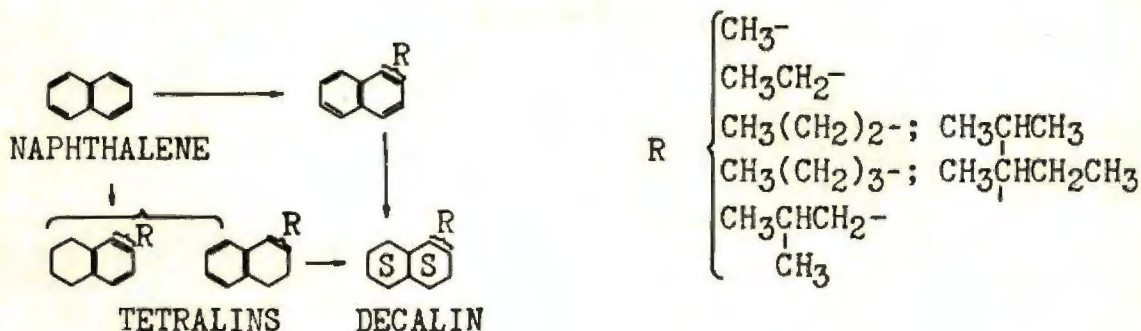
OUTLINE OF HYDROCARBONS INVESTIGATED - I

Figure 2.
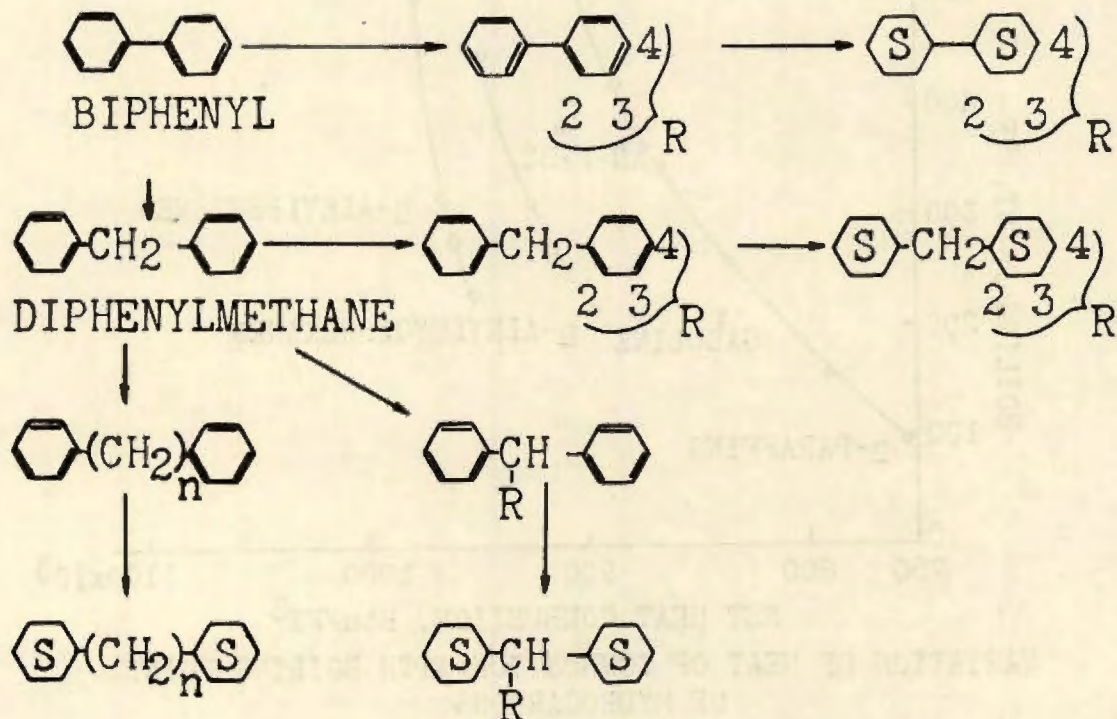
OUTLINE OF HYDROCARBONS INVESTIGATED - II

Figure 3.
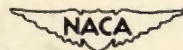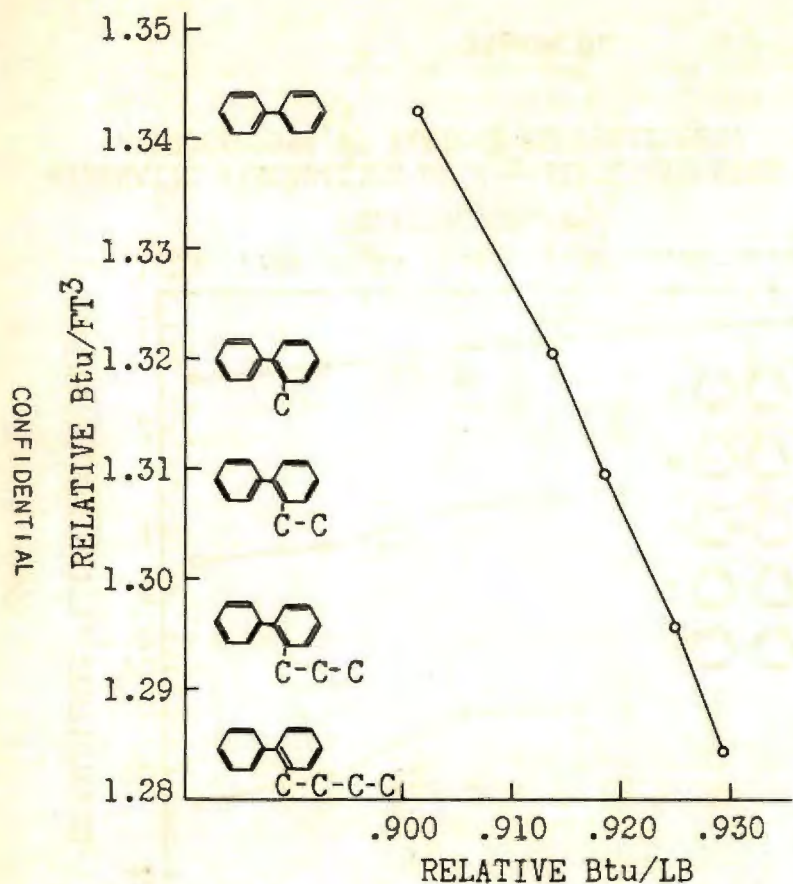
COMPARISON OF STRUCTURE AND NET HEAT OF
COMBUSTION OF 2-n-ALKYL BIPHENYL HYDRO-
CARBONS

Figure 4.
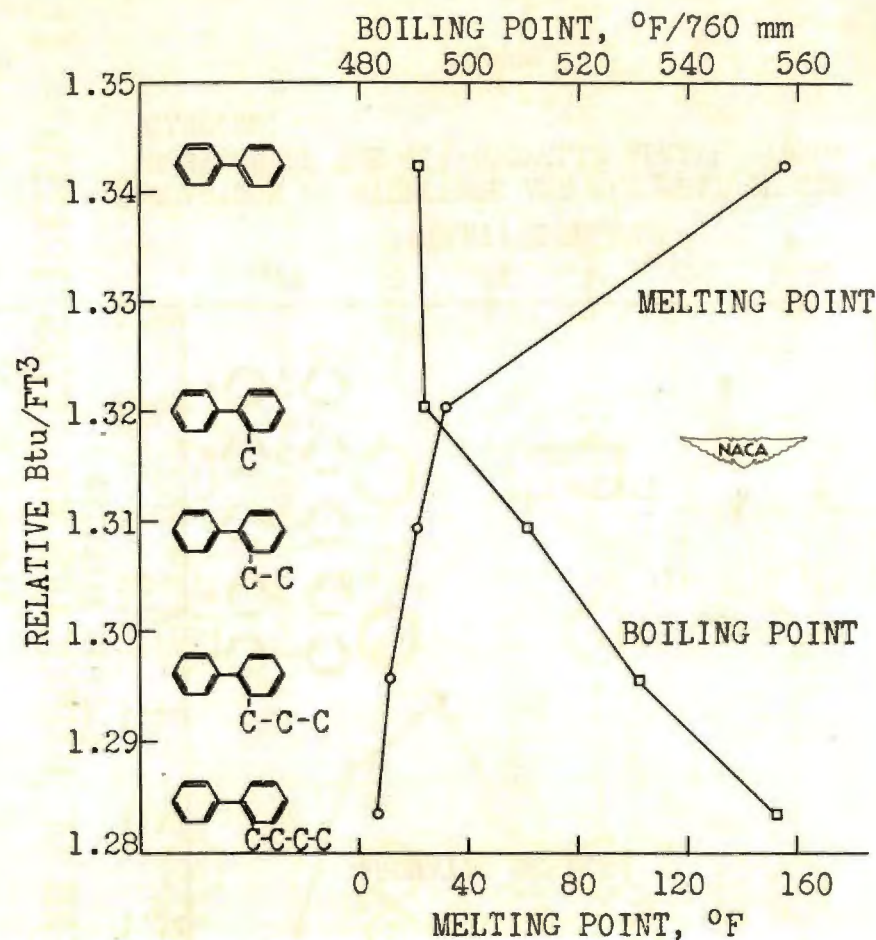
MELTING AND BOILING POINTS OF THE 2-n-ALKYL
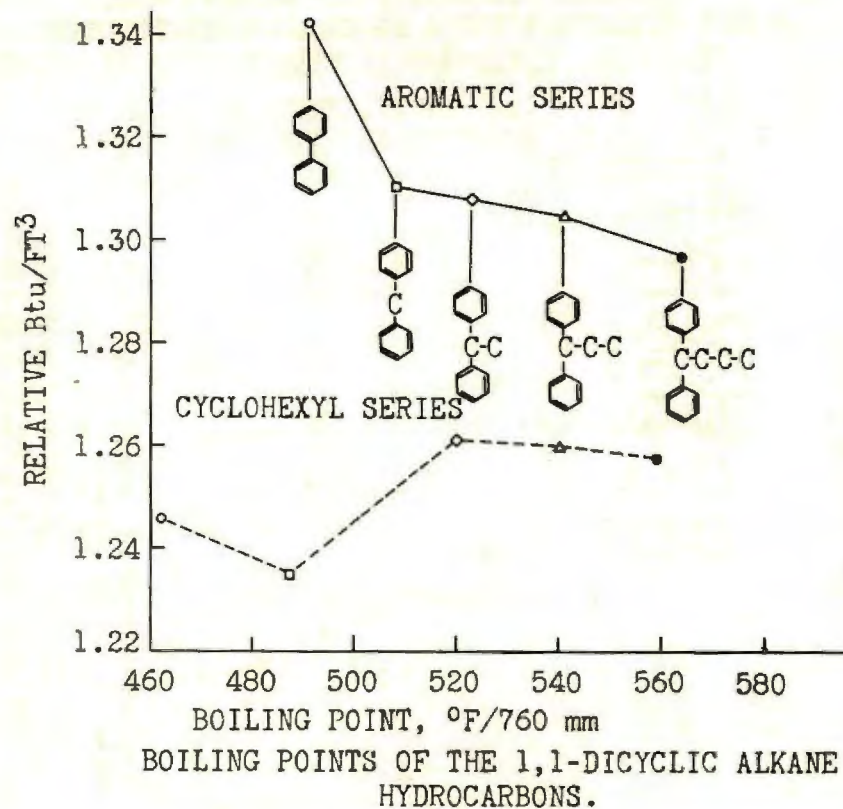BIPHENYL HYDROCARBONS

Figure 5.

KINEMATIC VISCOSITIES OF 2-n-ALKYL BIPHENYL
HYDROCARBONS AT VARIOUS TEMPERATURES.

Figure 6.

COMPARISON OF STRUCTURE AND NET HEAT OF COM-
BUSTION OF THE 1,1-DICYCLIC ALKANE HYDRO-
CARBONS.

Figure 7.

986-C

BOILING POINTS OF THE 1,1-DICYCLIC ALKANE
HYDROCARBONS.

Figure 8.

MELTING POINTS OF THE 1,1-DICYCLIC ALKANE
HYDROCARBONS

Figure 9.

KINEMATIC VISCOSITIES OF THE 1,1-DICYCLIC ALKANE
HYDROCARBONS AT VARIOUS TEMPERATURES.
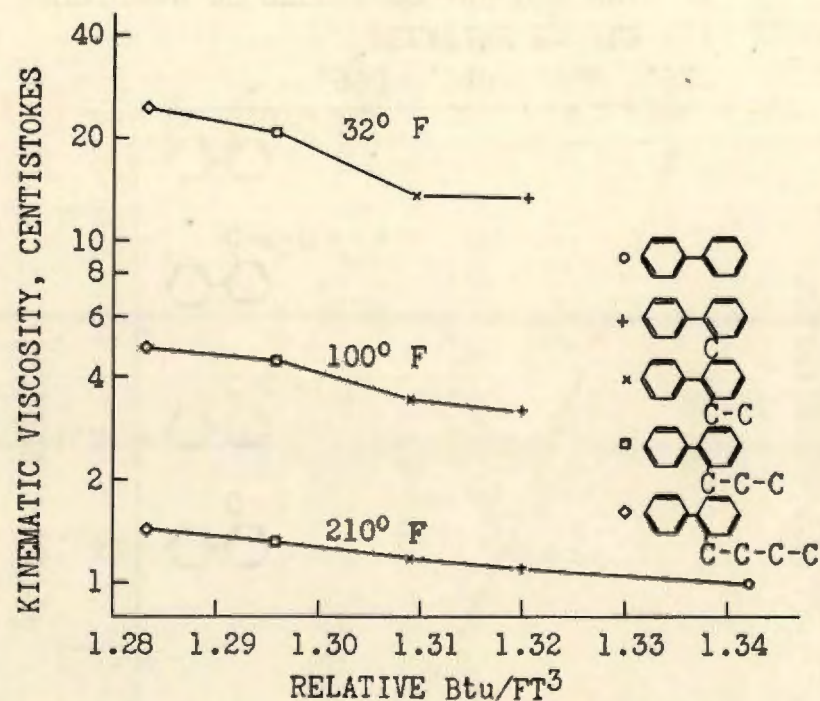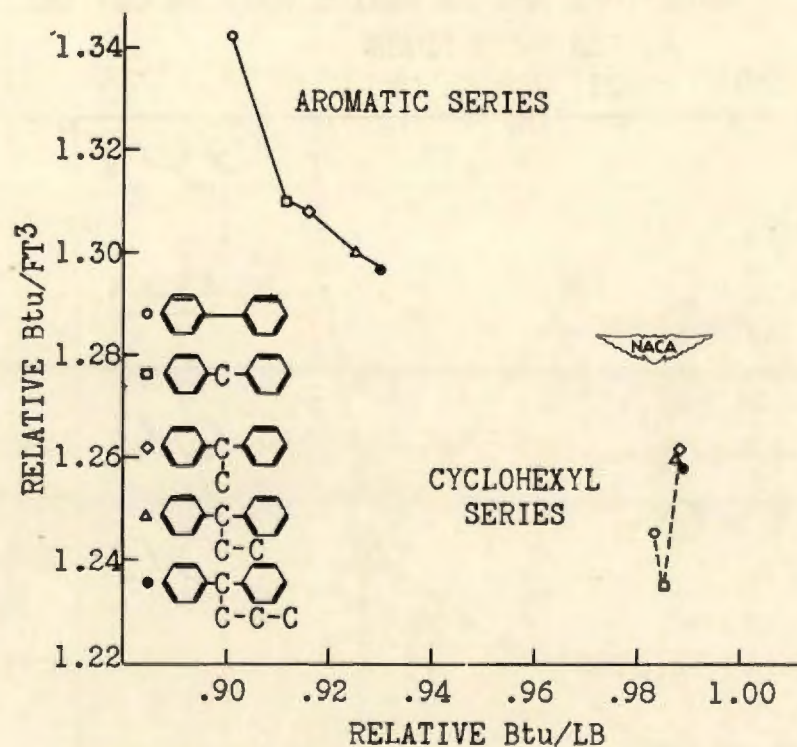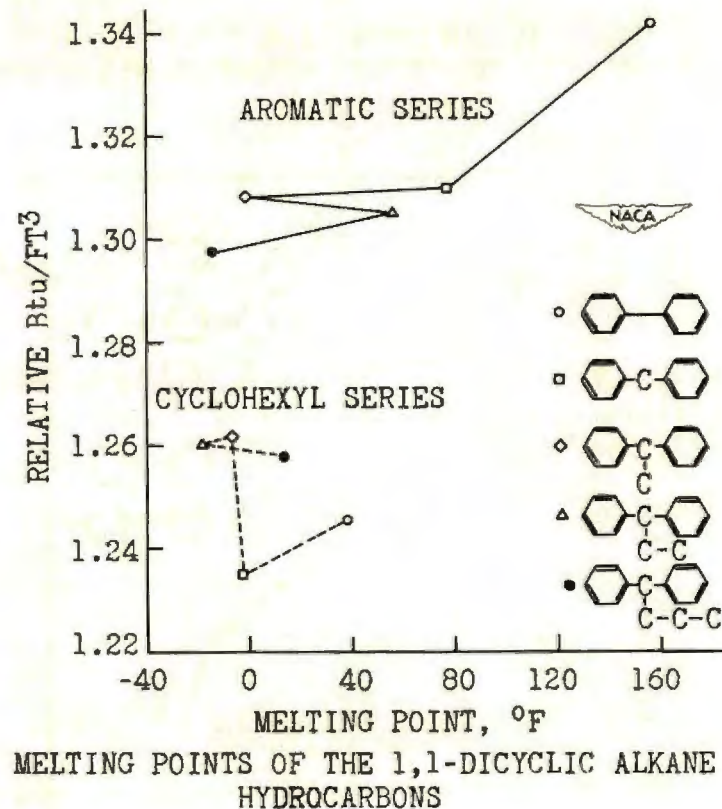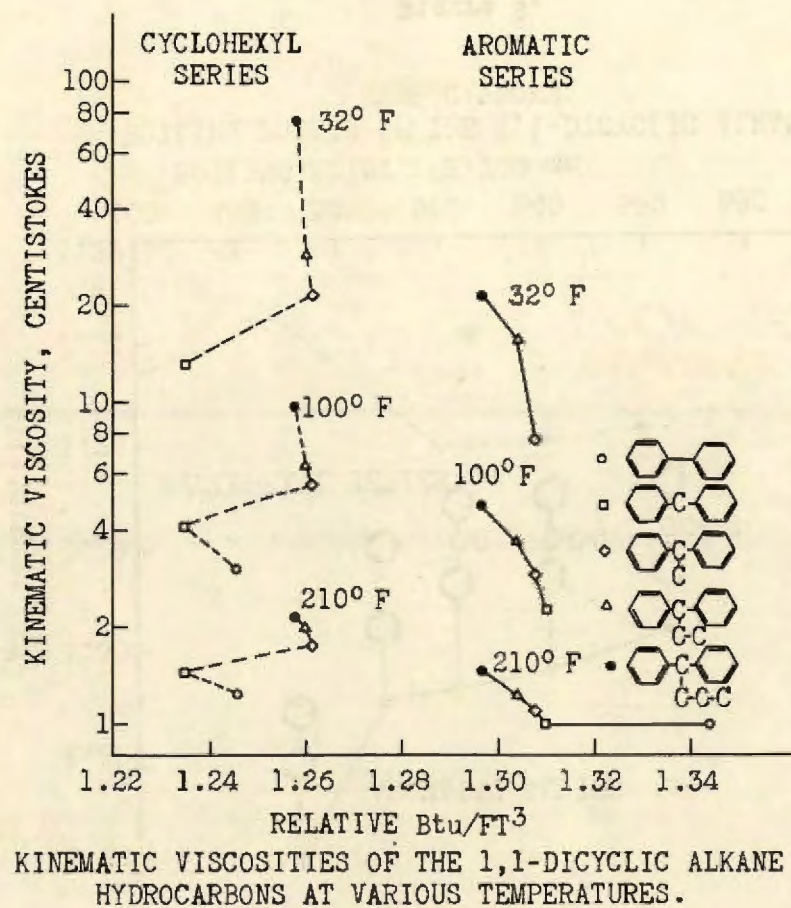
Figure 10.

COMPARISON OF STRUCTURE AND NET HEAT OF COM-
BUSTION OF THE α, ω-DICYCLIC ALKANE HYDRO-
CARBONS.

Figure 11.
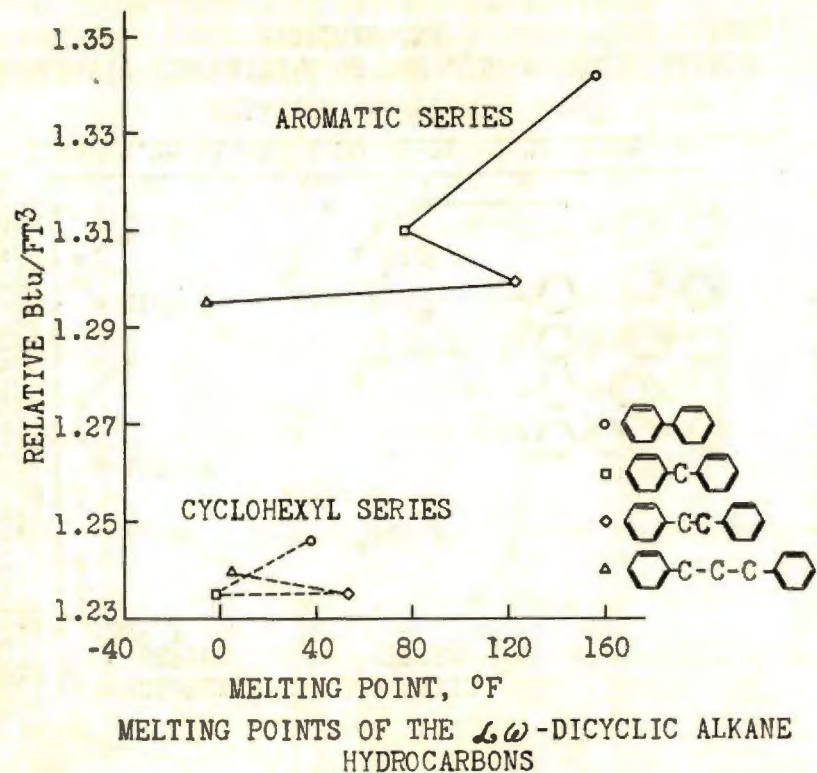
MELTING POINTS OF THE $\mathcal{L}\omega$-DICYCLIC ALKANE
HYDROCARBONS

Figure 12.

BOILING POINTS OF THE $\mathcal{L},\omega$-DICYCLIC ALKANE
HYDROCARBONS

Figure 13.

KINEMATIC VISCOSITIES OF THE $\angle, \omega$-DICYCLIC ALKANE
HYDROCARBONS

Figure 14.

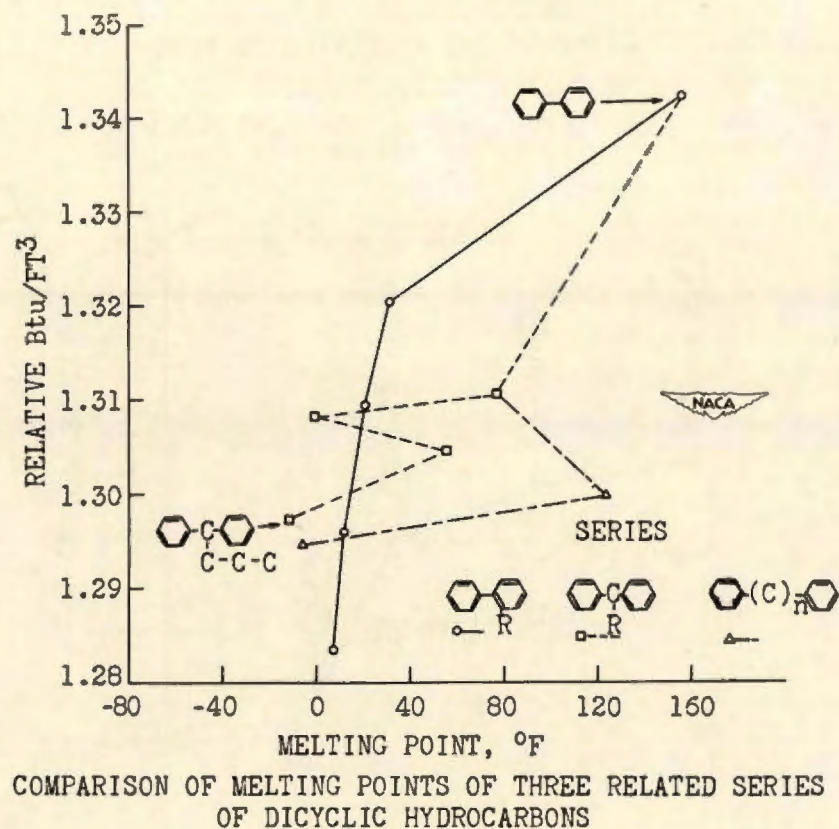COMPARISON OF MELTING POINTS OF THREE RELATED SERIES
OF DICYCLIC HYDROCARBONS

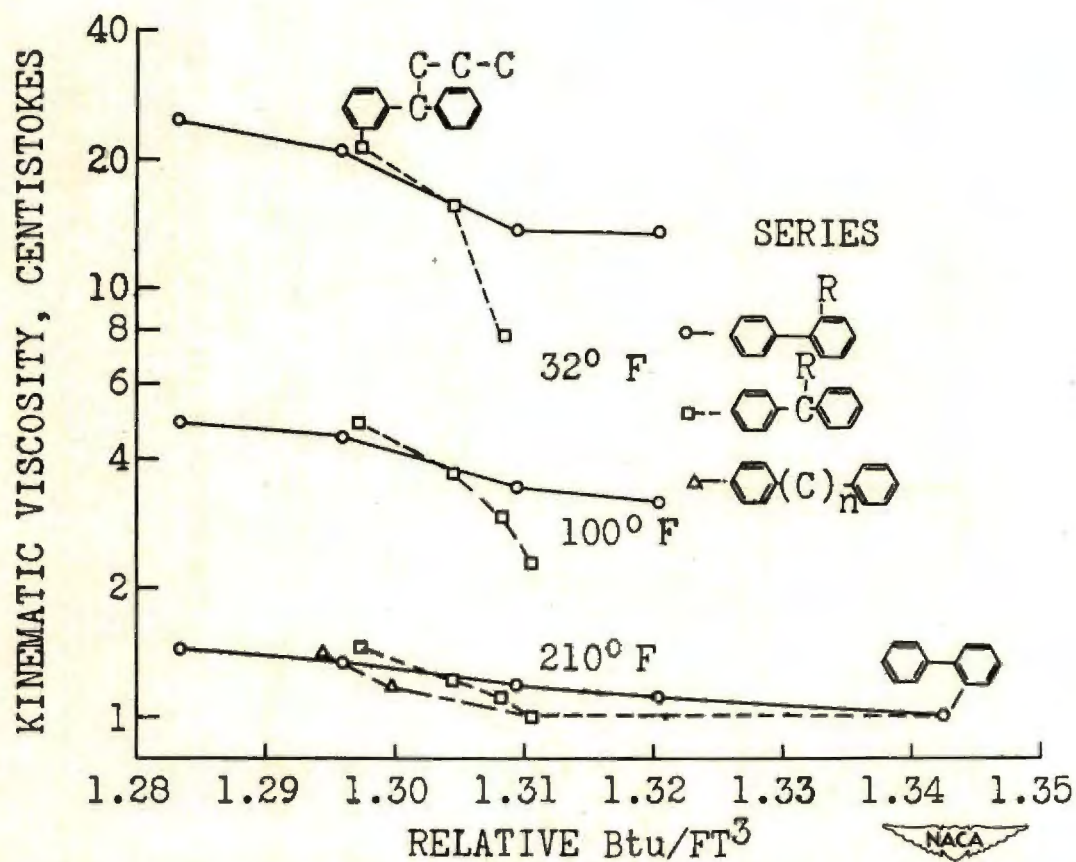**Figure 15.**

986-C
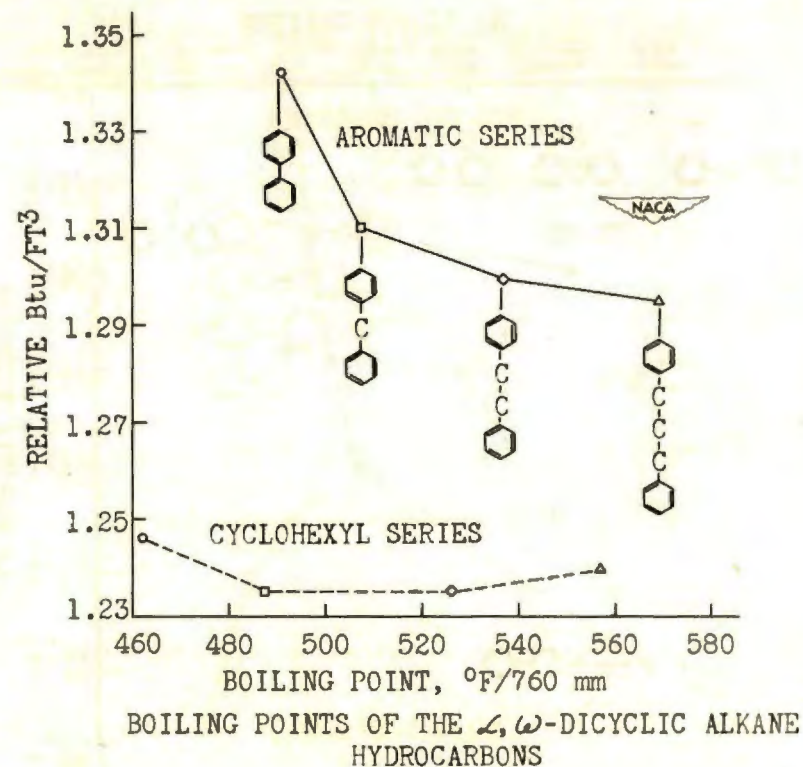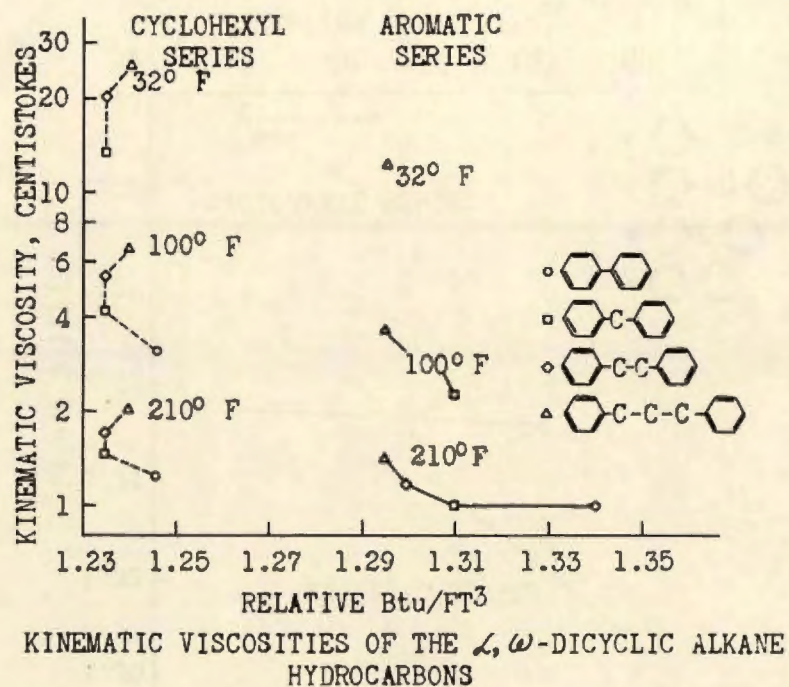
COMPARISON OF KINEMATIC VISCOSITIES OF THREE RELATED
SERIES OF DICYCLIC AROMATIC HYDROCARBONS

Figure 16.

EFFECT OF FUEL INJECTION CONDITIONS AND FUEL PROPERTIES

ON PERFORMANCE IN GAS-TURBINE COMBUSTORS

By Edmund R. Jonash

Flight Propulsion Research Laboratory

INTRODUCTION

Fuel research for jet-propulsion engine combustors involves not only careful control of the composition of the fuels being investigated, but also careful consideration of the various components of the combustor itself. It has been found that small changes in the combustor liner, air entry ports, or the fuel injection system can alter the performance, and, in some cases, even the relative performance of different fuels.

One component that is closely related to fuel studies and that influences, to a large extent, the performance of the combustor is the fuel nozzle. The function of the nozzle is to deliver the fuel to the combustor in a fine spray form, which is most conducive to rapid combustion. The combustion efficiency and flame blow-out depend to a large extent upon the fineness of this spray, its penetration, and its location. The fineness of the spray and its penetration are functions of the pressure drop across the nozzle. Figure 1 illustrates the effect of this pressure drop on the combustion efficiency of a turbojet combustor operated with standard-type constant-area fuel nozzles (reference 1). These data were obtained with an annular-type combustor operating at an inlet-air pressure of 9.2 pounds per square inch absolute, a velocity of 200 feet per second, and a temperature of 90° F. The two fuels investigated were AN-F-28 and Diesel fuel. Each curve (fig. 1) represents a test run with a different size fuel nozzle; the nominal volume rating of the nozzles in gallons per hour is indicated by the figures at the end of each curve. By successively changing the size of the nozzle, it was possible to operate the combustor over a range of injection pressures for each fuel flow rate.

From the results of this investigation, it is seen that, in general, at low heat input values the smaller nozzles produced the higher efficiencies; whereas at the higher heat inputs the larger nozzles gave the higher efficiencies, and, in the case of Diesel fuel, allowed burning at higher heat input conditions without flame blow-out. Flame blow-out is indicated by the perpendicular lines at the end of each curve.

The same data is plotted as combustion efficiency against fuel
nozzle pressure differential (fig. 2) with each curve representing
constant values of heat input. At low values of heat input, the
combustion efficiency of both fuels increased with fuel injection
pressure; whereas at higher values of heat input, the combustion
efficiency decreased with an increase in injection pressure.

APPARATUS

Inasmuch as it appeared desirable to control the fuel injec-
tion pressure with a single nozzle installation, the NACA-designed
nozzle shown in figure 3 was tested. A plunger, mounted on a
central shaft that is positioned by a spring and bellows, provides
valve action on a number of tangential holes of varying size. Fuel
enters at the top, flows through the nozzle body, through the
tangential holes which produce a swirling body of fuel, and out
the nozzle orifice in a fine, hollow-cone spray. The pressure of
the fuel on the bellows determines the plunger position required
for a certain fuel pressure differential. Sufficient tangential-
hole area is exposed to maintain this given pressure. By pre-
loading the plunger with a variable nitrogen pressure behind the
bellows, any desired pressure drop across the tangential holes
could be maintained at any flow rate within the design range.
This nozzle is completely described in reference 2.

A single combustor from a J33 turbojet engine was set up as
shown in figure 4. Air flow direction is from right to left.
Refrigerated air was passed through an A.S.M.E. orifice to meter
flow rates, through regulating valves to control flow quantities
and pressures, and passed into the combustor. The inlet-air tem-
perature, as measured by a single iron-constantan thermocouple,
was maintained by means of electrical preheaters. Fuel entered
the combustor through the single nozzle at the position shown in
figure 4 and burned in the inner liner of the combustor. Com-
bustor outlet temperatures were measured with several chromel-
alumel thermocouples.

FUEL-NOZZLE INVESTIGATION

The single combustor was operated at an inlet-air pressure of
7 pounds per square inch absolute, an inlet-air temperature of
40° F, and with air-flow rates from 0.61 to 1.05 pounds per sec-
ond. The combustion efficiency of one fuel, isooctane, was deter-
mined over a range of fuel injection pressure differentials at

constant values of fuel-air ratio with the NACA-designed nozzle. The results are shown in figure 5. Isooctane was investigated at air-flow rates of 0.61, 0.75, and 1.05 pounds per second. Contrary to what was expected from previous investigations, the combustion efficiency at constant fuel-air ratios remained substantially constant over a wide range of fuel injection pressure differentials. At high values of injection pressure differential, the combustion efficiency of isooctane tended to decrease with further increases in pressure differential.

In order to further investigate the effect of the fuel injection pressure differential on the combustion efficiency, two additional fuels, n-heptane and diisopropylbenzene, were tested. Figure 6 shows the results with n-heptane, where similar general trends were noted at air-flow rates of 0.61 and 0.85 pound per second. At the higher air-flow rate, a slight decrease in combustion efficiency with increase in pressure was noted. Figure 7 shows the same general trends with diisopropylbenzene, a high-boiling-temperature aromatic fuel. It is noted that the combustion efficiency is affected only at high fuel injection pressure differentials.

From these data it was concluded that a combustor operated with the fuel nozzle having a variable-tangential-hole-area mechanism was insensitive to a wide range of injection pressures (from 20 to 160 lb/sq in.) and results of fuel tests conducted at only one pressure would be indicative of the results to be expected at any fuel injection pressure within the range investigated.

FUEL INVESTIGATIONS

Previous investigations of the effect of fuel properties on the performance of turbojet combustors have, in general, indicated two results: (1) volatility of the fuel affects the combustion efficiency performance with low-boiling-temperature fuels showing higher combustion efficiency performance than high-boiling-temperature fuels, and (2) hydrocarbon structure affects performance to a smaller degree with paraffinic fuels showing somewhat higher combustion efficiencies than aromatic fuels.

These investigations, however, were conducted with constant-area fuel nozzles with the fuel nozzle pressure differential being dependent upon the type of fuel and upon the fuel flow rate. A study was therefore conducted to determine the effects of hydrocarbon structure and volatility on the combustion efficiency

performance of a combustor operated with a constant-pressure-
differential fuel nozzle. The combustor assembly and nozzle pre-
viously described were operated with the fuels shown in the
following table:

FUEL PROPERTIES

Fuel type	Fuel	A.S.T.M. distillation			Specific gravity	Lower heating value (Btu/lb)	H/C
		ibp	fbp	50%			
Paraffinic	n-Hexane	151	156	153	0.668	19,230	0.196
	2,3-Dimethyl-butane	134	136	135	0.666	19,200	0.196
	n-Heptane	202	206	206	0.688	19,150	0.192
	Isooctane	204	206	206	0.695	19,070	0.189
	n-Octane	250	254	252	0.712	19,100	0.189
	Diesel fuel	480	574	508	0.799	18,760	0.171
Aromatic	Benzene	172	176	173	0.877	17,260	0.084
	Diisopropyl-benzene	380	398	392	0.876	17,840	0.118

The paraffinic fuels are listed first, with five low-boiling-
temperature and one high-boiling-temperature fuel, and two
aromatic fuels, one low-boiling-temperature and one high-boiling-
temperature fuel. Tests with the diisopropylbenzene were
restricted to the nozzle pressure investigation because of the
high carbon-forming tendencies of the fuel. The Diesel fuel
tested was a high grade cetane-type paraffin. The A.S.T.M.
distillation data, the specific gravity, hydrogen-carbon ratio,
and the net heat of combustion are listed.

The fuel nozzle pressure drop for the tests was maintained at
25 pounds per square inch, the inlet-air pressure at 7 pounds per
square inch absolute, and the inlet-air temperature at 40° F. The
fuel flow rate was adjusted to maintain a constant feed of 376 Btu
per pound of air to the combustor while the mass rate of air flow
was gradually increased to points at which either flame blow-out
occurred or the combustor outlet temperatures decreased to values
considerably below normal operating temperatures of combustors.

The combustion efficiency of each of the pure fuels investi-
gated in relation to the mass air-flow rates is presented in

figure 8. Each fuel is represented by a different symbol and the
A.S.T.M. 50-percent distillation temperature of each fuel is noted
at the end of each curve. All fuels show a decrease in combustion
efficiency with increase mass air flow. This decrease, however,
was not the same for all the fuels tested; the fuels tend to show
greater differences in performance at the higher air-flow rates.
n-Octane and n-heptane burned with the highest combustion effi-
ciencies throughout the air-flow range investigated. Benzene, the
one aromatic fuel tested under these conditions, burned with effi-
ciencies slightly below n-octane and n-heptane. The combustion
efficiency of n-hexane, which has a 50-percent distillation tem-
perature of 153° F, was as low as Diesel fuel, which has a
50-percent distillation temperature of 508° F. Both fuels are of
the same hydrocarbon type. The normal-chain hydrocarbons,
n-octane and n-hexane, show higher combustion efficiencies than
do their branched-chain isomers, isooctane and 2,3-dimethylbutane.
The two conclusions that can be drawn from the results presented
in figure 8 are: (1) straight-chain paraffins burn with higher
combustion efficiencies than do branched-chain paraffins, and
(2) the effect of fuel volatility on combustion efficiency is not
as well defined as has been concluded from previous investigations.

The relation between combustion efficiency and the boiling
temperature of the fuels is shown in figure 9. Combustion effi-
ciency is plotted against the A.S.T.M. 50-percent distillation
temperature. Each curve represents a different mass air-flow
rate investigated. The straight-chain hydrocarbons are indicated
by the solid curves, and the branched-chain hydrocarbons by the
broken curves. Above a boiling temperature of about 200° F, the
combustion efficiency of the normal hydrocarbons decreased with
an increase in boiling temperature. In the low-boiling-temperature
range, n-hexane, which has a boiling temperature of 153° F, shows
lower combustion efficiencies than the higher-boiling-temperature
fuels, n-heptane and n-octane. This effect was also noted with
the two branched-chain paraffins, 2,3-dimethylbutane and isooctane.

FUEL-BLENDING INVESTIGATION

The effects of blending a low-boiling-temperature fuel with
a high-boiling-temperature fuel, both fuels being of the same
hydrocarbon type, are indicated in figure 10. The top curve shown
is n-octane, with eight carbon atoms, and the bottom curve, Diesel
fuel, with an average of 16 carbon atoms. The blend tested con-
tained 50-percent (by weight) n-octane and 50-percent (by weight)

Diesel fuel. Above a mass air-flow rate of 0.90 pound per second, the blend curve is between the pure component curves as would be expected. The combustion efficiency of the blend, however, decreased less with increase in air-flow rate than did either of the pure components and, at low air-flow rates, was equal to or lower than either of the pure components.

In order to further investigate the differences in combustion efficiency of straight-chain hydrocarbons and branched-chain hydrocarbons, a 50-percent (by weight) n-hexane and 50-percent (by weight) 2,3-dimethylbutane blend was prepared and tested at the conditions previously noted. Figure 11 presents the performance of two pure fuels and the 50-50 blend with combustion efficiency again plotted against mass air-flow rate. These fuels have an identical number of carbon atoms but vary in structure and boiling temperature as shown in figure 11. Again the combustion efficiency of the blend is between the two pure components at the higher air-flow rates, above about 0.75 pound per second. At lower air-flow rates, however, the combustion efficiency of the blend was equal to or lower than either of the pure components.

Isooctane and n-heptane are two paraffinic fuels that have identical boiling temperatures of 206° F and, hence, vary only in hydrocarbon structure. Several blends of these two fuels were prepared and retested under inlet-air conditions of 7 pounds per square inch absolute pressure and 40° F temperature over a range of mass air-flow rates. Fuel flow rate was again adjusted to feed 376 Btu per pound of air to the combustor. Reference tests with isooctane followed each blend test and the combustion efficiency of the blend was related to the isooctane reference test by the ratio shown as the ordinate on figure 12. The ratio of the combustion efficiency of the test fuel, or blend, to the combustion efficiency of isooctane is plotted against mass air-flow rate for each of the blends. The composition of each blend tested is shown at the end of each curve. The structures of the two pure components are also shown. The abscissa line, a ratio of 1.00, represents the performance of isooctane; all the blends show improved performance throughout the air-flow range. Again the greater differences in the performance of the fuels are noted at the higher air-flow rates with the pure n-heptane having a combustion efficiency about 25 percent higher than isooctane at the highest air-flow rate investigated.

The blending performance of the two fuels, n-heptane and isooctane, is indicated by a plot of the combustion efficiency ratio against the percent n-heptane in the isooctane blend for

several mass air-flow rates (fig. 13). It appears that percentages of n-heptane in an isooctane blend increased the combustion efficiency more than would be predicted from a straight-line blend relation. This is especially true at the higher air-flow rates. At the lower air-flow rates, the relation appears to approach a straight line, although the differences in the fuels at these conditions are quite small.

SUMMARY

In summary, these preliminary data have indicated several results:

1. In a J33 combustor operated with the NACA variable-area fuel nozzle, the fuel injection pressure differential affects combustion efficiency only slightly at the high altitude conditions investigated. The fuel pressure differential range investigated was from 20 to 160 pounds per square inch.

2. Differences in the combustion efficiency of fuels were more pronounced at high mass air-flow rates than at low mass air-flow rates.

3. Above a fuel boiling temperature of about 200° F, combustion efficiency decreased with further increases in boiling temperature, and below 200° F, combustion efficiency decreased with a decrease in boiling temperature.

4. In addition to the effects of fuel boiling temperature, differences in hydrocarbon structure can affect the combustion efficiency of a jet-engine combustor at some conditions: straight-chain hydrocarbons showed higher combustion efficiencies than branched-chain isomers.

5. Tests with blends of n-heptane and isooctane indicated a blending performance other than simple, straight-line relations.

REFERENCES

1. McCafferty, Richard J.: Effect of Fuels and Fuel-Nozzle Characteristics on Performance of an Annular Combustor at Simulated Altitude Conditions. NACA RM No. E8C02a (to be pub.).

2. Gold, Harold, and Straight, David M.: Gas-Turbine-Engine Operation with Variable-Area Fuel Nozzles. NACA RM No. E8D14, 1948.
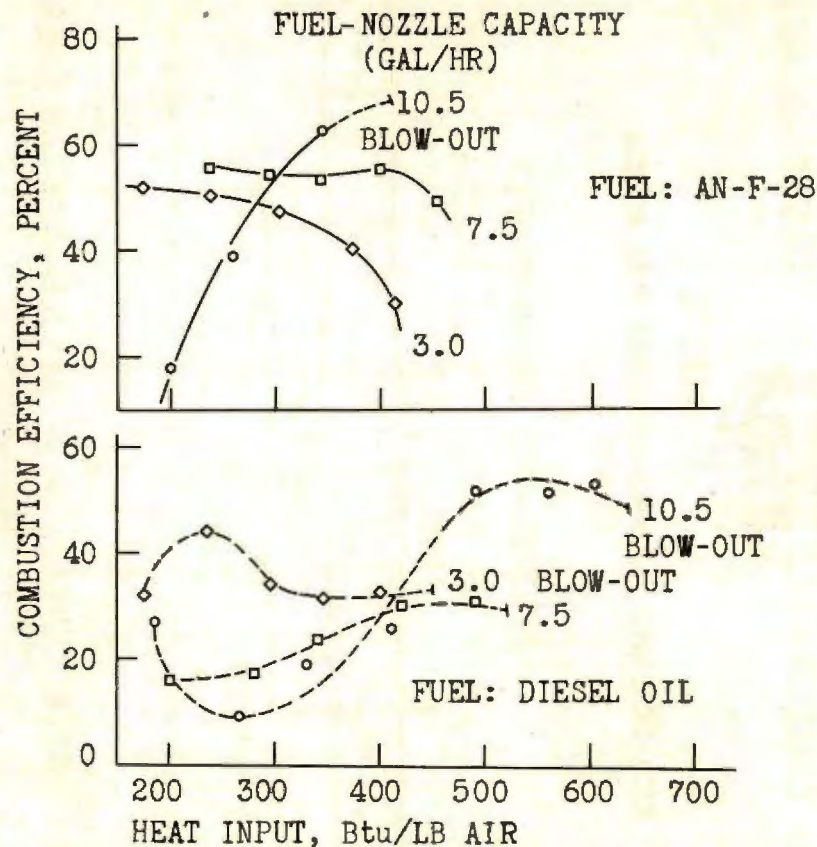
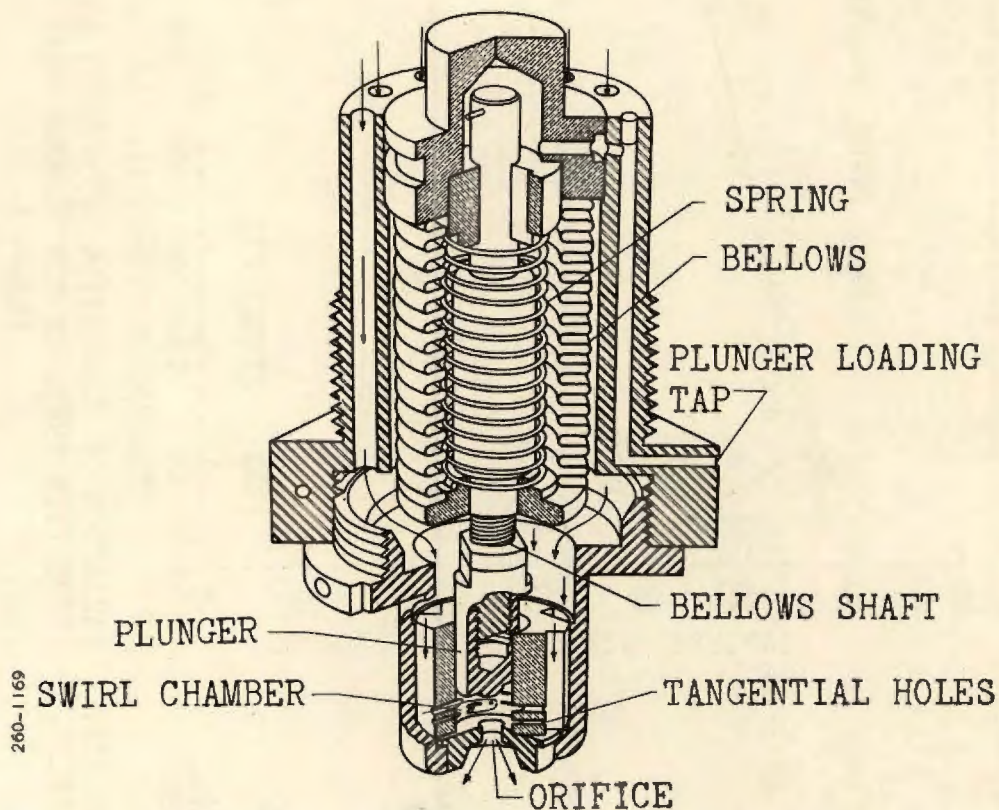VARIATION OF COMBUSTION EFFICIENCY WITH HEAT
INPUT FOR DIFFERENT CAPACITY FUEL NOZZLES.

Figure 1.
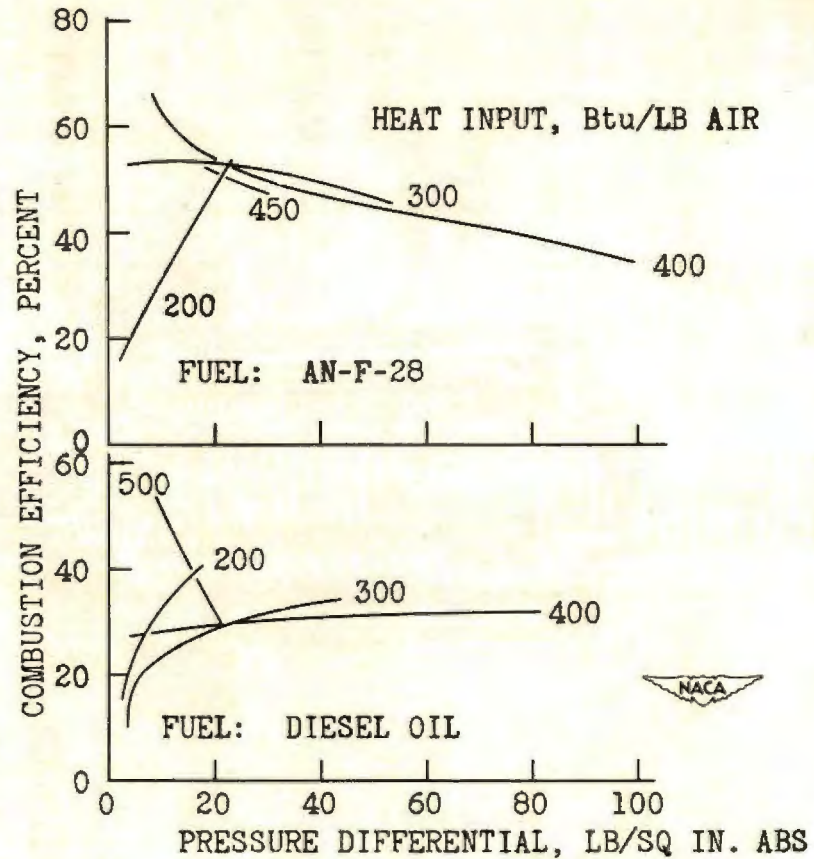
VARIATION OF COMBUSTION EFFICIENCY WITH FUEL
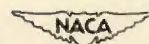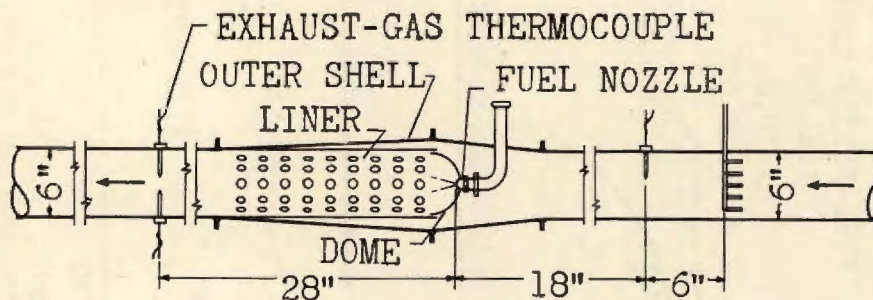INJECTION PRESSURE FOR SEVERAL HEAT INPUTS.

Figure 2.

NACA-DESIGNED VARIABLE-PRESSURE FUEL NOZZLE.
Figure 3.

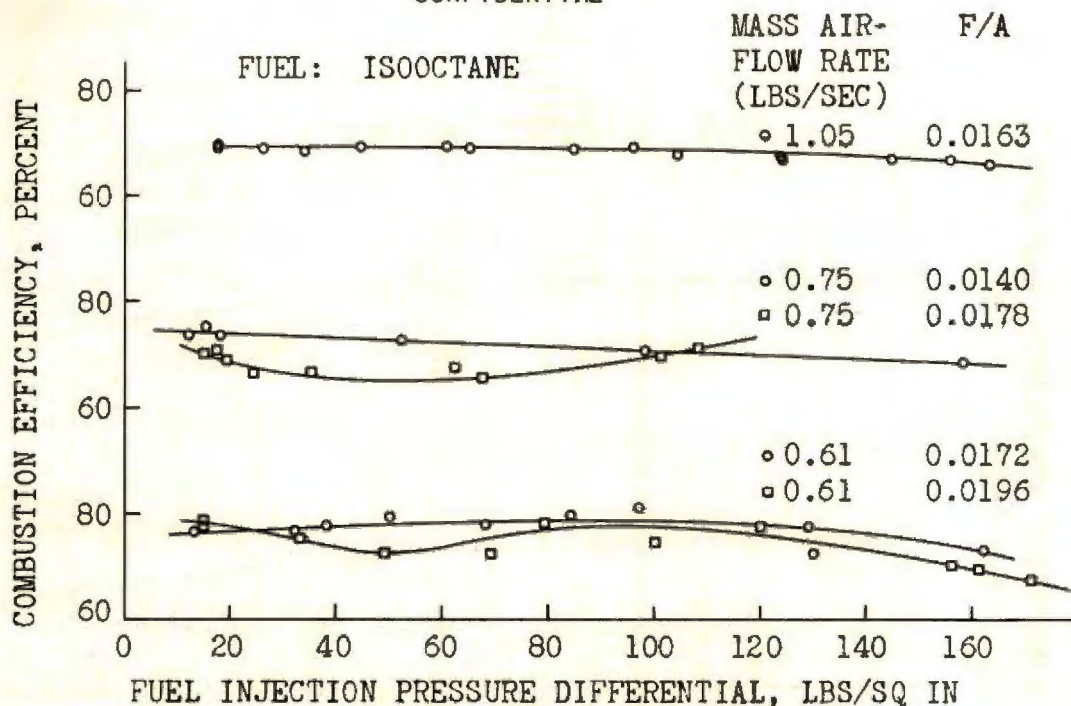
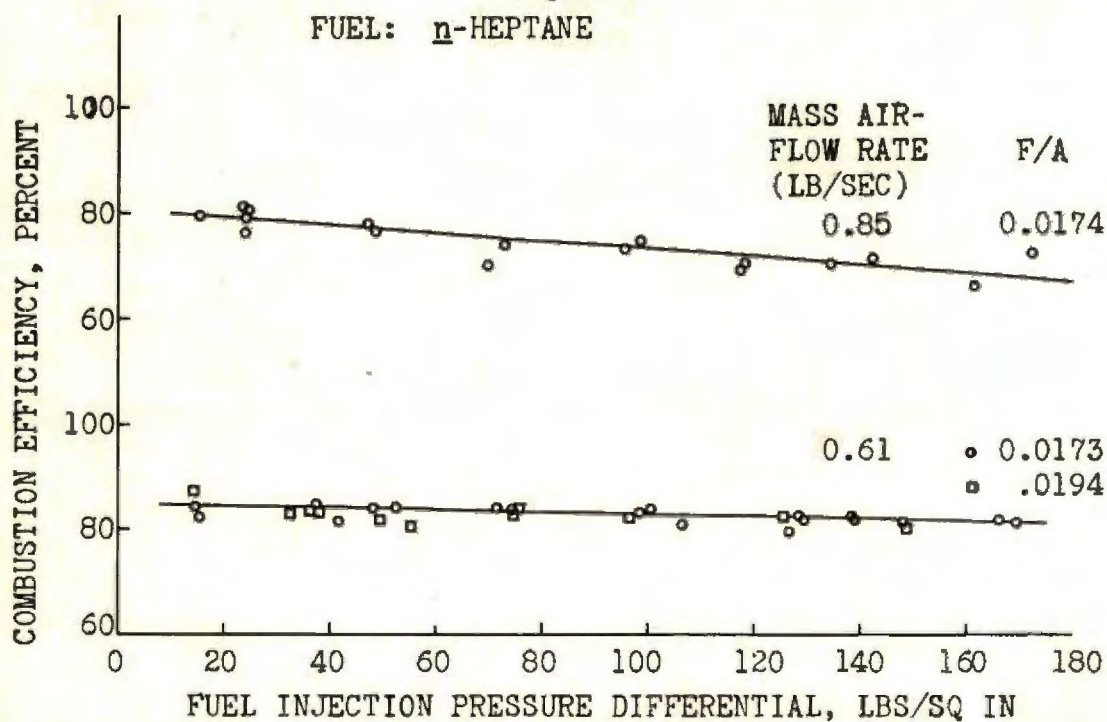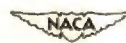
DUCTING AND INSTRUMENTATION OF SINGLE TUBULAR COMBUSTOR

Figure 4.

986-D

EFFECT OF PRESSURE DIFFERENTIAL OF NACA NOZZLE ON COMBUSTION
EFFICIENCY

Figure 5.

EFFECT OF PRESSURE DIFFERENTIAL OF NACA NOZZLE ON COMBUSTION
EFFICIENCY

Figure 6.

EFFECT OF PRESSURE DIFFERENTIAL OF NACA NOZZLE ON COMBUSTION
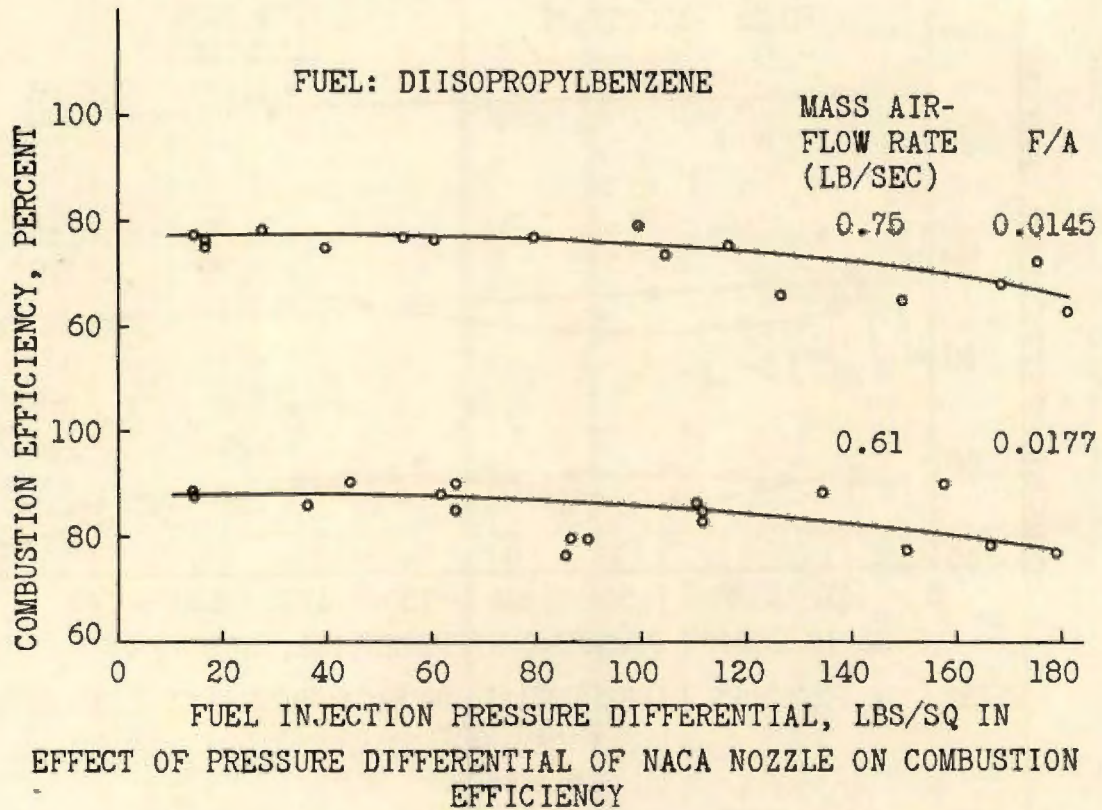EFFICIENCY
Figure 7.

CONFIDENTIAL

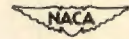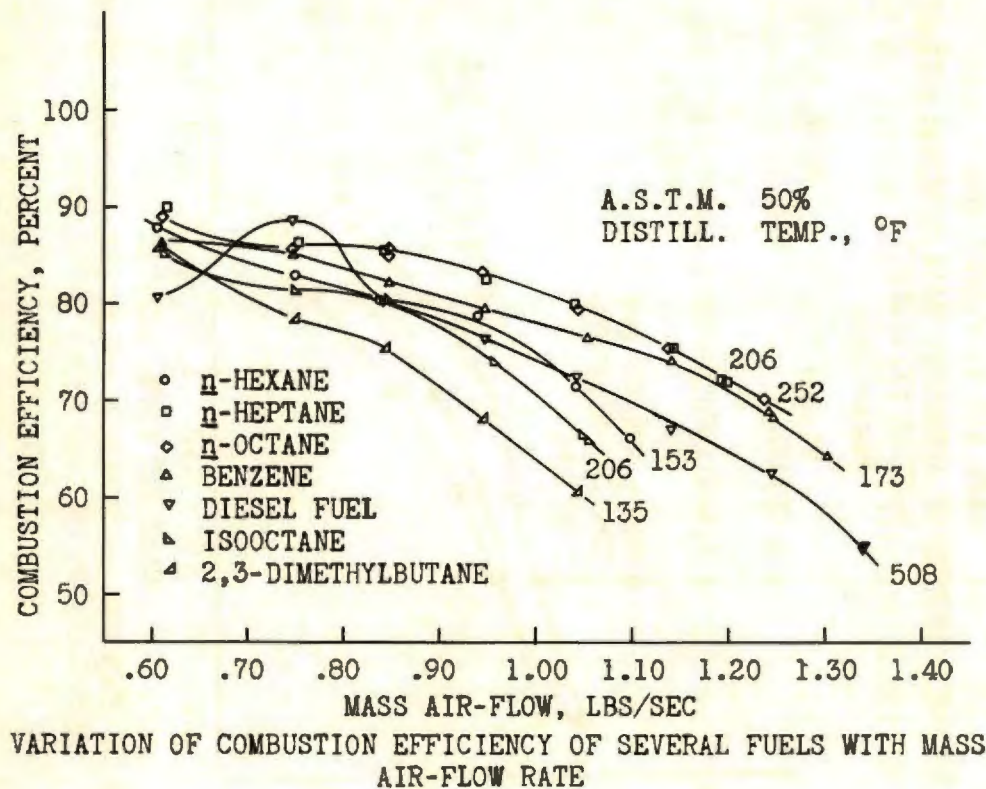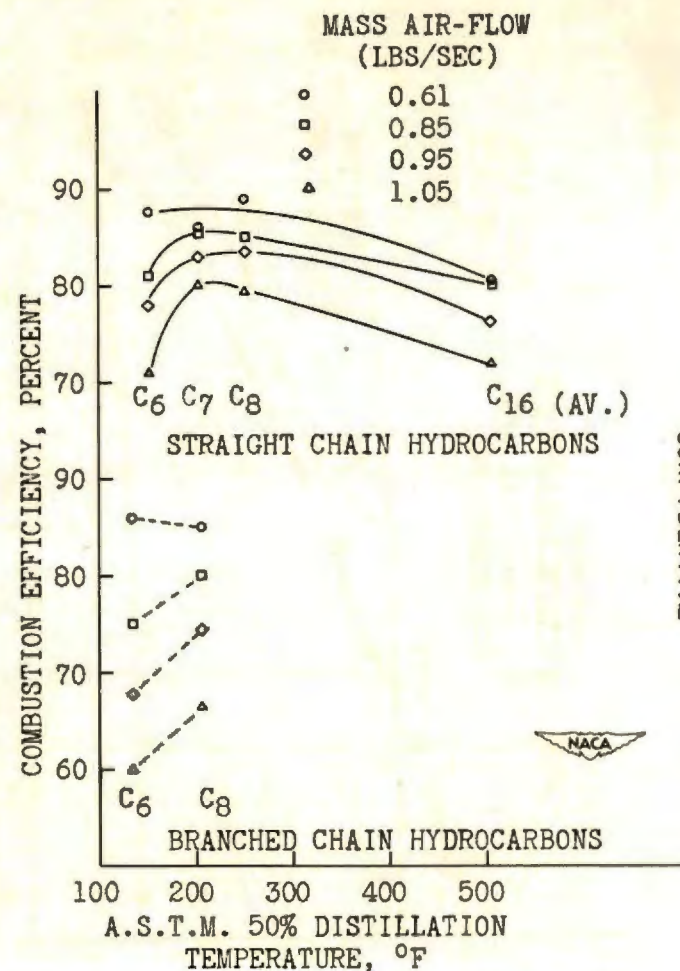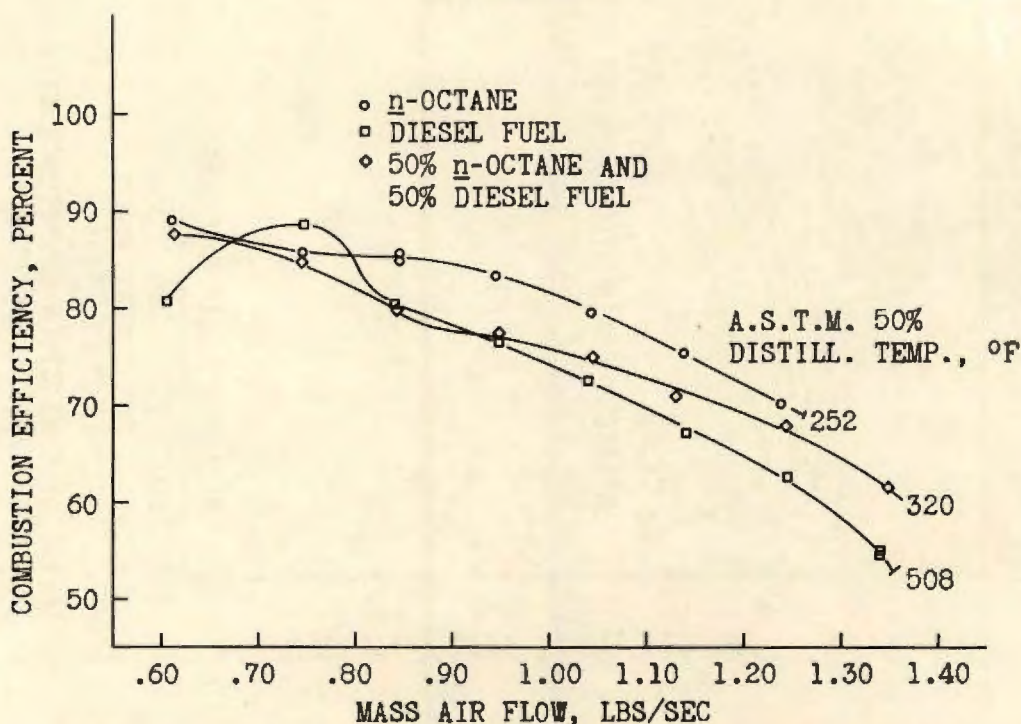VARIATION OF COMBUSTION EFFICIENCY OF SEVERAL FUELS WITH MASS
AIR-FLOW RATE

Figure 8.

CONFIDENTIAL

VARIATION OF COMBUSTION EFFICIENCY WITH
BOILING TEMPERATURE OF FUEL

Figure 9.

o n-OCTANE
□ DIESEL FUEL
◇ 50% n-OCTANE AND
  50% DIESEL FUEL

100

90

80

70

60

50

COMBUSTION EFFICIENCY, PERCENT

A.S.T.M. 50%
DISTILL. TEMP., °F

252

320

508

.60 .70 .80 .90 1.00 1.10 1.20 1.30 1.40

MASS AIR FLOW, LBS/SEC

EFFECT OF BLENDING OF STRAIGHT-CHAIN HYDROCARBONS ON COM-
BUSTION EFFICIENCY

Figure 10.

o n-HEXANE

□ 2,3-DIMETHYLBUTANE

◇ 50% n-HEXANE AND
  50% 2,3-DIMETHYL-
  BUTANE

H_2 H_2 H_2 H_2
$H_3C-C-C-C--C-CH_3$

  H   H
$H_3C-C-C-CH_3$
  CH_3 CH_3

100

90

80

70

60

50

COMBUSTION EFFICIENCY, PERCENT

A.S.T.M. 50%
DISTILL. TEMP., °F
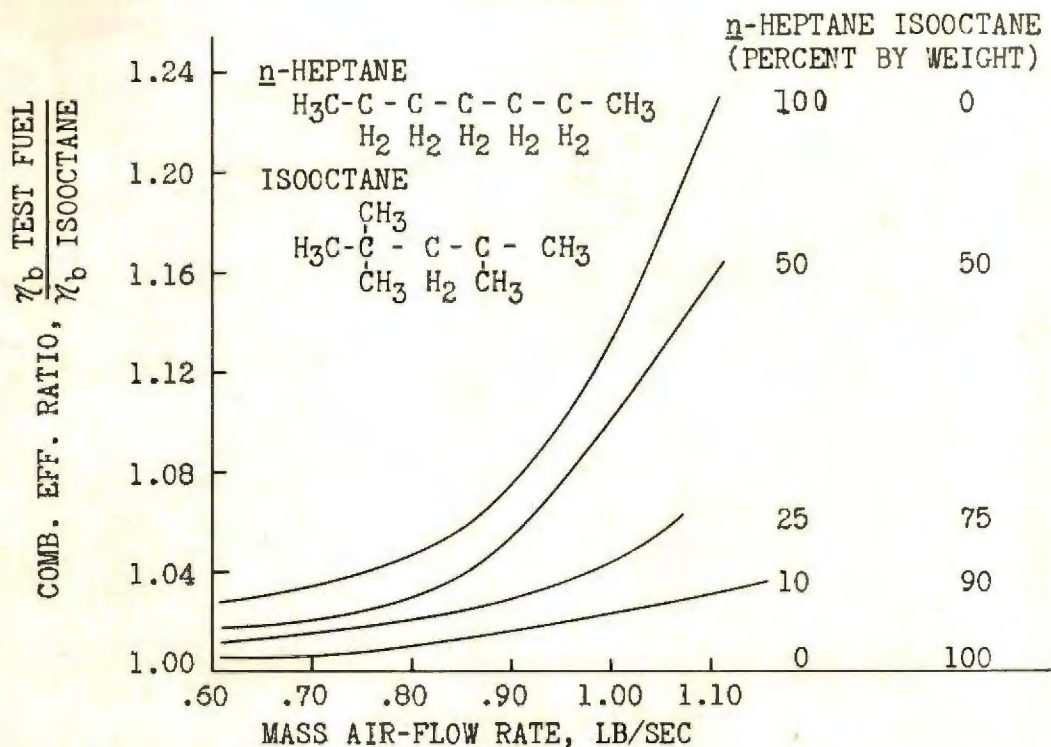
153

135

.60 .70 .80 .90 1.00 1.10 1.20 1.30

MASS AIR FLOW, LBS/SEC
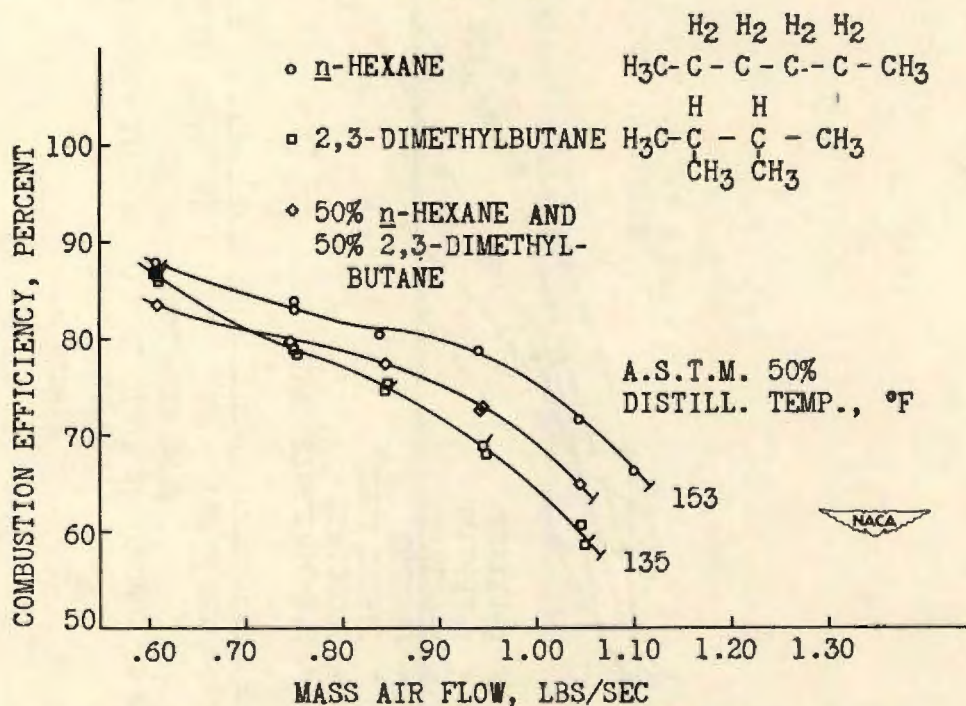
EFFECT OF BLENDING OF STRAIGHT-CHAIN AND BRANCHED-CHAIN
HYDROCARBONS ON COMBUSTION EFFICIENCY

Figure 11.

RELATIVE PERFORMANCE OF BLENDS OF n-HEPTANE AND ISOOCTANE

Figure 12.
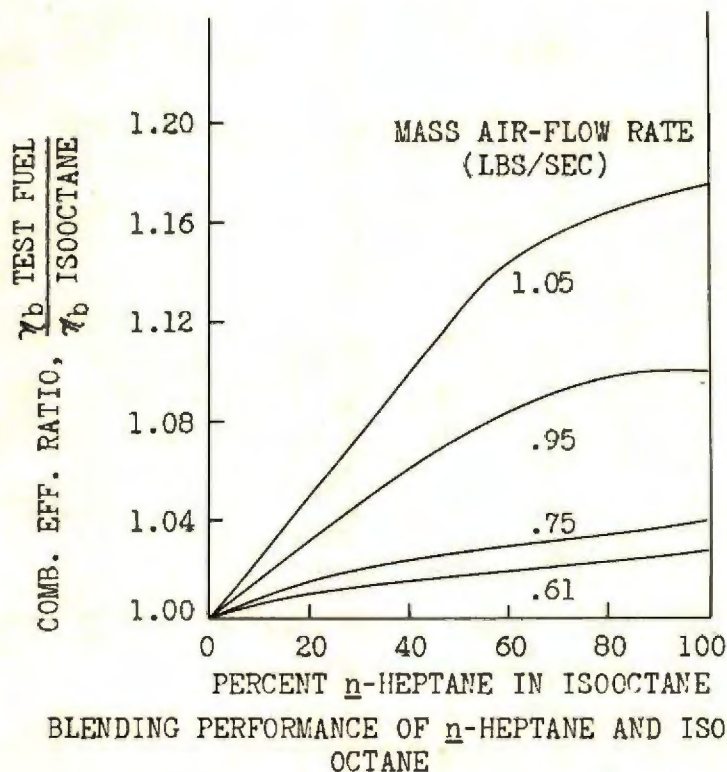

BLENDING PERFORMANCE OF n-HEPTANE AND ISO-
OCTANE

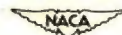**Figure 13.**

EFFECT OF FUEL VOLATILITY AND HYDROGEN-CARBON RATIO
ON CARBON FORMATION IN GAS-TURBINE COMBUSTORS

By Jerrold D. Wear

Flight Propulsion Research Laboratory

INTRODUCTION

The jet-engine fuel program conducted at the NACA Cleveland laboratory includes investigations to determine the effects of fuel properties on carbon deposition in jet-engine combustors. The effects of change in simulated engine conditions on carbon deposition were also investigated.

Published data (reference 1) of carbon deposition of seven fuels in an I-16 engine run at sea-level conditions indicated that the quantity of carbon deposited is apparently a function of the boiling point and the aromatic content of a fuel. The effects of these two factors, however, could not be isolated because the fuels used were complex hydrocarbon mixtures.

In an effort to isolate the effects of hydrocarbon type and boiling point on carbon deposition, 19 fuels, 12 of which were 95 or more percent pure, were evaluated in a 9.5B annular combustor (reference 2). Three of the fuels were investigated at six different simulated engine conditions to determine the effect of change in engine conditions on carbon deposition. The results are presented herein.

APPARATUS

In the 9.5B annular combustor (fig. 2), the combustion air is divided by the fuel manifold and enters the annular combustion zone from both sides through holes in the basket. The fuel is injected into the annular combustion zone by 12 nozzles evenly spaced around the fuel manifold. The carbon forms or is deposited around the nozzles at the back of the basket and on the sides of the basket between the longitudinal rows of air holes. Opening the combustor at the exhaust end makes it possible to observe the carbon formations.

The combustion zone and carbon formations photographed from the exhaust end are shown in figure 2. The view is upstream toward the

fuel nozzles. The light colored objects are large formations of
hard carbon on the basket. A considerable amount of carbon is
around the fuel nozzles on the back of the basket. The carbon was
obtained from benzene at simulated sea-level engine conditions for
a 2-hour run.

A diagrammatic cross section of a heavy carbon formation at the
fuel nozzle in the annular combustion zone is shown in figure 3. The
cross-hatched area represents carbon on the sides of the basket
between the longitudinal rows of the air holes and around the fuel
nozzles. The carbon on the basket is harder than that around the
fuel nozzles at the back of the basket.

RESULTS AND DISCUSSION

The effect of running time, other conditions constant, on the
carbon deposition of three fuels is shown in figure 4. Carbon weight
is plotted against running time at sea level and simulated 50-percent
rated engine speed. Fuel flow for any one engine condition was
obtained by setting the desired combustor inlet-air conditions and
adjusting the flow of AN-F-32 to give the required turbine tempera-
ture. This same fuel flow was used for the other fuels at this
engine condition. The fuels were aromatic solvent, benzene, and
AN-F-32. The quantity of carbon in the basket stabilized when the
rate of erosion and combustion of carbon on the basket is equal to
the rate of carbon deposition. The leveling of the curve indicates
that the rate of carbon removal by burning and eroding is approaching
the rate of carbon deposition after about 2 hours for aromatic
solvent and benzene.

A plot of carbon weight against altitude for aromatic solvent,
benzene, and AN-F-32 at simulated rated engine speed for
$1\frac{1}{4}$-hour run is given in figure 5. The values of combustion air
pressure, temperature, mass flow, and fuel-air ratio were the same
for all fuels at any one altitude, but varied with altitude.
Carbon formation decreased with increase in altitude; however, the
amount obtained with some fuels is significant at altitude conditions.

Carbon deposition as affected by simulated engine speed is
presented in figure 6. Carbon weight is plotted against simulated
engine speed at 20,000 feet for $1\frac{1}{4}$-hour run for aromatic solvent,
benzene, and AN-F-32. The values of combustion air pressure, temper-
ature, mass flow, and fuel-air ratio were the same for all fuels at

any one engine speed, but varied with engine speed. Carbon deposition increased with increase in simulated engine speed.

Investigation of three fuels at six different simulated engine conditions were made to determine if change in engine condition would change the order of carbon deposition among the fuels. Figure 7 is a plot of carbon weight at the different engine conditions for the fuels, aromatic solvent, benzene, and AN-F-32. The simulated engine test conditions are as follows:

Test condition	Simulated altitude (ft $\times 10^{-3}$)	Simulated engine speed (percentage rated)	Inlet-air total pressure (in. Hg absolute)	Inlet-air total temperature (^oF)	Fuel flow (lb/hr)	Overall fuel-air ratio	Run time (hr)	Turbine inlet temperature (^oF)
1	40	100	19.0	132	155.5	0.0282	$1\frac{1}{4}$	1315
2	20	50	18.9	43	116.5	.0224	$1\frac{1}{4}$	1045
3	30	100	30.8	153	172.0	.0202	$1\frac{1}{4}$	1320
4	0	50	40.0	100	157.5	.0175	$1\frac{1}{4}$	1280
5	0	50	40.0	100	157.5	.0175	2	1280
6	20	100	44.0	196	223.0	.0181	$1\frac{1}{4}$	1360

The order of carbon deposition among the fuels did not change with engine condition. These data suggest the possibility that one engine condition would be sufficient for relative carbon deposition investigations of the various fuels. Test condition 5 was used for these investigations.

The 19 fuels investigated (fig. 8) are classed as paraffins, olefins, aromatics, and mixtures. A fuel that contained less than 95 percent of any one class was considered as a mixture. The fuels are listed with increasing 50-percent evaporated temperature in each class. Each step of the staggered bars represents the weight of carbon obtained in check runs.

The carbon deposition obtained with the paraffins and olefins was small. The higher boiling olefin, $\underline{n}$-hexadecene-1, gave less carbon then diisobutylene, the lower boiling olefin. Although the carbon deposited in the basket with the two olefinic fuels was small, a thin layer of sooty carbon was deposited on the walls of the tail-pipe section. This sooty carbon was not obtained with the other type hydrocarbons.

The aromatic-type hydrocarbons gave the most carbon of the types investigated. There seems to be a general increase in carbon deposition with increase in boiling temperature for this class. There is some evidence of trend of carbon deposition with boiling temperature for the fuel mixtures; however, it is apparent there is another factor affecting the carbon deposition. Examination of the data indicated that hydrogen-carbon ratio and boiling temperature would correlate the carbon-deposition data. This will be shown in a later figure.

The effect of fuel blends on carbon deposition is shown in figure 9. This is a plot of carbon deposition of fuels A, fuels B, and blends of fuels A and B. The simulated engine conditions were sea-level altitude for 50-percent rated engine speed for a 2-hour run. The five blends investigated were: 50-50 percent by weight blend of isoheptane — AN-F-32, isoheptane — benzene, AN-F-32 — aromatic solvent, benzene — aromatic solvent; and a 70-30 percent by weight blend of aromatic solvent — monomethylnaphthalene. The blends of paraffin — mixed fuels, paraffin — aromatic, and mixed fuels — aromatics gave a general trend of carbon deposition. However, the aromatic — aromatic blends gave as much or more carbon than either of the fuels used to make the blends.

An attempt to correlate the carbon deposition of the various fuels with their 50-percent evaporated temperature and hydrogen-carbon ratio is shown in figure 10. This is a chart of 50-percent evaporated temperature, lines of constant hydrogen-carbon ratio, and carbon deposition. In order to find the ordinate of the chart, move up 50-percent evaporated temperature line of the fuel to the proper hydrogen-carbon ratio. This value of the ordinate is then plotted against the weight of carbon. The carbon deposition of the 19 fuels are plotted on this chart at the engine condition of 50-percent rated speed at sea level for a 2-hour run. The carbon weight varies from 1.0 to 145 grams. The data can be approximated by one straight line, except for the high-boiling-temperature olefin, fuel mixture, and aromatic. They gave less carbon than that predicted by the faired line. For a given hydrogen-carbon ratio, the carbon deposition of all fuels increases with 50-percent evaporated

temperature; for constant 50-percent evaporated temperature, the carbon deposition of all fuels increases with decrease in hydrogen-carbon ratio.

A correlation, to be of value, should rate the fuels in the same order at other engine conditions. Figure 11 shows data of three fuels at the six different engine conditions mentioned in figure 7. This chart is similar to the one shown in figure 10. The fuels are aromatic solvent, benzene, and AN-F-32. The symbols represent the different engine conditions. Again, the ordinate is obtained by moving up the 50-percent evaporated temperature line of the fuel to the proper hydrogen-carbon ratio. The weight of carbon is then plotted against this value of the ordinate. The same general trend is obtained at the various engine conditions, although the slopes of the faired lines are different.

In figures 12 to 14, carbon-deposition data obtained at three laboratories, A, B, and C (references 3 to 5, respectively), are plotted on charts similar to those given in figures 10 and 11; however, in order to expand the carbon-weight scale, the temperature abscissa and lines of constant hydrogen-carbon ratio have been omitted from the figures. The ordinates were obtained by moving up the 50-percent evaporated temperatures of the different fuels to the proper hydrogen-carbon ratios. The value of the ordinate of each fuel was then plotted against the weight of carbon obtained with that fuel.

Figure 12 presents data obtained at laboratory A of five fuel mixtures tested in an I-40 single combustor. The data can be approximated by one straight line.

Data obtained on an I-16 single combustor from laboratory B are shown in figure 13. One paraffin and two aromatic fuels deviated considerably from a straight line faired through the other data.

Figure 14 presents data obtained at laboratory C on an I-16 single combustor. One aromatic fuel showed a large deviation from the faired line.

SUMMARY

The following results were obtained from an investigation of the effect of fuel volatility and hydrogen-carbon ratio on carbon formation in gas-turbine combustors:

CONFIDENTIAL

     1. The carbon deposition of paraffinic, aromatic, and mixed
fuels at different engine conditions, in general, could be corre-
lated with hydrogen-carbon ratio and 50-percent evaporated temper-
ature. Carbon deposition increased with 50-percent evaporated tem-
perature at constant hydrogen-carbon ratio and with decreasing
hydrogen-carbon ratio at constant 50-percent evaporated temperature.

     2. Aromatic fuels produced more carbon than other classes of
fuels in the same boiling range because of their lower hydrogen-
carbon ratio.

     3. Carbon deposition decreased with increase in simulated
altitude, but is significant for some fuels at altitude conditions.

                            REFERENCES

1. Jonash, Edmund R., Barnett, Henry C., and Stricker, Edward G.:
     Investigation of Carbon Deposition in an I-16 Jet-Propulsion
     Engine at Static Sea-Level Conditions. NACA RM No. E6K01, 1947.

2. Wear, Jerrold D., and Busch, Arthur M.: Carbon Deposition
     Investigation of 19 Fuels in an Annular Turbojet Combustor.
     NACA RM (to be pub.).

3. Thwaites, H. L., and Rickles, N. H.: Internal Combustion Fuel
     Studies. Prog. Rep. Dec. 15, 1946 to Feb. 15, 1947. Rep.
     No. RL-7M-47(41), Res. Div., Esso Labs., Standard Oil Devel-
     opment Co., July 24, 1947.

4. Moore, R. A., and Giaccone, F. W.: Summary Rep. U. S. Gov't.
     Contract W-33-0-38 ac 8527. Rep. No. 46.23-DX, Res. and
     Development Labs., Socony-Vacuum Labs., Nov. 8, 1946.
     (AMC Proj. No. MX-587.)

5. Bert, J. A.: G.E. I-16 Jet Propulsion Burner Tests. Prog. Rep.
     No. 13, Calif. Res. Corp., Sept. 1, 1947. (Army Contract
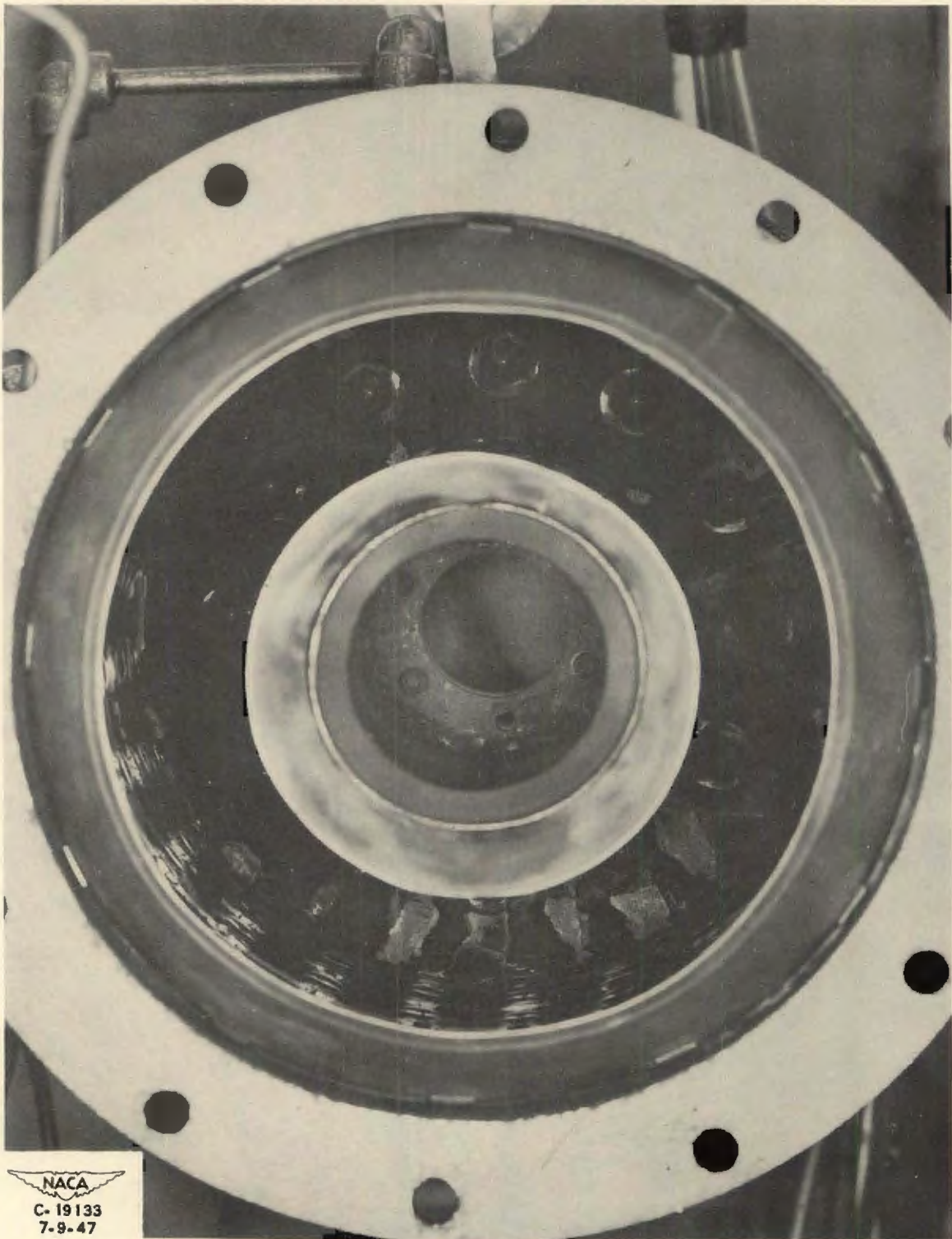   No. W-33-038 ac — 9083.)
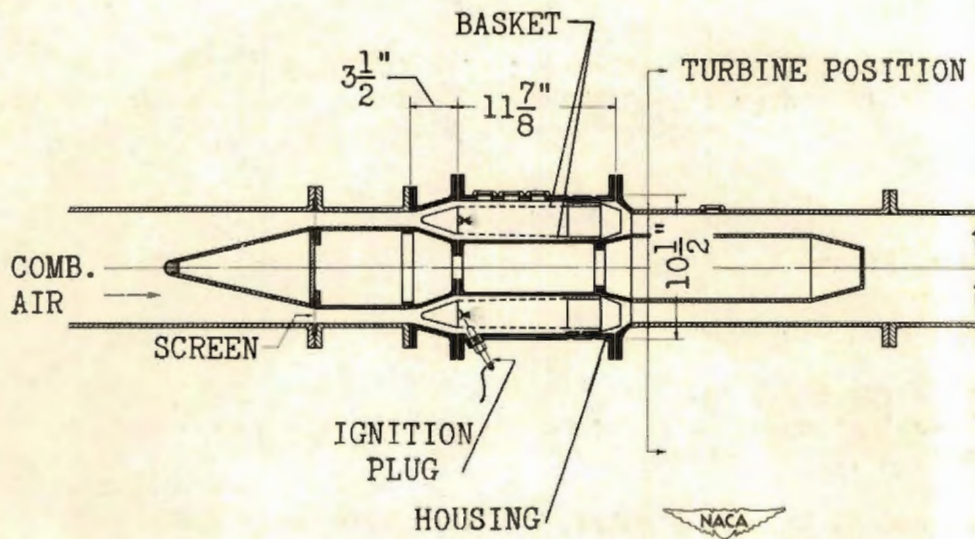
ANNULAR COMBUSTOR.
Figure 1.

Photograph of carbon formation in annular combustor

Figure 2.
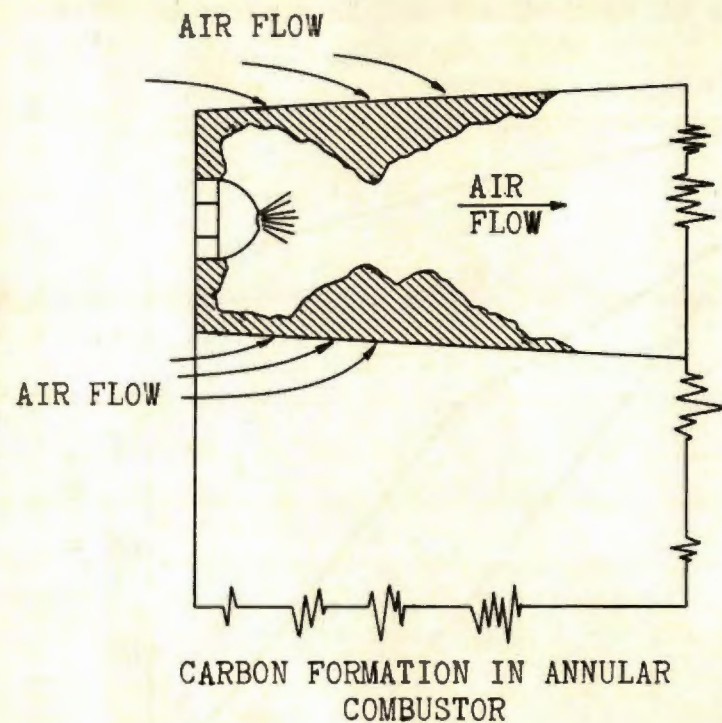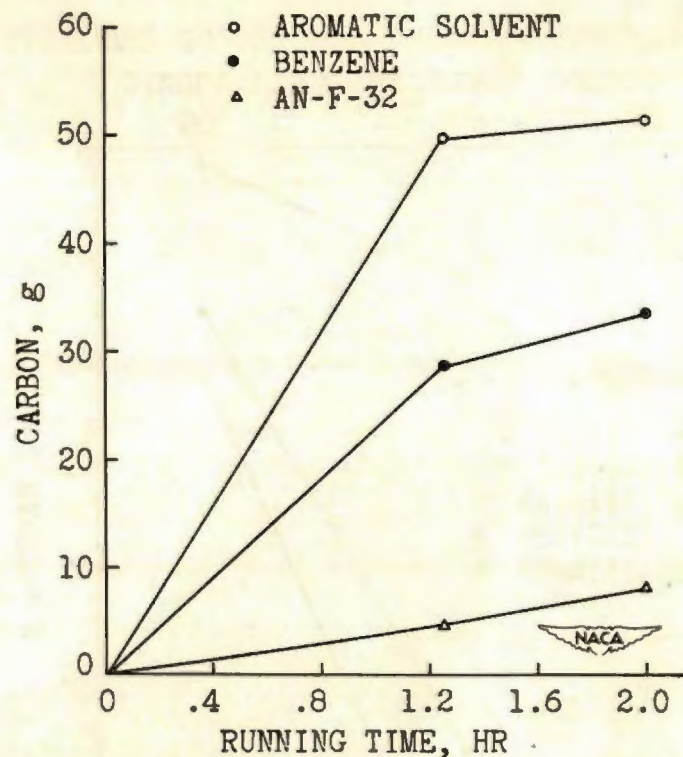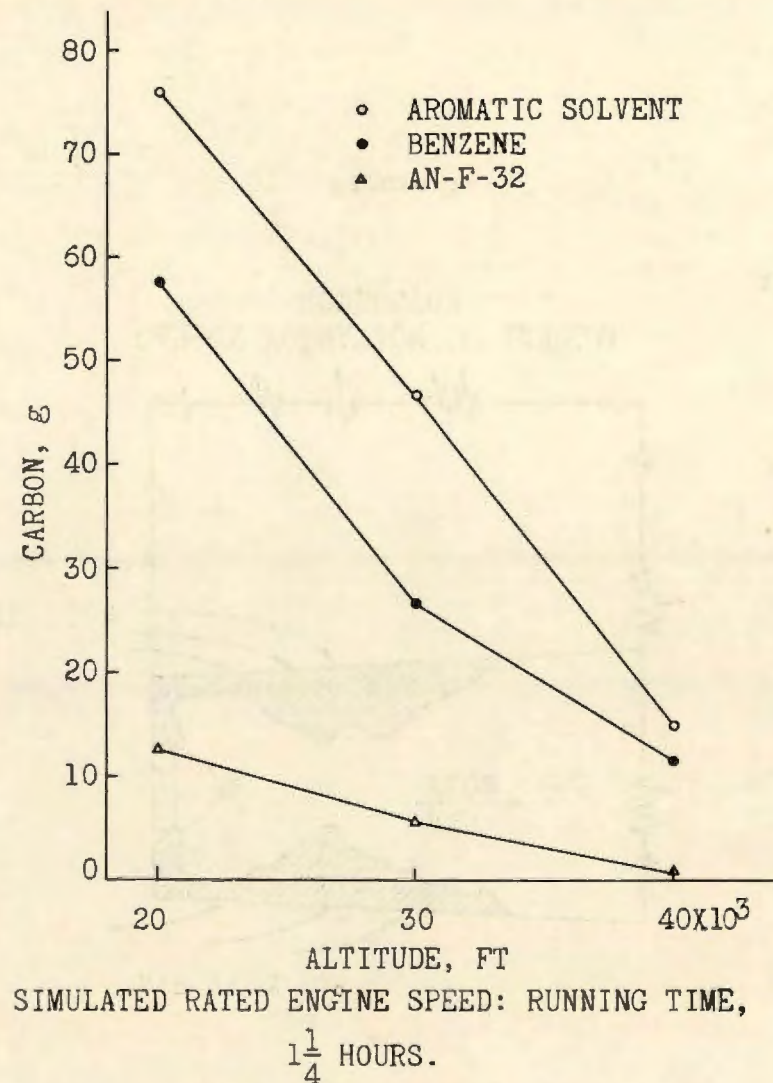
CARBON FORMATION IN ANNULAR
COMBUSTOR

Figure 3.

ALTITUDE, SEA LEVEL; SIMULATED ENGINE SPEED,
50 PERCENT OF RATED.
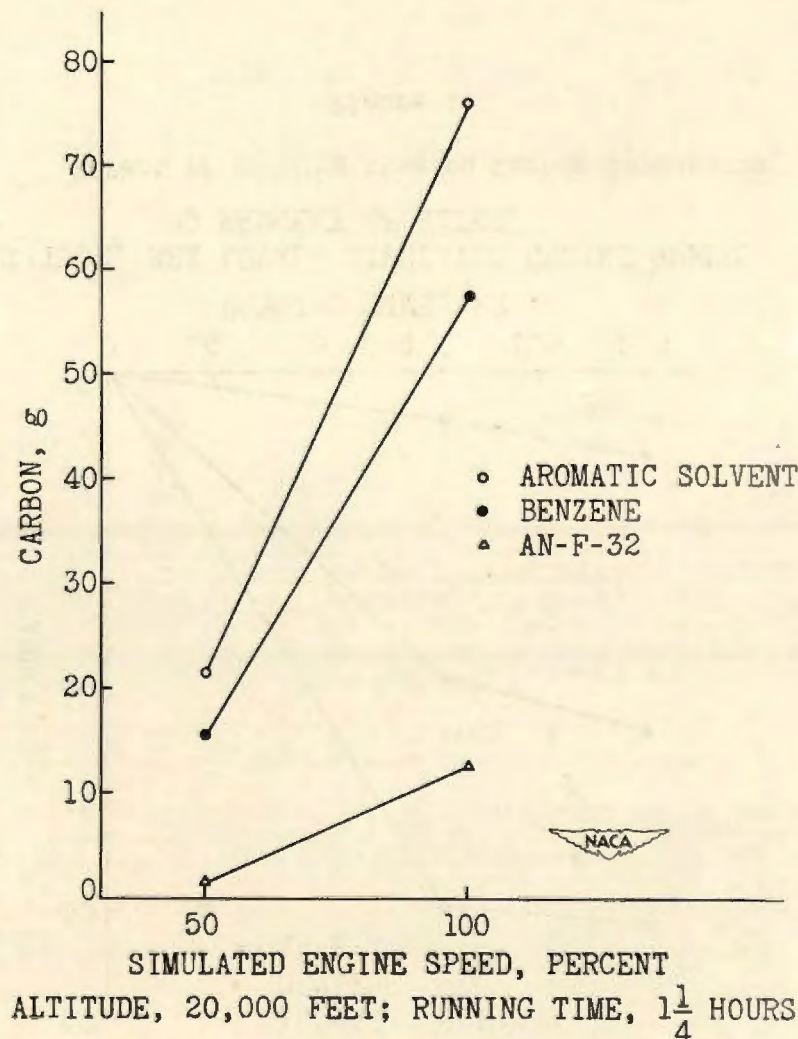
Effect of running time on Carbon deposition

Figure 4.

SIMULATED RATED ENGINE SPEED: RUNNING TIME, $1\frac{1}{4}$ HOURS.

Effect of altitude on carbon deposition

Figure 5.

SIMULATED ENGINE SPEED, PERCENT

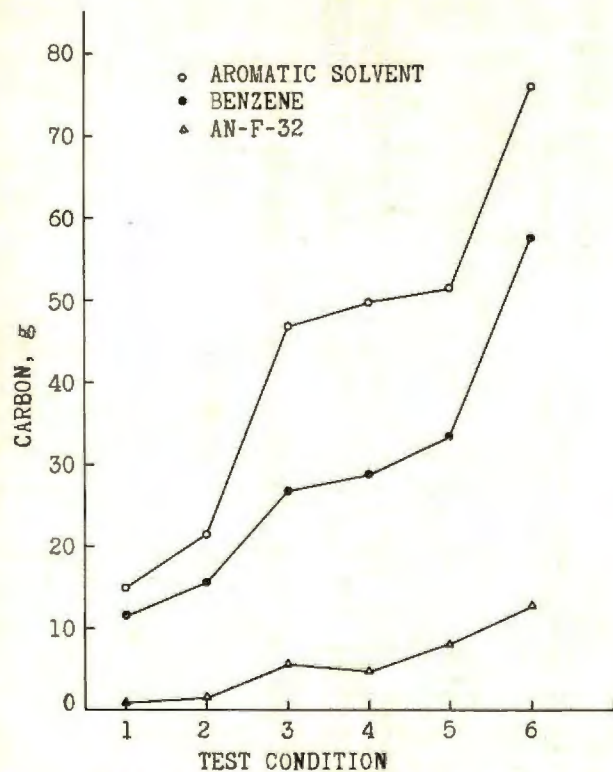ALTITUDE, 20,000 FEET; RUNNING TIME, $1\frac{1}{4}$ HOURS.

Effect of simulated engine speed on carbon deposition.

Figure 6

CONFIDENTIAL

CONFIDENTIAL

Effect of test conditions on
carbon deposition.

Figure 7.

| FUEL	A.S.T.M. 50% EVAP. TEMP. (°F)	ARO- MATICS (VOL %)
PARAFFINS		
COM. ISOHEPTANE	180	-------
PARAFFINIC SOLVENT	345	2
OLEFINS		
DIISOBUTYLENE	214	-------
n-HEXADECENE-1	522	-------
AROMATICS		
BENZENE	173	98
BLEND NO. 1	257	98
ETHYLBENZENE	270	98
XYLENE	278	98
AROMATIC SOLVENT	324	98
BLEND NO. 2	350	98
TRIISOPROPYLBENZENE	444	98
ME NAPHTHALENE	460	98
MIXTURES		
BLEND NO. 3	170	45
AN-F-28R	216	16
BLEND NO. 4	258	6
BLEND NO. 5	352	54
AN-F-32	370	13
MICHIGAN CRUDE	512	16
DIESEL	516	23

ALTITUDE, SEA LEVEL; SIMULATED ENGINE SPEED, 50 PERCENT OF RATED;
RUNNING TIME, 2 HOURS.

Effect of 50-percent evaporated temperature and fuel hydro-
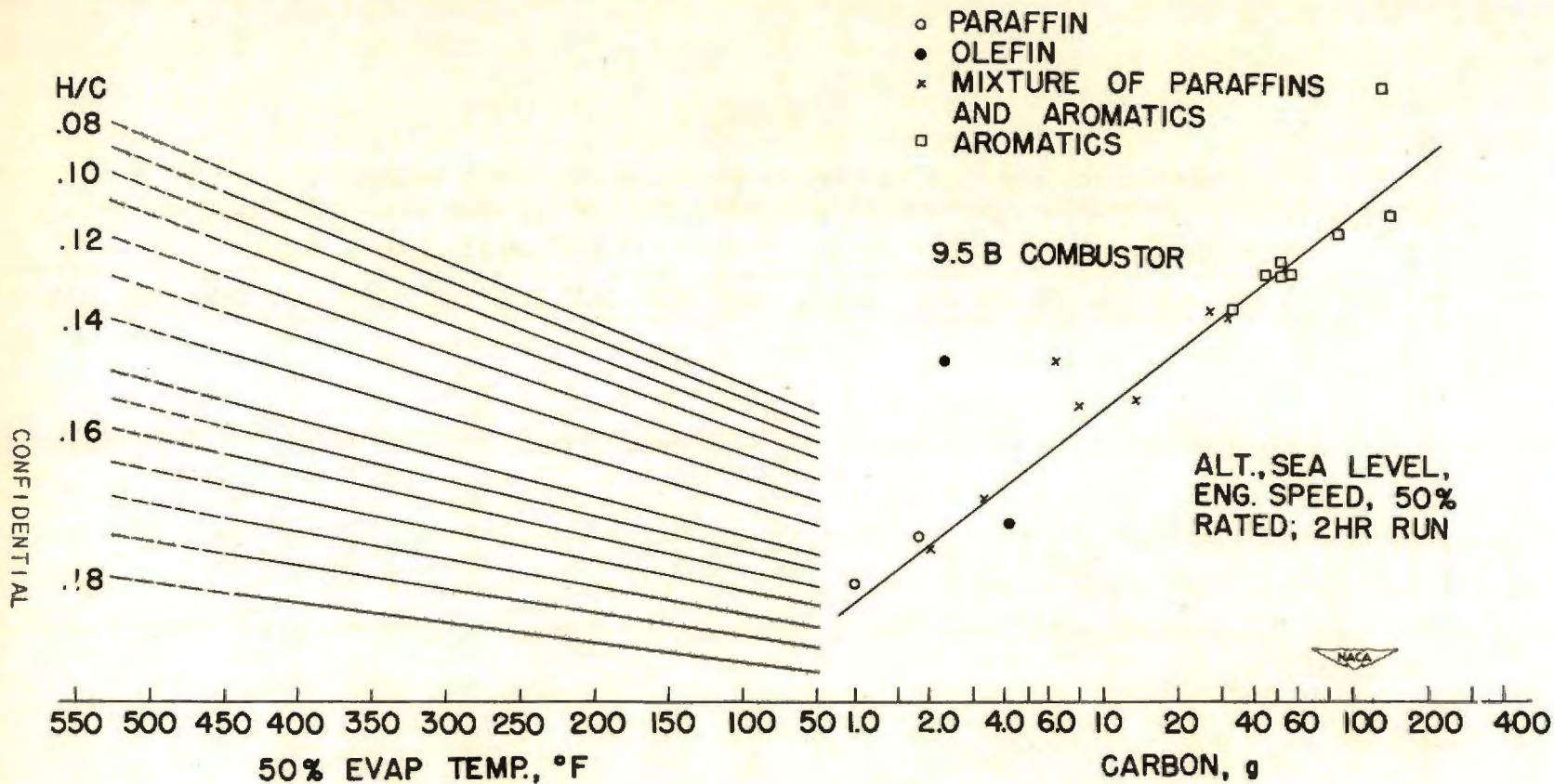carbon type on carbon deposition.

Figure 8.
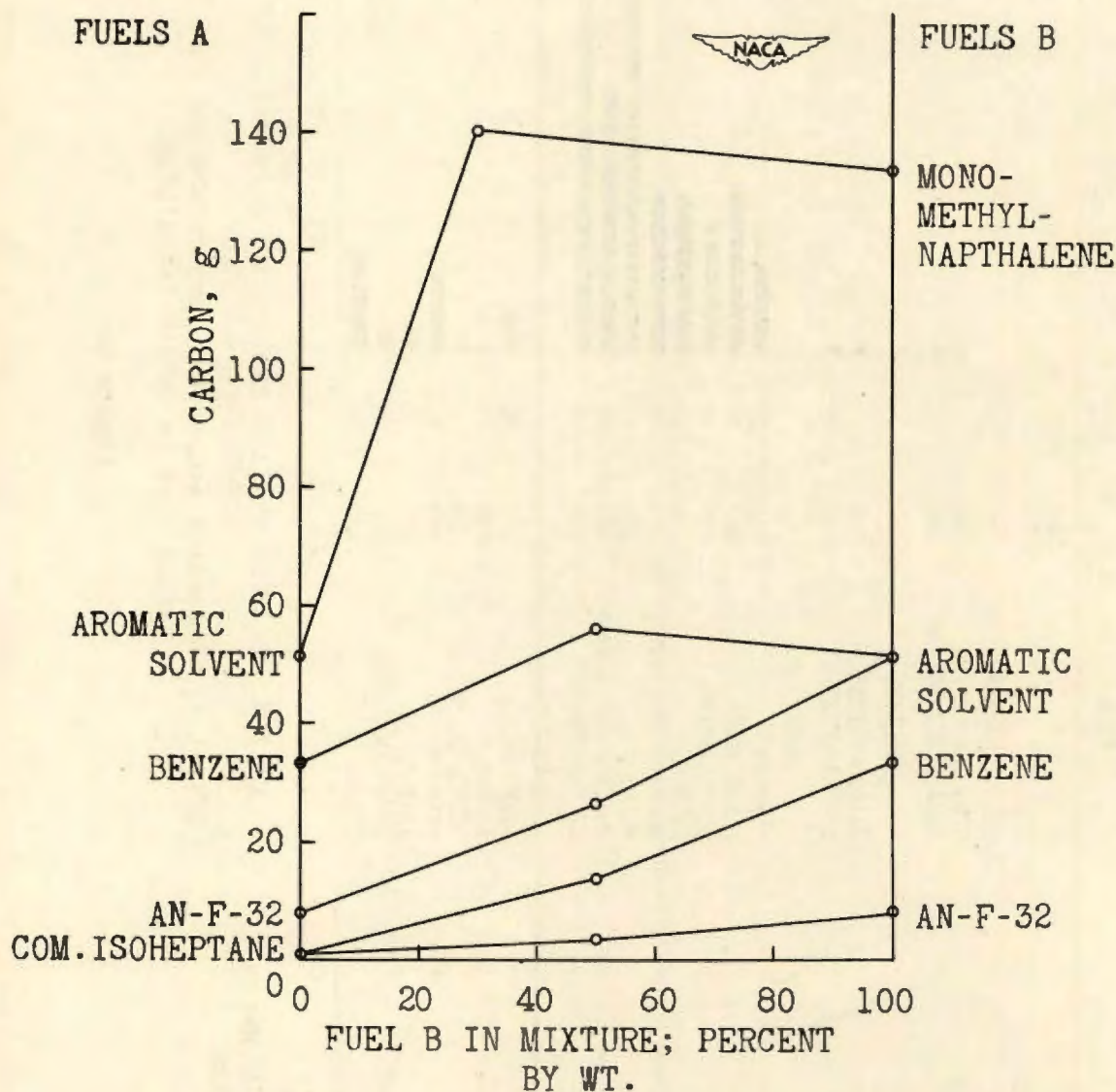
ALTITUDE, SEA LEVEL; SIMULATED ENGINE SPEED,
50 PERCENT OF RATED; RUNNING TIME, 2 HOURS.

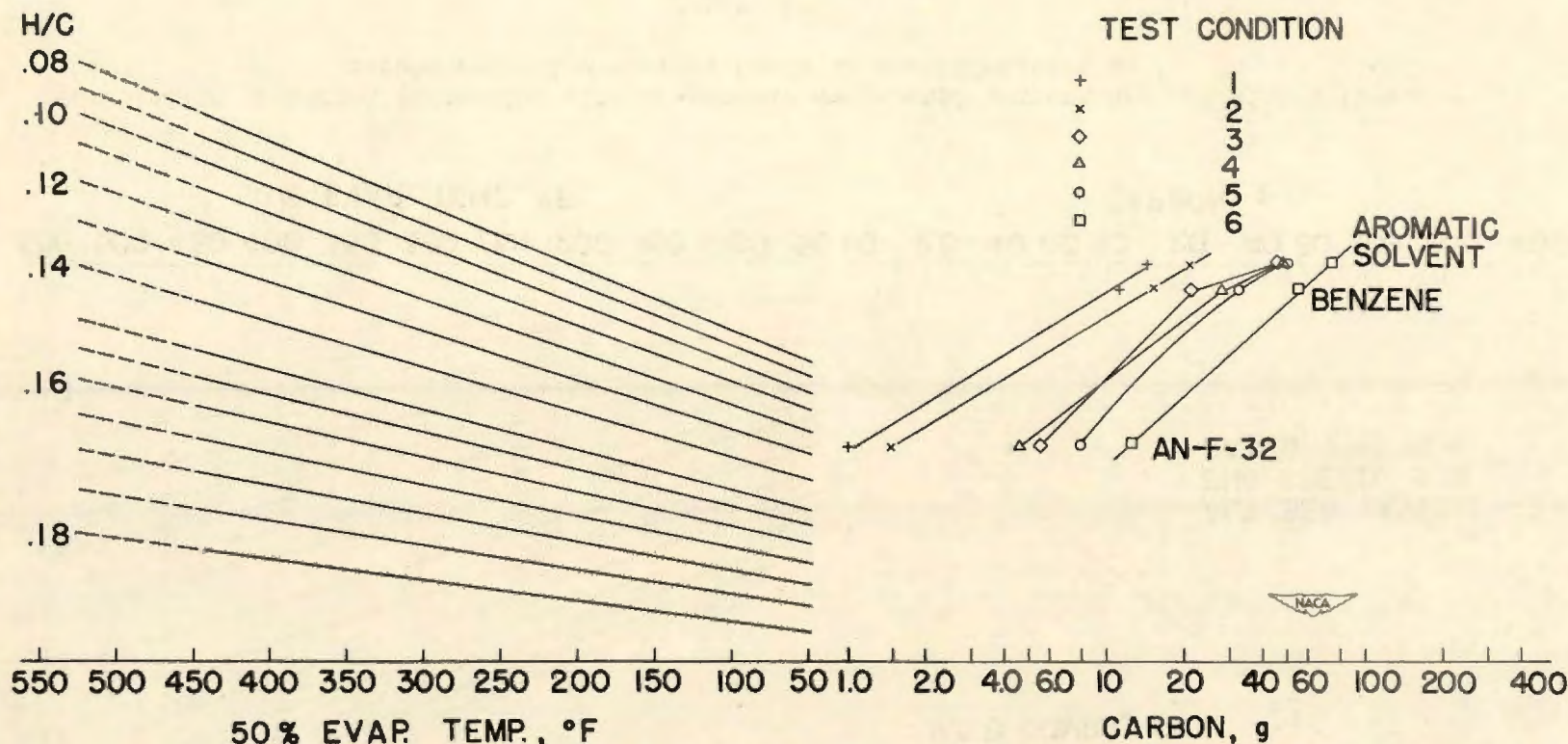Effect of fuel blends on carbon deposition.

Figure 9.

Correlation of carbon deposition with 50-percent evaporated temperature and with nitrogen--carbon ratio for various fuels at test condition 5.
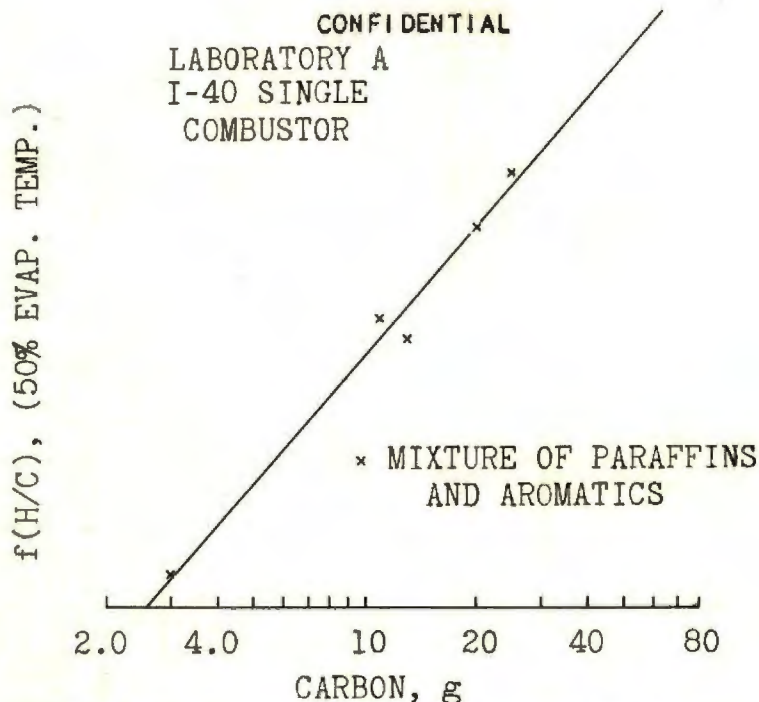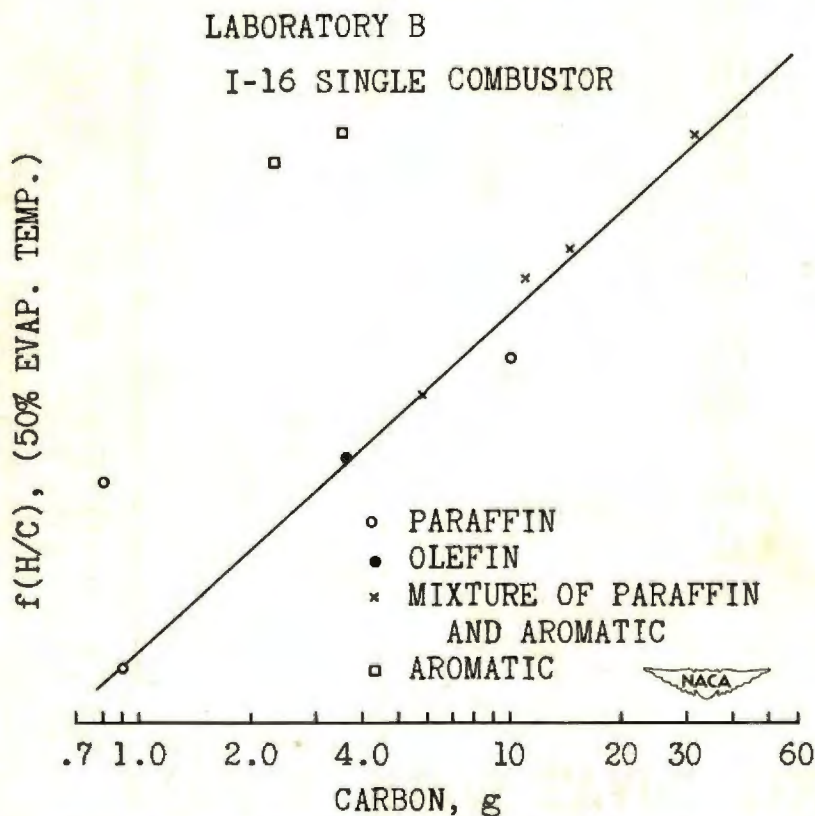
Figure 10.

Correlation of carbon deposition with 50-percent evaporated temperature and with hydrogen-carbon ratio for three fuels, each at six test conditions.

Figure 11.

LABORATORY A
I-40 SINGLE
COMBUSTOR

f(H/C), (50% EVAP. TEMP.)

× MIXTURE OF PARAFFINS
AND AROMATICS

2.0   4.0   10   20   40   80

CARBON, g

Carbon-deposition data from laboratory A correlated with 50-percent evap-
orated temperature and with hydrogen-carbon ratio for five fuels.

Figure 12.

LABORATORY B

I-16 SINGLE COMBUSTOR

f(H/C), (50% EVAP. TEMP.)

o   PARAFFIN
•   OLEFIN
×   MIXTURE OF PARAFFIN
     AND AROMATIC
□   AROMATIC   NACA

.7 1.0   2.0   4.0   10   20 30   60

CARBON, g

Carbon-deposition data from laboratory B correlated with 50-percent evap-
orated temperature and with hydrogen-carbon ratio for ten fuels.

Figure 13.

Carbon-deposition data from laboratory C correlated with 50-percent evaporated temperature and with hydrogen-carbon ratio for eight fuels.
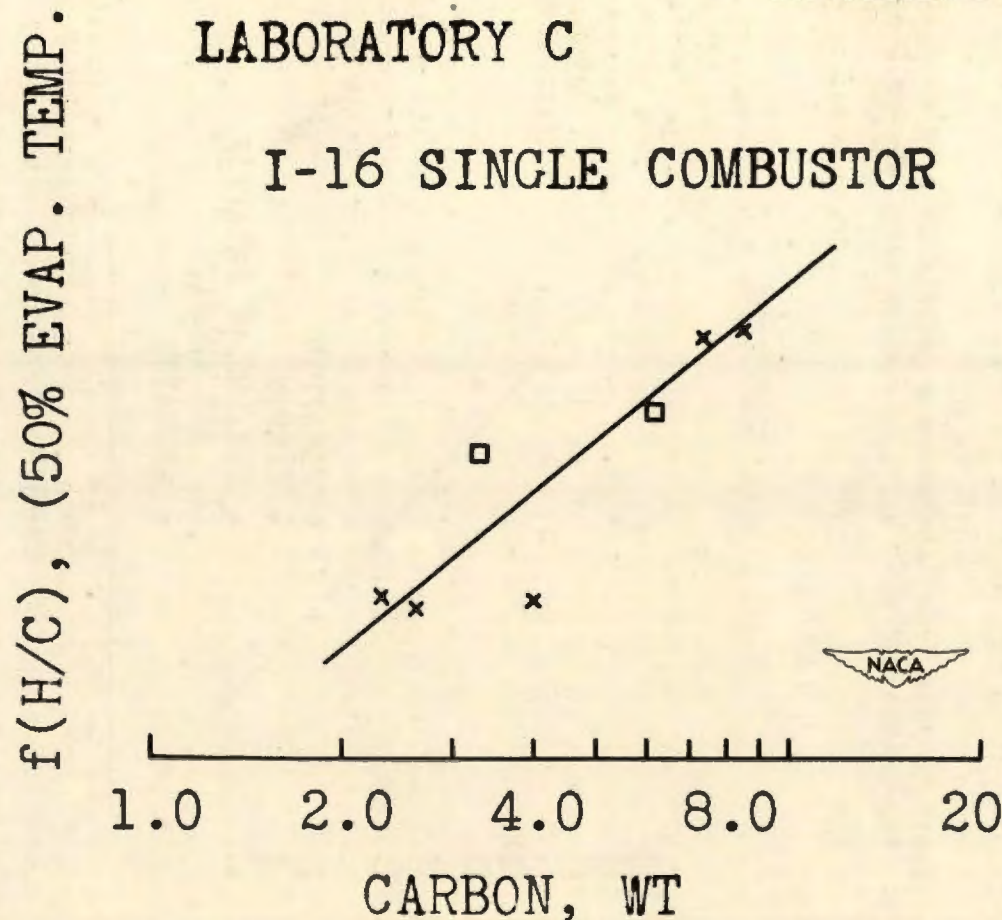
Figure 14.

INFLUENCE OF MOLECULAR STRUCTURE OF HYDROCARBONS

ON RATE OF FLAME PROPAGATION

By Thaine W. Reynolds and Earl R. Ebersole

Flight Propulsion Research Laboratory

INTRODUCTION

As part of an investigation being conducted at the NACA Cleveland laboratory to determine the effect of structure on the flame speed of a fuel, a study of the relation of unsaturation and of chain length to the uniform flame movement in a quiescent fuel-air mixture for 16 straight-chain hydrocarbons up to six carbon atoms in length and for four cyclic hydrocarbons has been made in a horizontal glass tube with an internal diameter of 2.5 centimeters.

Coward and Hartwell (reference 1) have shown that the fundamental flame speed of a fuel, or the burning rate at any point normal to the surface of the flame, is constant over the flame surface and is dependent only upon the fuel-air composition of the mixture.

Several investigators (references 2 to 5) have shown that in a tube closed at one end and ignited from the open end, the flame travels through the combustible mixture with a uniform velocity over a part of the tube length. The magnitude of this uniform velocity for any fuel at a constant temperature and pressure is dependent upon (1) the fuel-air ratio of the mixture, (2) the diameter of the tube, and (3) the direction of propagation, that is, whether upward, downward, or horizontal.

The uniform flame velocity, that is, the linear rate of flame travel through the tube, is equal to the product of the fundamental flame speed times the area of the flame surface divided by the cross-sectional area of the tube. Thus, by measurements of the uniform flame velocity, the fundamental flame speeds of different combustible mixtures can be relatively compared.

All results reported herein are presented as the variation of the uniform flame velocity with mixture composition and are given in graphical form.

CONFIDENTIAL

APPARATUS AND EXPERIMENTAL PROCEDURE

The flame-speed measuring apparatus consisted of a glass tube, $13\frac{1}{2}$ feet long, with an internal diameter of 2.5 centimeters. The apparatus assembled for the introduction of a fuel-air mixture is shown in figure 1. Two electrodes, which were located in the tube .2 inches from the open end and were connected to the secondary of a 10,000-volt transformer, were used to ignite the mixture.

In order to establish the uniformity of the flame travel and the reproducibility of the results, the speed of the flame was first measured by four ionization gaps, consisting of tungsten wires, located in pairs at 6-inch intervals from the open end of the tube. An electromotive force of 24 volts was impressed across the gaps. The impulse created when a circuit was completed by ionization in the flame front was amplified and photographically recorded along with traces from a timing fork at 1/100-second intervals. The use of four ionization gaps enabled the determination of the speed to be made over three successive parts of the tube and thus to establish the uniformity of the flame travel over that part of the tube. The flame travel was found to be uniform within ±2 percent for a distance of 12 inches starting at the first gap.

The data presented herein were taken using an electronic timing device. This device consisted essentially of two photoelectric cells located at points 6 and 18 inches from the end of the tube, respectively. The impulses caused by the flame front passing the photoelectric cells, after passing through suitable amplifying circuits, were used to start and to stop an electric timer graduated in 1/60-second intervals.

The source and the estimated purity of the fuels used in this investigation are listed in table I.

Gaseous mixtures of each fuel with air were made up in 12-gallon carboys and were allowed to become completely homogeneous by standing several hours before samples were withdrawn. The combustion tube was evacuated to a pressure of at least 1 millimeter of mercury absolute and the sample was introduced and brought up to atmospheric pressure by means of the modified Toepler pump. At least 5 minutes were allowed for the mixture to become quiescent, the stopper was carefully removed, and the mixture was ignited. An average of three such determinations for each fuel-air mixture was taken to obtain the values for flame velocity reported. At the peak flame-speed values, the mean deviation of all the determinations was about ±2 percent.

CONFIDENTIAL

DISCUSSION OF RESULTS

The results of the investigation of the straight-chain hydro-carbon fuels are shown in figures 2 to 6. Fuels with the same number of carbon atoms per molecule are shown together on the same figure, so that the effect of increasing unsaturation in a molecule of given size may be noted. Uniform flame velocity is plotted against fuel-air ratio. The range of the stoichiometric fuel-air ratios for all the fuels shown is from 0.062 to 0.075. The peak flame velocity for all fuels occurred at fuel-air ratios from 10 to 30 percent richer than stoichiometric with the excep-tion of benzene, the peak value of which occurred at approximately 60 percent richer than stoichiometric.

The increase in peak flame velocity of a triple-bond over a double-bond hydrocarbon in a molecule of given size is greater than the increase of a double over a single bond. The effect of one triple bond is greater than that of two conjugated double bonds as is shown by a comparison in the four-carbon and five-carbon series (figs. 4 and 5).

The results for the cyclic hydrocarbons are shown in figure 7. Cyclopropane had the highest flame speed of the compounds tested. Cyclohexene showed an increase in peak flame velocity of about 12 percent over the corresponding saturated ring compound, cyclo-hexane. The increase in peak flame velocity for benzene over cyclohexene was only about 4 percent. The cycloparaffins, cyclo-propane and cyclohexane, had higher peak flame velocities than the corresponding straight-chain paraffins, propane and hexane (figs. 3 and 6, respectively). Similarly, cyclohexene showed a slightly higher flame velocity than 1-hexene.

A plot of the peak uniform flame velocity obtained against the number of carbon atoms per molecule for the straight-chain compounds is shown in figure 8. The n-alkane hydrocarbons all had essentially the same peak flame speed. It can be seen from this figure that the effect of increasing unsaturation in a molecule of given size is greatest in the smaller molecules and drops off rapidly as the chain length is increased. Some effect is still apparent, however, in chains of six carbon atoms. With this number of carbon atoms, the peak flame speed of the n-alkyne hydrocarbon is still about 25 percent greater than the flame speed of the corresponding n-alkane hydrocarbon. The point for acetylene on figure 8 was estimated from fundamental flame-speed data taken from reference 6.

SUMMARY OF RESULTS

From an investigation of quiescent fuel-air mixtures in a 2.5-centimeter tube, it was found that for hydrocarbons up to six carbon atoms per molecule:

1. The straight-chain paraffin hydrocarbons had essentially the same peak flame speed.

2. Increasing the unsaturation in a molecule of given size increased the peak flame speed. This effect was most pronounced in the smaller molecules and dropped off rapidly as the chain length was increased.

3. Increasing the length of the carbon chain in an unsaturated straight-chain compound decreased the peak flame speed.

REFERENCES

1. Coward, H. F., and Hartwell, F. J.: Studies in the Mechanism of Flame Movement. Part II. The Fundamental Speed of Flame in Mixtures of Methane and Air. Jour. Chem. Soc., pt. II, 1932, pp. 2676-2684.

2. Wheeler, Richard Vernon: The Propagation of Flame in Mixtures of Methane and Air. The "Uniform Movement". Jour. Chem. Soc. Trans., vol. 105, pt. II, 1914, pp. 2606-2613.

3. Mason, Walter, and Wheeler, Richard Vernon: The "Uniform Movement" During the Propagation of Flame. Jour. Chem. Soc. Trans., vol. 111, pt. II, 1917, pp. 1044-1057.

4. Coward, H. F., and Hartwell, F. J.: Studies in the Mechanism of Flame Movement. Part I. The Uniform Movement of Flame in Mixtures of Methane and Air, in Relation to Tube Diameter. Jour. Chem. Soc., pt. II, 1932, pp. 1996-2004.

5. Lewis, Bernard, and von Elbe, Guenther: Physics of Flames and Explosions of Gases. Jour. Appl. Phys., vol. 10, no. 6, June 1939, pp. 344-359.

6. Jost, Wilhelm: Explosion and Combustion Processes in Gases. McGraw-Hill Book Co., Inc., 1946, table 21, p. 122.

TABLE I - SOURCE AND PURITY OF FUELS USED

| Hydrocarbon	Source	Minimum estimated purity (mole percent)

Paraffins
  Ethane
  Propane
  Butane
  Pentane
  Hexane
	
	Ohio Chemical & Mfg. Co.
	Ohio Chemical & Mfg. Co.
	Ohio Chemical & Mfg. Co.
	Phillips Petroleum Co.
	Phillips Petroleum Co.
		
		95
		99.9
		99
		99
		95

Olefins
  Ethylene
  Propylene
  1-Butene
  2-Pentene
  1-Hexene
	
	Ohio Chemical & Mfg. Co.
	Ohio Chemical & Mfg. Co.
	The Matheson Company, Inc.
	Phillips Petroleum Co.
	OSU Res. Foundation, A.P.I. Res. Project 45
		
		99.5
		99.5
		99
		95
		99

Diolefins
  1,3-Butadiene
  1,3-Pentadiene
	
	Ohio Chemical & Mfg. Co.
	OSU Res. Foundation, A.P.I. Res. Project 45
		
		98
		99

Acetylenes
  Propyne
 	
  1-Butyne
 	
  1-Pentyne
  1-Hexyne
	
	OSU Res. Foundation, A.P.I. Res. Project 45
	OSU Res. Foundation, A.P.I. Res. Project 45
	Farchan Research Laboratories
	Farchan Research Laboratories
		
		99
		
		99
		
		95
		95

Cycloparaffins
  Cyclopropane
  Cyclohexane
	
	Ohio Chemical & Mfg. Co.
	Dow Chemical Co.
		
		99.5
		98

Cycloolefins Cyclohexene	 Eastman-Kodak Co.	 95
Aromatics Benzene	 Barrett Div., The Allied Chemical & Dye Corp.	 98
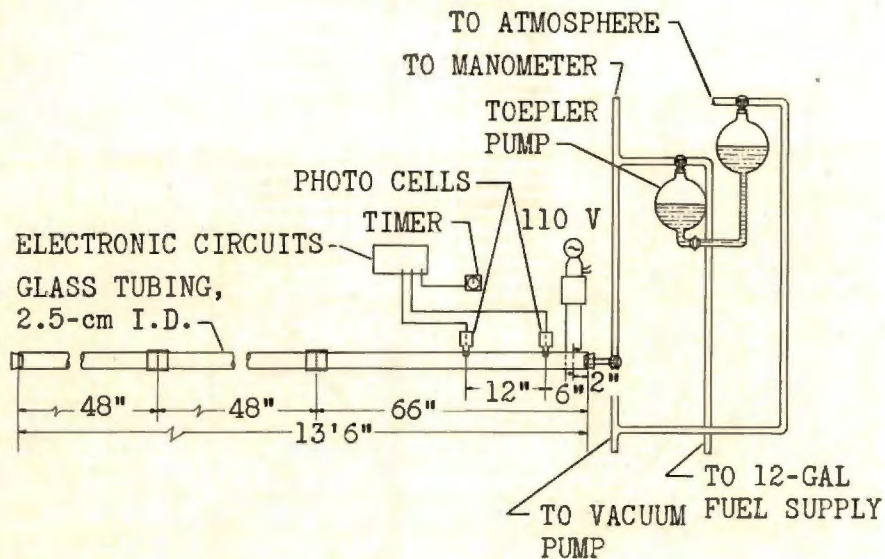
FLAME-SPEED MEASURING APPARATUS.
Figure 1
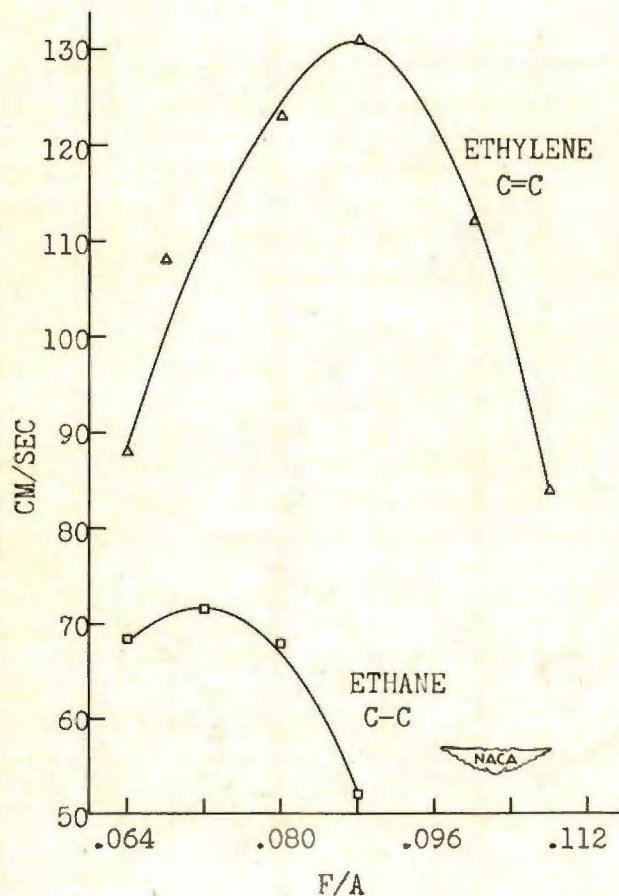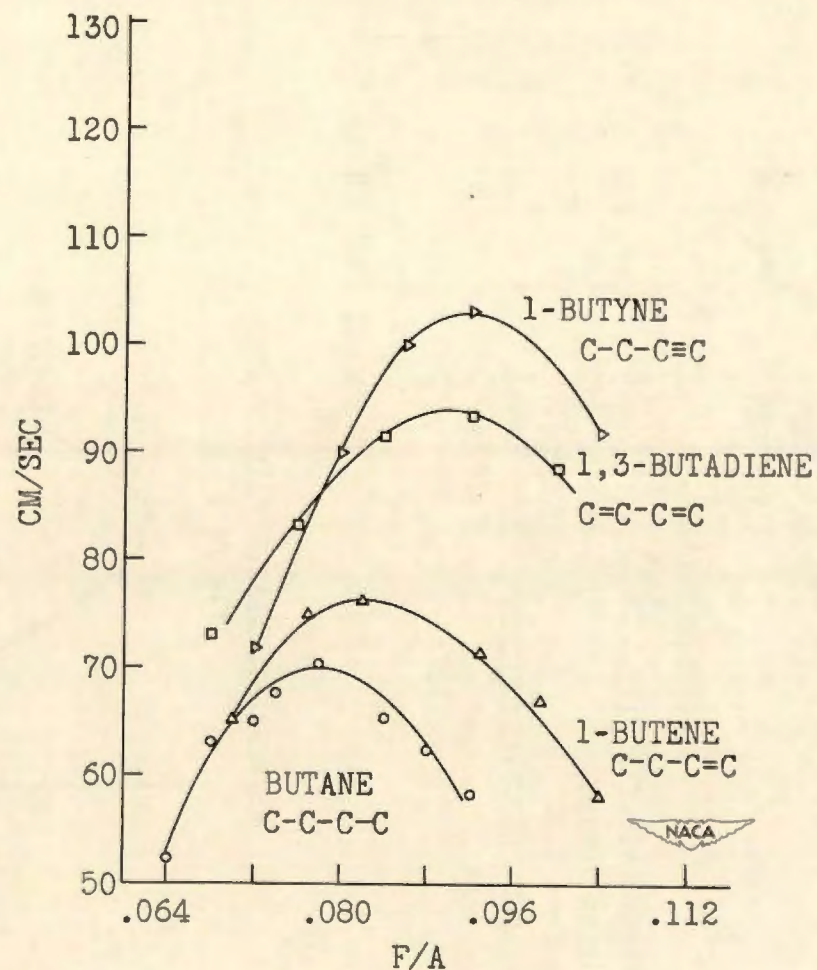

C-2 HYDROCARBONS
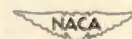FLAME SPEED VERSUS FUEL-AIR RATIO
Figure 2

CONFIDENTIAL
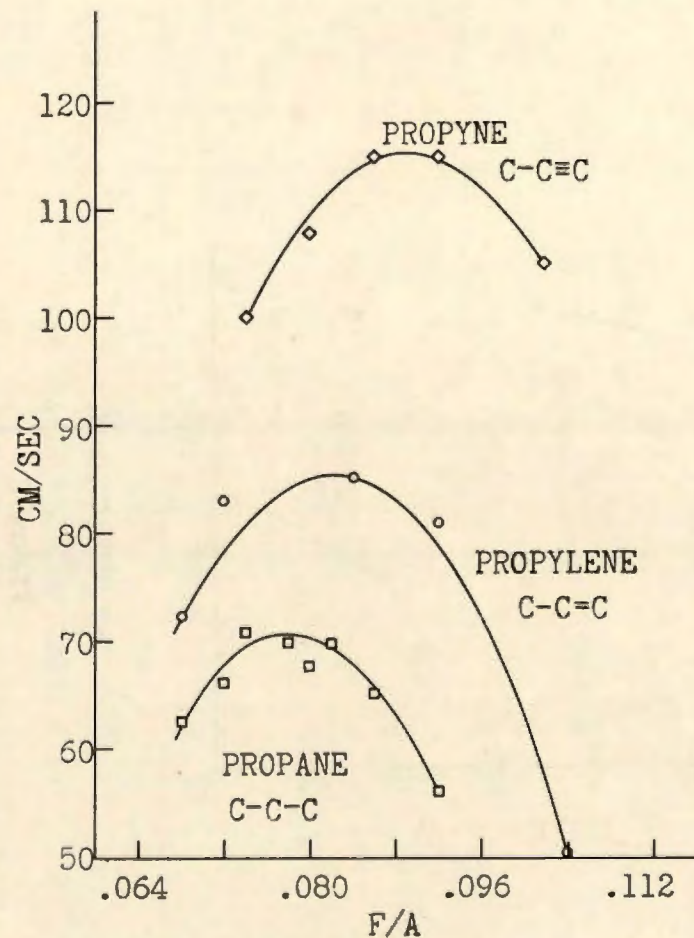
C-3 HYDROCARBONS
FLAME SPEED VERSUS FUEL-AIR RATIO
Figure 3

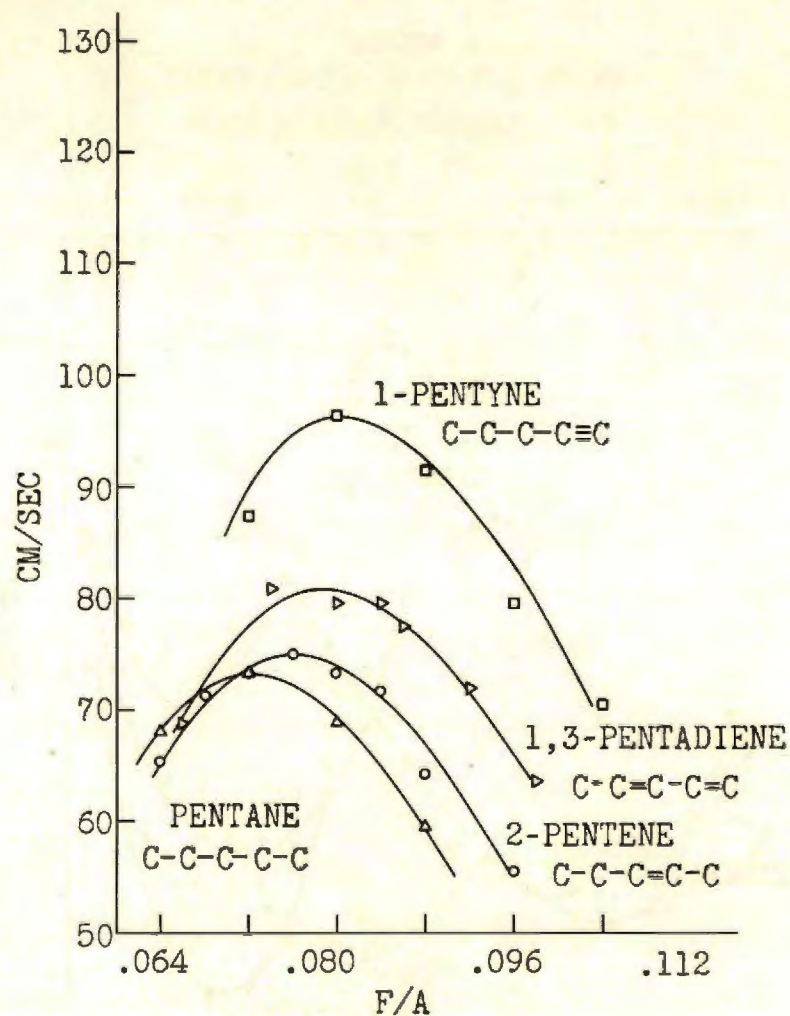C-4 HYDROCARBONS
FLAME SPEED VERSUS FUEL-AIR RATIO
Figure 4

C-5 HYDROCARBONS

FLAME SPEED VERSUS FUEL-AIR RATIO

Figure 5

C-6 HYDROCARBONS

FLAME SPEED VERSUS FUEL-AIR RATIO

Figure 6

CYCLOPROPANE
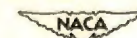
BENZENE

CYCLOHEXENE

CYCLOHEXANE

CM/SEC

F/A

CYCLIC HYDROCARBONS

FLAME SPEED VERSUS FUEL-AIR RATIO

Figure 7

CM/SEC

n-ALKYNES
C≡C-R

1,3 DIENES
C=C-C=C-R

C=C-R
n-ALKENES

n-ALKANES
C-C-R

NACA
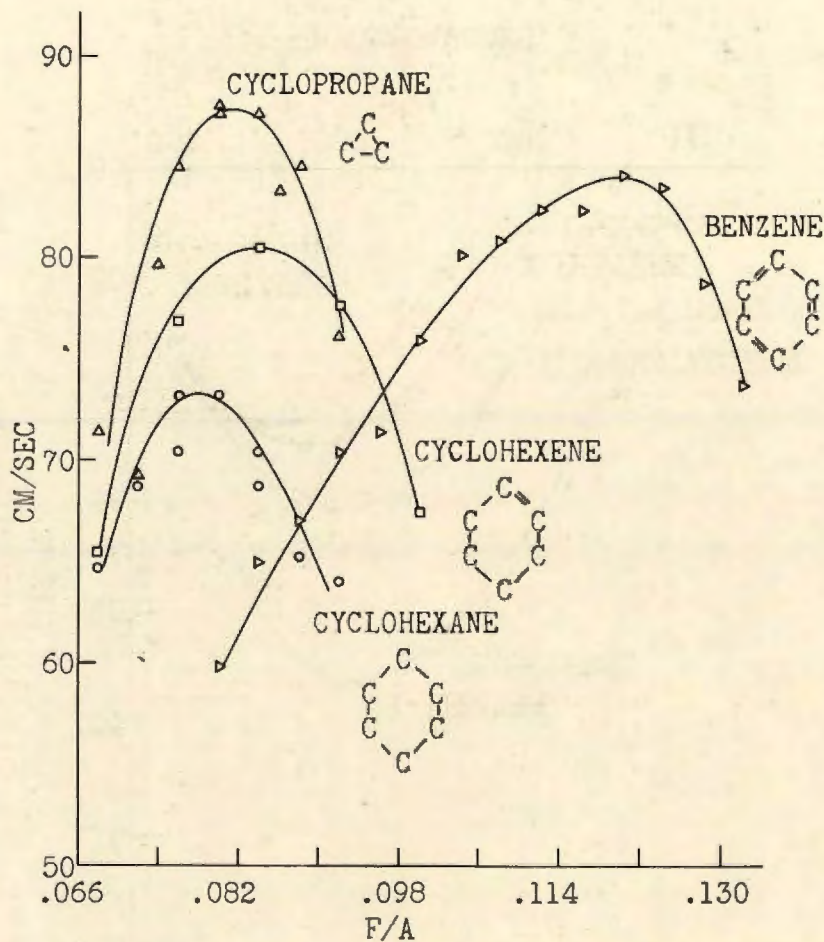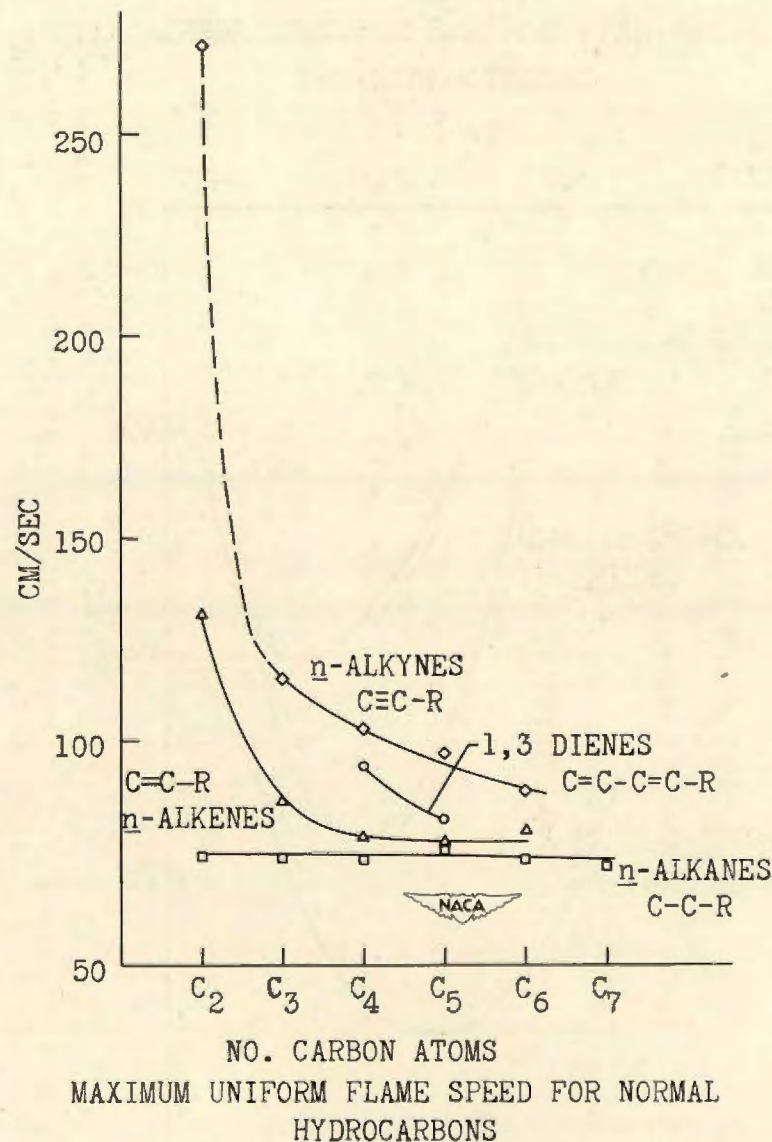
NO. CARBON ATOMS

MAXIMUM UNIFORM FLAME SPEED FOR NORMAL
HYDROCARBONS

Figure 8

COMBUSTION OF METALLIC FUELS

By Melvin Gerstein

Flight Propulsion Research Laboratory

INTRODUCTION

The problem of finding a fuel capable of achieving large thrusts at high Mach numbers and of occupying a minimum volume has led to a study of some of the factors affecting the performance of fuels. Some of these factors are

(1) Heat of combustion per pound of fuel
(2) Heat of combustion per cubic foot of fuel
(3) Maximum flame temperature
(4) Flame speed
(5) Altitude operational limits

The first two factors are related to the available energy of the propellant. In comparing fuels for performance, it is desirable to select those supplying the maximum heat release per unit weight of fuel, hence the heat of combustion per pound is important.

In considering the range of supersonic missiles in which a limited space is available for fuel storage, the second factor, the heat of combustion per cubic foot of fuel, becomes important. It is desired that the maximum energy release from any given volume of fuel that can be stored in the missile be obtained. This condition can be fulfilled by a fuel with a large heat of combustion and a high density. It is obvious that the density factor can be achieved most readily with solid propellants. Many of these solid propellants, in particular the free metals, have high heats of combustion. The use of powdered metals as fuels will be considered later.

Although the energy released from a given weight and volume of propellant are important factors affecting performance, this energy release must be accomplished under conditions favoring the development of a high thrust. In particular, the energy release must be rapid and must raise the optimum mass flow through the combustion chamber to a temperature producing maximum thrust at each flight condition. Only if these conditions are realized is the energy output useful in propulsion. The need for meeting these conditions accounts for the consideration of flame temperature and flame speed in the list of important factors.

Because most supersonic missiles are designed for high altitudes, the altitude operational limit is important. The fuel must be capable of igniting at low pressures and burning smoothly and efficiently under altitude conditions.

A proper evaluation of high energy propellants must consider all of these factors in addition to others not listed herein. The high energy fuels program of the NACA Cleveland laboratory includes research to determine the types of fuel likely to meet these requirements. Some progress toward a solution of these problems has been made.

RESULTS AND DISCUSSION

Calculations of the flame temperatures of various fuels show that metals and metallic compounds produce high temperatures. In addition many of these fuels have high heats of combustion and high densities.

Maximum Flame Temperature

The effect of the maximum flame temperature on thrust can be seen in figure 1. The thrust per unit combustion-chamber area is plotted against the temperature rise in the combustor for a missile flying at 50,000 feet. Each curve represents a flight Mach number ranging from 1.5 to 3.5. The solid lines represent an air velocity of 250 feet per second at the inlet of the combustion chamber and the broken lines indicate a variable inlet velocity calculated to give choking at the combustor exit. The bars indicate the approximate ranges of maximum temperature rise for each of three fuels, gasoline, aluminum, and beryllium. Because accurate thermodynamic data are not available for aluminum and beryllium, only the approximate temperature ranges are shown. At a Mach number of 3.5, a thrust of 3000 pounds per square foot is attained with gasoline, whereas aluminum is capable of producing a thrust of 4200 pounds per square foot and beryllium, a thrust of 5100 pounds per square foot. These values indicate that for a unit of given frontal area, beryllium produces one and two-thirds times as much thrust as gasoline or conversely, for a given thrust, a unit using beryllium as a fuel needs only three-fifths the frontal area of a unit using gasoline. This reduction of frontal area of the engine is especially important in supersonic missiles because of high external drag.

The temperatures required to obtain high thrust with metallic fuels presents a materials and cooling problem. If the temperature

rise is restricted to the maximum attainable from gasoline by burning the metals at lean mixtures, the frontal area of the engine cannot be reduced; however, the frontal area of the fuel tanks can be reduced because beryllium contains four times as many British thermal units per cubic foot as gasoline, and aluminum contains about three times as much as gasoline. When beryllium is used as a fuel, the same amount of energy can be stored in a fuel tank one-fourth the size of a gasoline fuel tank. Gasoline has a heat of combustion of 840,000 Btu per cubic foot, aluminum has a heat of combustion of 2,250,000 Btu per cubic foot, and beryllium, 3,110,000 Btu per cubic foot; these values indicate the advantages of metallic fuels. The two solid fuels discussed are not the only fuels giving high performance but illustrate the type of fuel being considered. The utility of such fuels as beryllium would be limited because of availability and cost.

In order to evaluate the performance of metallic fuels which include the study of thrust, flame temperature, and behavior of the solid products of combustion, a 2-inch burner was set up. Powdered aluminum was chosen as the first fuel because it would present most of the problems of metallic fuels and is relatively abundant and easy to handle. It did not seem feasible to burn the solid metal inasmuch as it was expected that the solid would soon become coated with oxide and combustion would stop. It was then decided that a finely divided power, 200 mesh or finer, would be the easiest form of the metal to burn, although the use of solid fuels in powdered form greatly reduces the advantage of the high density. For actual use in a missile, some method of carrying the fuel in solid form but still suitable for burning would have to be found.

A sketch of the burner used to evaluate high energy propellants is shown in figure 2. The burner consists of a 2-inch stainless-steel tube immersed in a cooling trough. The trough was necessary because the high flame temperature of aluminum caused the uncooled tube to deteriorate in a few seconds. The powder, contained in a 1-inch-diameter tube, is forced by a piston through a rapidly rotating slitted disk into the combustion chamber. Forcing the powder through the slitted disk greatly improves the powder-air distribution. The powder is ignited by means of electrodes located downstream of the injector. By the time stable combustion has been reached, the electrode wires have melted and burning continues without the aid of a spark. In more recent tests, the electrodes have been replaced by a gun-powder fuse placed in a tube mounted flush with the surface of the burner. The fuse is electrically ignited and burns for about 3 seconds, which is long enough for the flame to reach stability and continue burning. A flame holder can also be inserted in the plane of the electrodes.

A photograph of the burner with the cooling jacket removed (fig. 3) shows the long tube containing the aluminum powder and the motor that operates the rotating disk. The burner exhausts through a window to the atmosphere.

One of the biggest problems encountered is the solid product formed by combustion. If spark plugs are used to ignite the fuel, solids soon accumulate about the electrodes and eventually from 50 to 90 percent of the combustor area is blocked. If a gun-powder fuse is used to ignite the mixture and is mounted flush with the surface of the burner as previously described, deposits do not form but the burning is intermittent due to the absence of a flame holder. The accumulation of solids on a circular flame holder after a 50-second run is illustrated in figure 4. The clean flame holder blocked only about 30 percent of the area, but the deposits soon doubled the area blocked. The use of a cylindrical rod as a flame holder gave a similar result although the original blocked area was only about 15 percent. The only solution that presented itself was to clean the flame holder during the run. The cleaning was accomplished by moving the rod back and forth through a close-fitting sleeve. This type of flame holder is being investigated at the present time. Preliminary results indicate that the moving flame holder has a tendency to stop as solids begin to accumulate, but, if kept moving, remains clean during the entire run.

In addition to the flame holder, any projection or rough spot in the combustion chamber will accumulate solids. The deposits formed on a thermocouple probe and on the smoothly machined parting line between the combustion chamber and the nozzle connected by flanges is shown in figure 5. These flanges were removed in later burners and the combustion chamber and nozzle are formed from a continuous piece of tubing with no parting line. This construction has considerably reduced the formation of deposits.

The accumulation of solids makes the evaluation of metallic fuels difficult because the change in the cross-sectional area of the combustion chamber changes the pressure drop through the burner and as a result also the thrust. Attempts are being made at the present time to measure the thrust obtained using aluminum as a fuel. A water-cooled thrust target is being used for this purpose.

Estimates of the combustion efficiency have been made by an analysis for free aluminum in the solid deposits. The solids accumulated at the flame holder contain about 20 percent free aluminum, which indicates a combustion efficiency of 80 percent, whereas the solids in the exhaust contain only 6 percent free aluminum, indicating a combustion efficiency of 94 percent.

Flame Speed

Another factor affecting fuel performance, which is being investigated, is flame speed. For a unit of given frontal area, there is an optimum mass flow through the combustion chamber governed by flight conditions. Although it is possible to burn many of the conventional fuels at high velocities to reach the optimum flow, some of the high density hydrocarbons do not burn rapidly enough. The addition of flame promoters, however, might make these fuels more suitable. For this reason a study is being made of the flame speeds of various substances. At present only the rate of flame propagation in homogeneous, quiescent mixtures is being investigated. A study of the effect of turbulence will be made at a later date.

The flame-speed measuring apparatus is shown in figure 6. The flame tube is made of pyrex, 1 inch in diameter and 8 feet long. One end of the tube is equipped with a ground-glass joint, which can be removed to open the tube to the atmosphere just before firing. Fuel is admitted from the closed end of the tube and is measured by a manometer. Air is introduced from each end of the tube to facilitate mixing. Enough air is added to bring the pressure inside the tube to atmospheric pressure. Mixing is accomplished by means of an iron cart with disks at each end. The cart is moved back and forth inside the tube by means of a magnet. This method of mixing was used to avoid handling the inflammable mixture any more than necessary because of the sensitivity of diborane-air mixtures to ignition. Even with these precautions, some mixtures exploded prematurely, which may have been due to the heat of mixing. The effectiveness of the mixing was determined by the reproducibility of the results after different intervals of mixing.

The rate of flame propagation is measured by means of photo cells connected to an electronic timer. The timer and photo cell circuit were calibrated by means of a rotating mirror. An accuracy of about 3 percent in the region of five-thousandths of a second was found. This time interval is the shortest measured in this investigation.

The rate of flame propagation in diborane-air mixtures is shown in figure 7. The rate of flame propagation in centimeters per second is plotted against fuel-air ratio. The curve extends almost to the stoichiometric fuel-air ratio. Attempts to measure the flame speed at fuel-air ratios of about 0.09 led to mixtures which preignited each time; it is expected however that this mixture would give a flame speed near the maximum and that it would require very little energy to cause ignition. Investigations to eliminate

preignition of diborane-air mixtures are being conducted in order to
study the remainder of the curve.

The speeds attained with lean mixtures are high and reach
approximately 5000 centimeters per second at a fuel-air ratio of 0.065.
Hydrocarbons in the same tube give peak flame speeds of about
100 centimeters per second. Investigations are now being made to
determine whether diborane has a catalytic effect on the flame speeds
of conventional fuels. It may prove to be a useful additive.

SUMMARY

These preliminary investigations have shown that (1) metallic
fuels can be burned in a ram-jet combustion chamber to produce stable
flames and (2) diborane is capable of burning at high velocity.
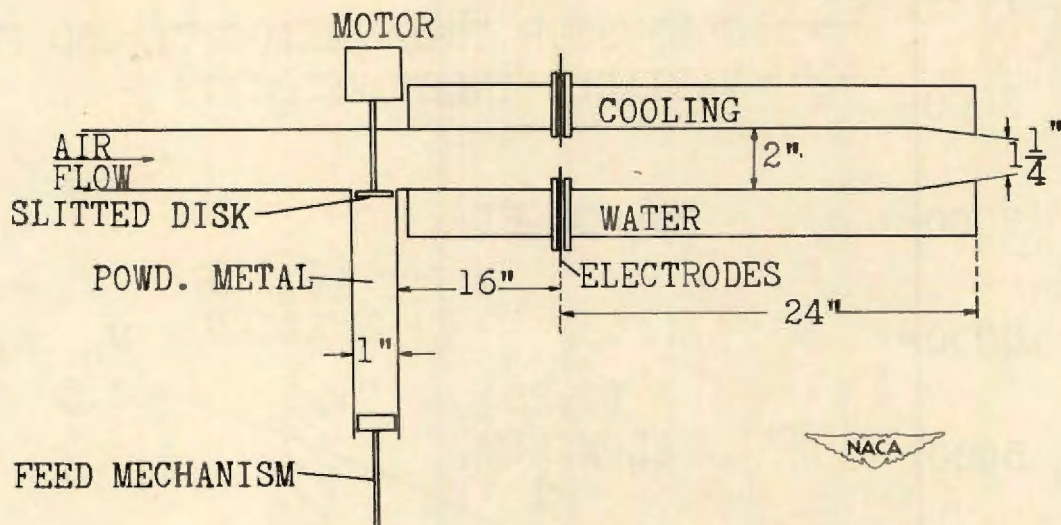
986-G
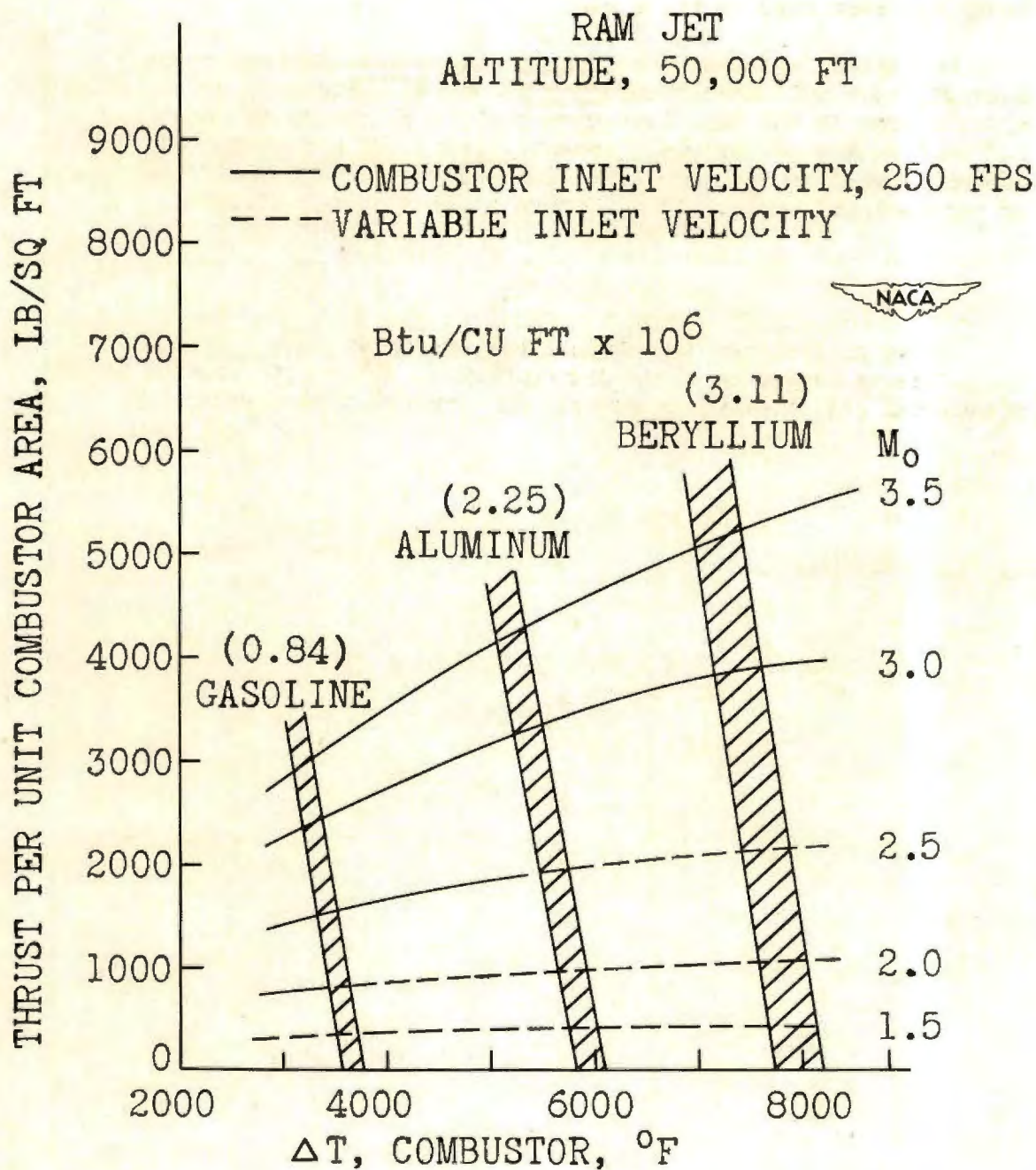
Effect of temperature rise on performance.
Figure 1.

POWDERED METAL RAM JET.

Figure 2.

NACA
C- 18138
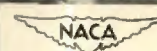3. 14. 47
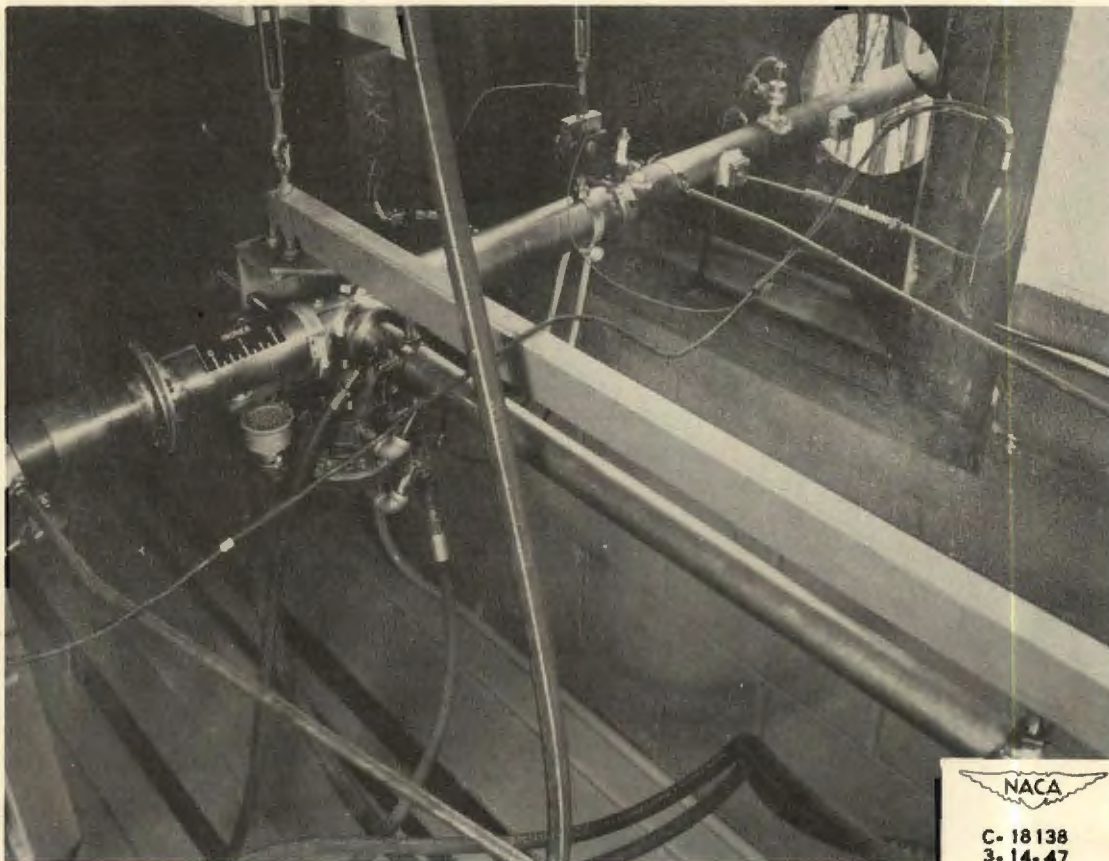
Two-inch combustor for metallic fuel.
Figure 3.

986-G
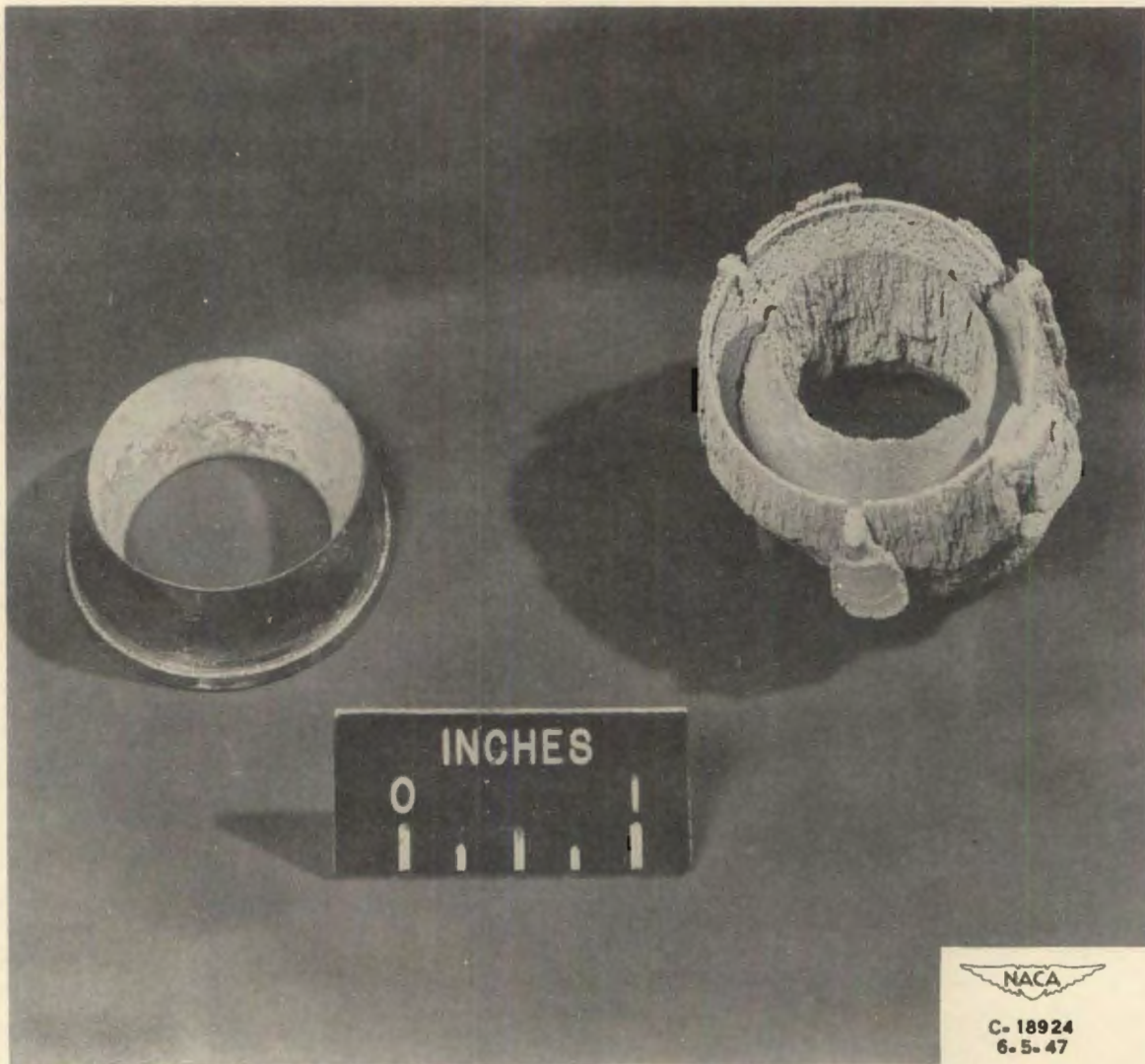
FLAME HOLDER DEPOSITS

Figure 4.

986-G
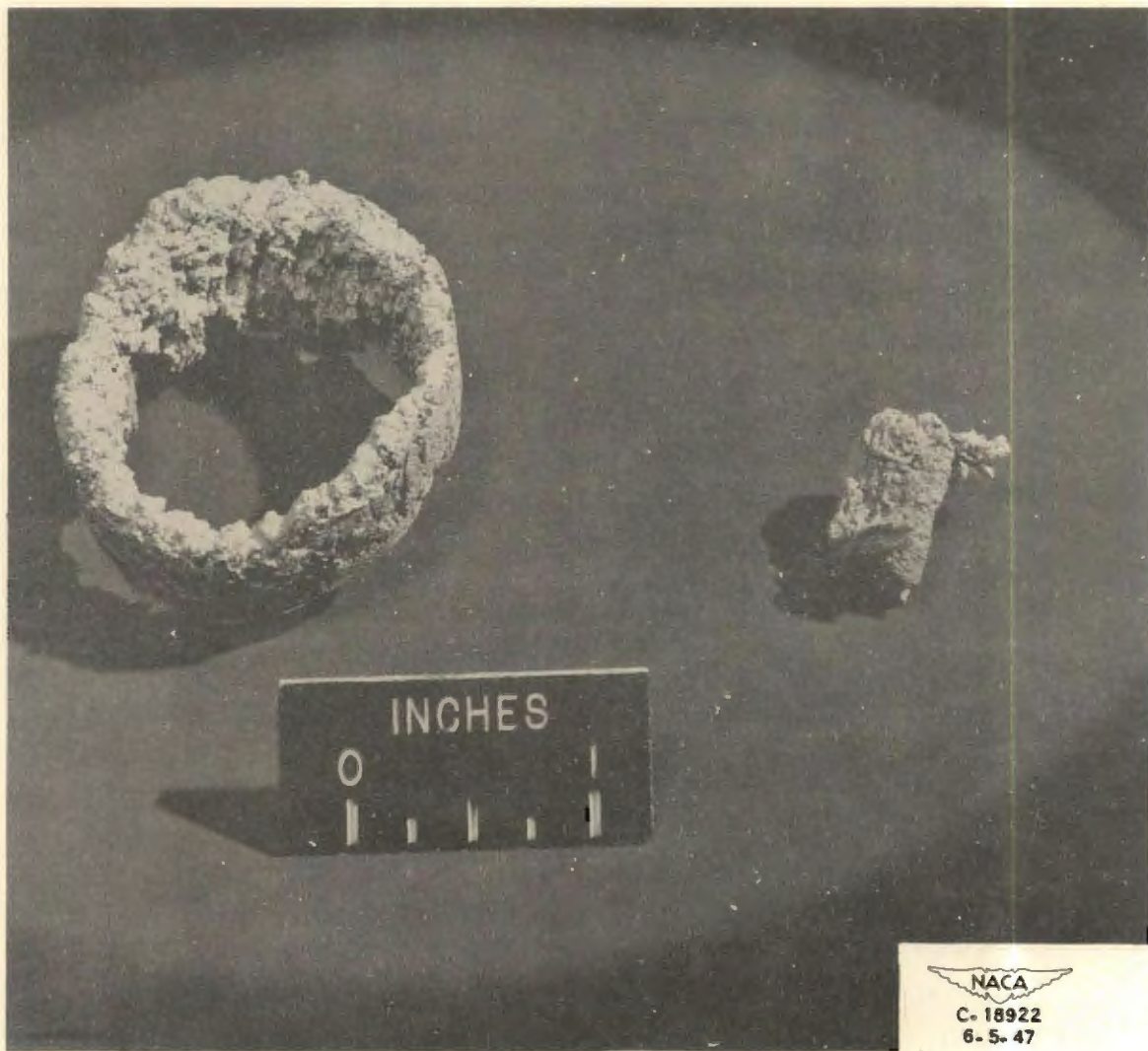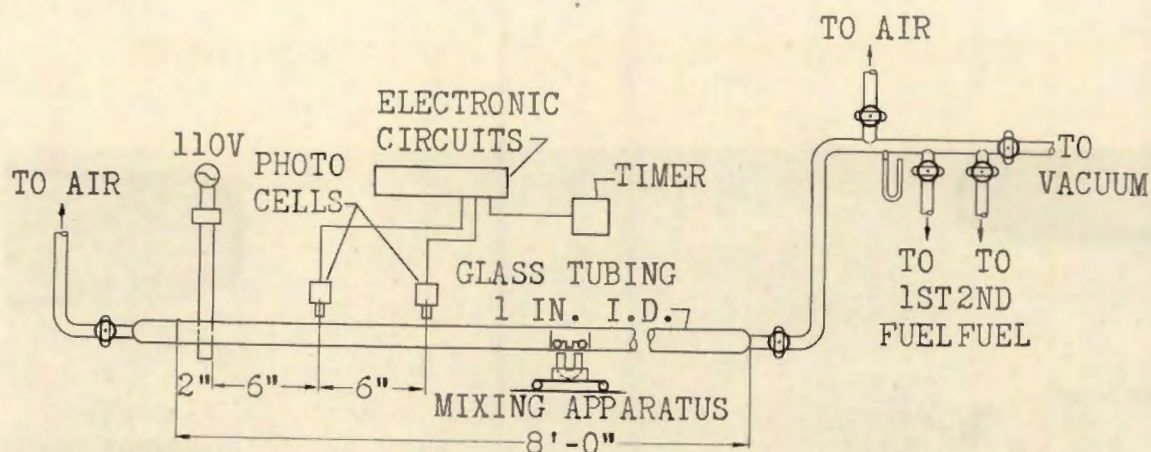

DEPOSITS ON NOZZLE AND PROBE

Figure 5.

FLAME SPEED MEASURING APPARATUS
Figure 6.
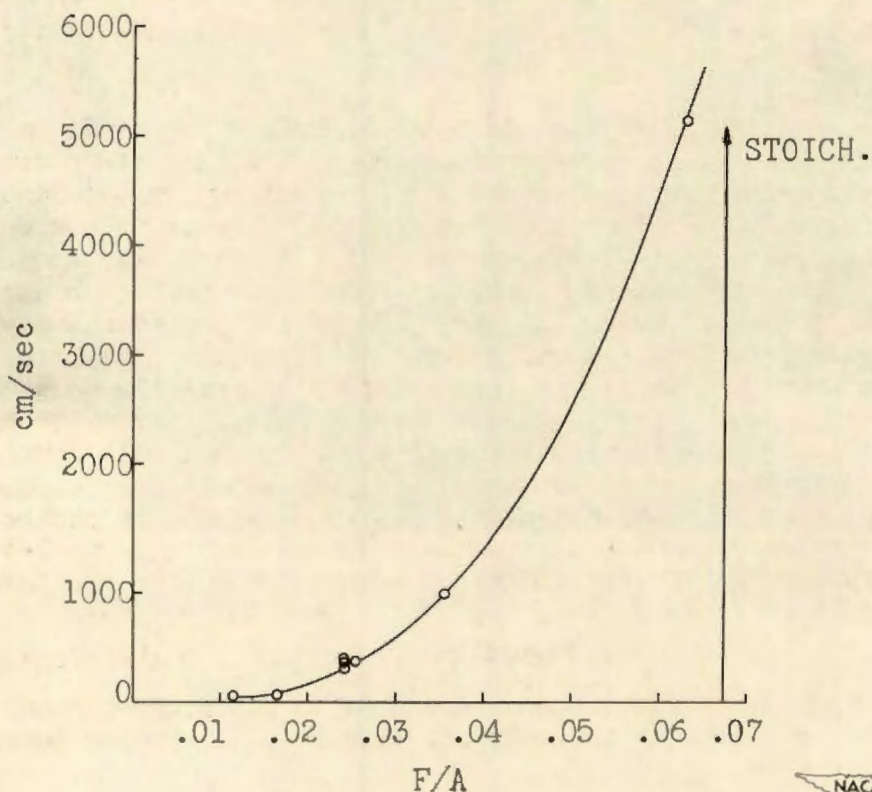
DIBORANE FLAME SPEED
Figure 7.

DETERMINATION OF CARBON-HYDROGEN GROUPS OF HYDROCARBONS

BY INFRARED MEASUREMENTS (1.10 TO 1.25 MICRONS)

By Robert R. Hibbard

Flight Propulsion Research Laboratory

INTRODUCTION

During the past 25 years, a considerable amount of research
has been devoted to the development of methods for the analysis
of fuels. Procedures are now available that yield satisfactory
accuracies in the determination of the amount of paraffin, cyclo-
paraffin, olefin, and aromatic in gasoline-range samples and con-
siderable progress has been made in developing methods for a
similar analysis of heavier stocks. In order to more completely
characterize a fuel, it would be desirable to have, in addition
to the above data, information on the amount of chain branching
in paraffins and the degree of paraffinic substitution in cyclo-
paraffins and aromatics.

The limitations of methods that classify a fuel only as to
its aromatic, olefin, cycloparaffin, and paraffin content are
illustrated in table I, in which are listed three of the nine
heptanes. The heptanes vary in molecular structure from a com-
pound that has all seven carbon atoms in a single chain to one
that still has seven carbon atoms but has three carbons branching
from a four carbon chain. All are 100-percent paraffin and should
be so determined by the usual methods of analysis. All have
7 carbon atoms and 16 hydrogen atoms and therefore the same chem-
ical formula and the same carbon-hydrogen ratio. The first com-
pound is the well-known reference fuel, n-heptane, with zero
rating on the octane number scale, and the last is triptane, an
excellent fuel in a spark-ignition engine. Methods of analysis,
which group these compounds together, do not give all the data
necessary for the differentiation of these fuels. In the last
two columns of table I are listed the number of CH_3 and

CH_2 groups per molecule. These fuels show marked differences
in the relative number of these groups with the higher octane
number being found for the compound that has the greater number
of CH_3 groups.

Another example of the limitations of conventional methods of analysis is shown in table II in which the molecular structures of two of the eight C_9 aromatics are given. Both fuels are 100-percent aromatic by the usual methods of analysis, both have nine carbon atoms and twelve hydrogen atoms per molecule and therefore the same chemical formula. Again there are differences between these fuels in their engine performance. In the F-4 test the first aromatic (1,3,5-trimethylbenzene) has a better rich rating that the second compound (n-propylbenzene), although the difference is not as marked as it is between n-heptane and triptane. In the last three columns of table II are listed the number of CH_3, CH_2, and aromatic CH groups per molecule. Again, in this case, better knock-limited performance is obtained with the fuel having the greater number of CH_3 groups.

APPARATUS AND CALCULATIONS

The previous paper on the effect of molecular structure on knock-limited performance of aromatics showed that not only the number of carbon-hydrogen groups, but also their position on the ring, is important. There are analytical methods that completely identify hydrocarbons (that is, show both the number of groups and the exact position). However, these methods cannot be applied to fuels that have a very large number of components and because the numbers of these groups apparently have considerable bearing on fuel performance, it was considered important to find methods for their determination.

In the middle thirties, work done by several investigators at the Bureau of Standards and summarized in reference 1 indicated that the various carbon-hydrogen groups could be determined by absorption spectroscopy in the near infrared. The near infrared is the region just beyond the red limit of human vision and data are obtained in this region by use of an absorption spectrometer.

The essential components of an absorption spectrometer are shown in figure 1. A light source emits a wide range of wavelengths, much wider than the human eye can see. The light, in passing through the sample in the cell, has some wavelengths selectively removed, or absorbed, by the sample. The portion of the radiation that is not absorbed by the sample enters the prism and is variably refracted to split the radiation into its various wavelength components. Radiation of a relatively narrow range of wavelengths pass through the exit slit and are measured by a thermocouple. An amplifier and recorder complete the apparatus. The wavelength of the radiation being measured can be varied by rotation of the prism.

One of the early obstacles in the use of the near infrared region was the necessity of using an instrument of greater resolving power than those commonly available. However, it was found that a few simple modifications of a Perkin-Elmer infrared spectrometer would give an instrument that was satisfactory for work in this region. The Perkin-Elmer instrument is a common but very good small prism spectrometer and is found in many industrial laboratories. A tungsten ribbon lamp was substituted for the Globar source that is supplied with the instrument and the rocksalt prism was replaced with one of glass because glass has better dispersion in the near infrared (that is, spreads out the refracted radiation more) than does rock salt.

When an absorption spectrometer is used to "see" the colors of fuels in the near infrared, the CH_3, the CH_2, and the aromatic CH groups are found to absorb light at slightly different wavelengths. Table III is a table of these wavelengths. The aromatic CH groups in hydrocarbons absorb light that has a wavelength of 1.14 microns (a micron μ being 1/1000 of a millimeter), the CH_3 group absorbs wavelengths of 1.19 μ, and the CH_2 group, 1.21 μ. Because there is a spread of only 0.02 μ between the wavelengths at which the CH_3 and CH_2 groups absorb, good resolving power is required.

In order to put this tabular data into a graphical form, figure 2 shows an idealized spectrum of a paraffin hydrocarbon in the near infrared. The function of the amount of light absorbed plotted against the wavelength of light shows that the CH_3 group has peak absorption at 1.19 μ and the CH_2 at 1.21 μ. If the sample contained only CH_3 groups, the spectrum would be that shown by the light solid line and if it contained only CH_2 groups, the dotted line would result. The work at the Bureau of Standards showed that, if the proper function were used to express the amount of light absorbed, the height of these inner peaks would be almost directly proportional to the concentration of these groups for any compound in a single class of hydrocarbons. This fact indicates that a spectrometer can be calibrated with a few typical hydrocarbons and then used to determine the concentration of the different types of carbon-hydrogen group in any compound or mixture of compounds of the same class. This procedure differs from the usual absorption spectroscopy method in which individual hydrocarbons can only be determined after calibration with those same materials. The infrared has been widely used for the analysis of refinery streams such as liquified petroleum gases and alkylates

in which there are only a moderate number of compounds present. In
these infrared analyses of refinery streams, as many as 10 hydro-
carbons have been determined simultaneously. However, in fuels,
and especially in the high-boiling jet fuels, the number of com-
pounds present generally runs into the tens or hundreds of thousands.
The usual infrared analysis cannot be applied to these complex mix-
tures, whereas the near infrared analysis of functional groups should
be completely operable.

Because most paraffins contain both CH_3 and CH_2 groups,
the spectrum actually obtained is that shown by the heavy solid
line of figure 2. There is an interference by the CH_2 groups
in the determination of CH_3 groups at 1.19 μ and a similar
interference by CH_3 in the determination of CH_2 groups at
1.21 μ. It is therefore necessary to use a simultaneous equation
form of solution shown in table IV. The average number of CH_3
and CH_2 groups per molecule (these are the integer values shown
in the last columns of tables I and II) are the unknowns x and
y, respectively. The function of light absorption, which is nearly
directly proportional to the concentrations of these groups, is the
molar extinction ϵ and is defined by the equation given in
table IV. Inasmuch as figure 2 showed that the function ϵ varies
with wavelength, the wavelength must be stipulated. Simultaneous
equations of the type given in table IV can then be set up. The
coefficients A, B, C, and D are constants and are obtained
by calibrating the instrument with a few typical compounds of the
same class. The values of ϵ can be experimentally determined
and for paraffins would be determined at 1.19 and 1.21 μ. When
the values for ϵ at the two wavelengths and for the four coef-
ficients are known, the quantities x and y (the number of
CH_3 and CH_2 groups per mole) can be readily calculated.

The values for A, B, C, and D do not depend on the
compound and can be applied to any compound of a given class or
to mixtures containing any number of components. At the bottom
of table IV are the values determined by the NACA Cleveland
laboratory and by the Bureau of Standards for these coefficients.
When, in addition to the CH_3 and CH_2 groups, the aromatic
CH group is being analyzed, ϵ must be determined at a third
wavelength (1.14 μ) and additional coefficients must be estab-
lished by calibration to give three simultaneous equations.

RESULTS AND DISCUSSION

The Bureau of Standards showed the potentialities of the near infrared analysis about ten years ago but it seems to have been little used, possibly for two reasons: First, the Bureau used a very large spectrometer of a type not found or easily matched in industrial laboratories. And secondly, although satisfactory results were obtained with paraffins, too few cycloparaffins and aromatics were studied to establish the accuracies obtainable on these two classes of hydrocarbons. Therefore, the aims of this investigation were to determine (1) whether a commercially available, small prism spectrometer could be easily modified to yield adequate data in the near infrared and (2) whether satisfactory analytical results could be obtained on classes of hydrocarbons other than paraffin.

Optical tests proved the modified Perkin-Elmer spectrometer to be capable of separating absorption bands, which are only $2/1000$ μ apart. Additional proof of the worth of the instrument lies in the agreement between the calibration coefficients A, B, C, and D obtained by NACA and by the Bureau of Standards (table IV). In absorption spectroscopy it is unusual to obtain any closer agreement in calibration constants even with supposedly identical instruments. When values are obtained that are in as good agreement as those shown, it can be concluded that the instruments are substantially equal for the near infrared analyses. As to the second aim, to determine whether accurate results could be obtained on all classes of hydrocarbons, the data presented herein will show the degree of success attained.

Paraffins

Applying the constants shown in table IV to the analysis of paraffins yielded the results found in table V. The structures of two typical paraffins are shown in table V. These compounds are typical paraffins in that the carbon atoms are either in straight chains as shown for n-heptane, or in branched structures as shown for isooctane. Paraffins always have only one bond between adjacent carbon atoms. Typical results only are given. It was determined by near infrared analysis that n-heptane has 2.0 CH_3 groups and the structure shows it to have 2.0; the

error is therefore zero. For this compound, the determined number of CH_2 groups is 5.4; the actual number, 5.0; and the error, 0.4. Similarly, for isooctane the determined number of CH_3 groups is 5.2 and the number shown by the structure is 5.0; for the CH_2 groups, 0.8 is determined and 1.0 is actually present.

It should be emphasized at this point that the inaccuracies are not experimental errors. The experimental error is of the order of 0.05 for each type of carbon-hydrogen group. The analytical errors arise from the lack of true constancy of absorption of the same groups in different compounds. For instance, one CH_3 in n-heptane does not absorb light to exactly the same extent as does one CH_3 group in isooctane. Therefore, when it is assumed that the optical properties of these groups are identical in all compounds, and that is the assumption made by setting up A, B, C, and D as constants, analytical inaccuracies result.

The average and maximum values of error observed for these 4 plus 17 other paraffins examined are shown at the bottom of table V. The trend in the errors found for 21 paraffins is not discernible as a function of either molecular weight or the amount of branching, and presumably the same accuracy would be obtained on any number of the more than 100,000 paraffins, which are possibly present in a wide-cut jet fuel. The average errors for paraffins (0.24 for CH_3 and 0.28 for CH_2 groups) are almost identical to those obtained by the Bureau of Standards with a much larger spectrometer and with different paraffin compounds. It is therefore demonstrated that a commercially available small prism spectrometer yields useful analytical data in the near infrared region.

Cycloparaffins

At the top of table VI are the structures of three typical cycloparaffins, which, like the paraffins, have only a single bond joining adjacent carbon atoms, but differ from the paraffins in that at least a part of the molecule is in a ring. The cycloparaffins and paraffins are very much alike in both chemical and physical properties and, because methods are not available for separating them, it is necessary to use the same spectrometer calibration for both classes (that is, the numerical values for the coefficients A, B, C, and D found for paraffins must be used for cycloparaffins).

Listed in table VI are the results obtained on four cyclopentanes. For the first compound, cyclopentane, 3.2 CH_3 groups are determined where none is actually present and only 1.7 CH_2 groups where 5.0 should have been found. The third compound, ethyl cyclopentane, has a determined number of 3.1 CH_3 groups where only 1.0 is present and 2.9 CH_2 groups

where 5.0 are shown by the structure. The average analytical errors for these four and eight additional compounds are 1.9 for the CH_3 and 1.5 for the CH_2 groups. These errors are so large that they obviously make the results useless.

Because a method that works for paraffins and not for cycloparaffins is of limited use, a search was made for some independently determinable value that could be used as a correction factor. Such a factor was found to be the weight percent ring as determined by the method given in reference 2. The weight percent ring is the percent of the total number of carbon atoms in the ring and is 100 percent for cyclohexane, 100 percent for cyclopentane, and 71 percent for ethyl cyclopentane.

In figure 3, the errors in the determination of CH_3 groups are plotted against the independently determinable weight-percent-ring factor. The data for four cyclopentanes (table VI) are shown by the circles on figure 3. Inasmuch as this plot is to be used as a correction factor, it is desirable to assume zero correction at zero-percent ring and a linear correction as a function of percent ring. Therefore, a straight line is drawn through the origin. Data points for the four cyclopentanes fall on the indicated line; however, the different series of cycloparaffins show deviations which require a different line to be drawn for each series. For instance, the cyclohexane data requires a line of about one-half the slope of the cyclopentane line. The decalin series closely approaches the cyclohexanes in their deviations and the two ring cyclohexanes are similar to the cyclopentanes. Inasmuch as the method given in reference 2 does not differentiate between the types of cycloparaffin ring present, an average line must be used when only the weight percent ring can be determined, which is the usual case.

A similar plot for the deviations in the determination of CH_2 groups is given in figure 4. In this figure, the sign of the deviations is negative. The cyclopentane data points fall on the line of greatest slope, the decalins require but little correction, and the cyclohexanes require considerably more correction. Some justification may be required for drawing the indicated line through the two ring cyclohexane points (fig. 4). In this semiempirical approach, it was necessary to have a zero correction at zero-percent ring; therefore, the line must run through the origin. In the paraffin data, where there were no complicating factors such as weight percent ring, the average deviations were about 0.3 group and the maximum 0.6 group. It is

therefore not surprising that the points should fall away from
their respective lines by the amounts shown. It is more sur-
prising that such good agreement with a straight line function
was found for so much of the data. Again in this figure the
average line drawn must be used in cases when the type of cyclo-
paraffin is unknown.

In order to determine the amount of error introduced by use of
the average correction factors for the different series, average
lines were used to obtain the corrected data shown in table VII.
At the top of this table are the molecular structures for two
additional series of cycloparaffins: 3-methylbicyclohexyl, which
has two joined cyclohexane rings, and isopropyl decalin, which
has two six-member rings with two carbon atoms common to each
ring. Listed in this table are the determined and correct values
for the number of CH_3 and CH_2 groups for one of each of the
four series of cycloparaffins. For 3-methylbicyclohexyl, the
analytical results corrected by use of the average lines are
1.6 CH_3 groups where 1.0 is actually present and 8.8 CH_2 groups
where 9.0 should have been found. For isopropyl decalin,
1.4 CH_3 groups instead of 2.0 are determined and 8.0 CH_2 groups
instead of 7.0. The average analytical errors of 0.56 CH_3 and
0.86 CH_2 group are admittedly large.

These errors, however, are a considerable improvement over
the uncorrected results observed previously and represent the
maximum probable error in the analysis of a cycloparaffinic fuel.
Errors of this order would be obtained if the cycloparaffins in
a fuel were all of a single series, the series being unknown. If
methods, which will allow the determination of the type of cyclo-
paraffin present in a fuel, are developed in the future, the
probable errors in analysis will be the 0.08 and 0.16 values
shown at the bottom of table VII. These values were obtained by
using the appropriate correction lines for each series rather
than the average lines. If a cycloparaffin sample were truly
average in composition (that is, if equal amounts of the four
series were present), then the analytical error should be close
to these lower values since the average correction line would
be very nearly the ideal one.

Single Ring Aromatics

The molecular structures of three single ring aromatics are
shown in table VIII. In all aromatics there is a six-carbon-atom
ring with alternate single and double bonds between adjacent

carbon atoms. The aromatics can be easily separated from the paraffins and cycloparaffins and therefore a new calibration was made yielding new values for the coefficients.

The simplest single ring aromatic is benzene. It has neither CH_3 nor CH_2 groups, but has 6.0 aromatic CH groups. For benzene, the number of groups determined by near infrared analysis is 0.0 CH_3, 0.1 CH_2, and 5.9 aromatic CH groups. For p-xylene, the determined number of CH_3 groups is 2.3 and the actual number shown by structure is 2.0; the determined number of CH_2 is 0.1 where it should have been zero; and 3.0 aromatic CH groups are found by analysis where 4.0 is the correct number. For 15 single ring aromatics, the average errors are those indicated in table VIII. In this class of compounds the deviations were random except when para-substitution was present. Aromatics are para-substituted when the two carbon atoms on opposite sides of the ring have either CH, CH_2, or CH_3 groups attached to them. In this case, the determined values for the number of aromatic CH groups were always low, the results on p-xylene being an example. No independent method for estimating the degree of para-substitution is known and therefore these inaccuracies in the determination of the aromatic CH group must be accepted.

Two Ring Aromatics

Molecular structures for two types of two ring aromatics are shown in table IX. These may be compounds like 3-methylbiphenyl, which has two aromatic rings joined by a single bond, or like tetralin, which has an aromatic ring joined with a cycloparaffin ring with two carbon atoms common to both rings. There are many other classes of aromatic compounds with two or more rings. For 3-methylbiphenyl, the near infrared analysis shows 1.3 CH_3 groups, -0.2 CH_2 group, and 8.7 aromatic CH groups where the correct values are 1.0, 0.0, and 9.0, respectively. For tetralin, the determined values for these groups are 0.1, 4.0, and 3.7 where the actual values are 0.0, 4.0, and 4.0. For the nine two ring aromatics examined, the average errors are 0.12 CH_3, 0.20 CH_2, and 0.48 aromatic CH group. Again para-substituted compounds yielded low results in the determination of the aromatic CH group.

Blends

All the results shown have been obtained on single pure compounds and show the magnitude of errors that might be expected in the analysis of single components. They also serve as a basis for estimating the maximum probable inaccuracies that would be expected in the analysis of multicomponent fuels. Because most of the deviations observed in all these single component data were random (that is, there was a shotgun pattern of plus and minus errors), it would be expected that these plus and minus deviations would largely cancel out in the analysis of blends containing a large number of components. This should also be true in the analysis of fuels where thousands or even hundreds of thousands of compounds are likely to be present. Tables X to XIII show the results obtained on blends prepared from pure hydrocarbons.

The data resulting from the analysis of five blends of paraffins, each containing ten components, are shown in table X. The true number of CH_3 and CH_2 groups per mole are not integer values as they were for the single compounds but are average numbers calculated from the known compositions of these blends. The average analytical errors for these five blends are 0.08 CH_3 and 0.13 CH_2 group. These results do not deviate extensively from the limits of experimental measurements and are, as expected, an improvement over the average errors of about 0.3 group, which was obtained for 21 paraffins examined singly. The data in table X show the order of accuracy that would be expected in the analysis of the paraffinic fractions of hydrocarbons.

Five cycloparaffin blends yielded the results show in table XI. In this case, the method described in reference 2 was used to determine the weight percent ring and the infrared data were corrected by using the average lines from figures 3 and 4. These blends were prepared containing relatively large amounts of first one, then another of the various series of cycloparaffins. This approach appears to be unfavorable but parallels the condition existing in the analysis of fuels where the relative amounts of the various series are unknown. The average errors of 0.20 and 0.37 for the CH_3 and CH_2 groups, respectively, are somewhat higher than those obtained for paraffins, as would be expected.

Paraffin - cycloparaffin blends were analyzed and the results are shown in table XII. The analyzed weight percent ring is given for these blends along with the determined and true content

of CH_3 and CH_2 groups. The 0.25 average error in the determination of CH_3 groups is higher than anticipated but the 0.15 average error for CH_2 groups is about that expected.

For blends of single ring aromatics, the results shown in table XIII were obtained. The average analytical errors, less than 0.1 for the three groups, are very low. In fact, the errors are better than should be expected in the analysis of aromatic fuels because it is possible that the fuel samples could have moderate or high amounts of para-substituted components and, under these circumstances, would show a lower concentration of aromatic groups than was actually present.

Petroleum Streams

In addition to the work on pure hydrocarbons, analytical data were obtained on petroleum streams. Inasmuch as there is no alternate method for obtaining actual CH_3, CH_2, and CH content, the results of the near infrared determination cannot be checked for accuracy. Therefore, only two paraffinic streams have been selected to show what can be done with actual fuel samples. In table XIV are the results for an alkylate and for a hot-acid octane, both predominately C_8 paraffins. From molecular weight determinations, the average number of carbon atoms per molecule has been calculated and the results of near infrared determination of CH_3 and CH_2 groups are shown; also calculated was the ratio of CH_3 to CH_2 groups, which is a measure of the amount of branching in a paraffin. The more highly branched the compound, the higher is the ratio. The values for alkylate are found to be 4.4 CH_3 and 1.8 CH_2 groups per mole, giving a ratio of 2.4:1. For hot-acid octane, the analysis shows 4.6 CH_3 and 0.8 CH_2 groups, giving a ratio of 5.8:1. Because there is no direct method to check these results, it can only be suggested that knock rating might parallel the CH_3/CH_2 ratio since, in general, the more highly branched the paraffin, the higher the octane number. In this case the F-4 rich rating with 4 ml TEL was used and gave a performance number of 140 for alkylate and slightly over 200 for hot-acid octane. On this basis, these knock rating results appear to confirm the infrared analyses.

SUMMARY

It is believed that the near infrared method can be used to determine the concentrations of carbon-hydrogen groups in fuel samples. This information has not been previously obtainable and should be a powerful tool in hydrocarbon research.
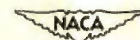
REFERENCES

1. Rose, Frank W., Jr.: Quantitative Analysis, with Respect to the Component Structural Groups, of the Infrared (1 to 2µ) Molar Absorptive Indices of 55 Hydrocarbons. RP 1072, Jour. Res. Nat. Bur. Standards, vol. 20, Jan.-June 1938, pp. 129-157.

2. Lipkin, M. R., Martin, C. C., and Kurtz, S. S., Jr.: Analysis for Naphthene Ring in Mixtures of Paraffins and Naphthenes. Ind. and Eng. Chem. (Anal. ed.), vol. 18, no. 6, June 1946, pp. 376-380.

TABLE I
TYPICAL HEPTANES (C_7H_{16})

STRUCTURE	PER-CENT PARAF-FIN	NO. C ATOMS/ MOLE	NO. H ATOMS/ MOLE	NO. CH_2/ MOLE	NO. CH_3/ MOLE
$H_3-C-C-C-C-C-C-C-H_3$ (with H_2 H_2 H_2 H_2 H_2)	100	7	16	5	2
$H_3-C-C-C-C-C-CH_3$ (with H_2, CH_3 branch, H_2 H_2, H)	100	7	16	3	3
$H_3C-C-C-CH_3$ (with H_3 H_3 branches, CH_3 below, H)	100	7	16	0	5

TABLE II
TYPICAL NINE CARBON AROMATICS (C_9H_{12})

NACA

STRUCTURE	PER-CENT ARO-MATIC	NO. C ATOMS/ MOLE	NO. H ATOMS/ MOLE	NO. CH_3/ MOLE	NO. CH_2/ MOLE	NO. ARO CH/ MOLE
(trimethylbenzene ring structure with three CH_3 groups)	100	9	12	3	0	3
(benzene ring with $-C-C-CH_3$ chain, H_2 H_2)	100	9	12	1	2	5

TABLE III

NEAR INFRARED ABSORPTION
WAVELENGTHS
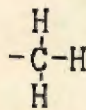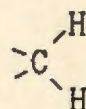
WAVELENGTH (MICRONS)	FUNCTIONAL GROUP	
1.143	AROMATIC	$\overset{\cdot}{C}{-}H$
1.190	PRIMARY	$-\overset{\displaystyle H}{\underset{\displaystyle H}{C}}{-}H$
1.212	SECONDARY	$\overset{\displaystyle H}{\underset{\displaystyle H}{>}}C$

TABLE IV

FORM OF CALCULATIONS

x = AVERAGE NO. CH_3 GROUPS PER MOLECULE
y = AVERAGE NO. CH_2 GROUPS PER MOLECULE

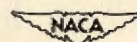$$\epsilon_{(\mu)} = \frac{\text{LOG} \dfrac{100}{100 - (\% \text{ LIGHT ABSORBED BY SAMPLE})}}{\text{CONC. OF SAMPLE} \times \text{THICKNESS OF CELL}}$$
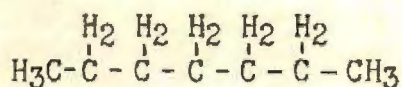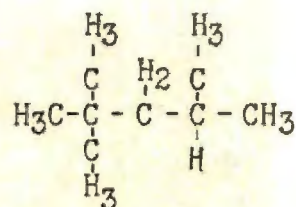
$\epsilon_{1.190\mu} = Ax + By$
$\epsilon_{1.212\mu} = Cx + Dy$

	A	B	C	D
NACA	0.0260	0.0098	0.0066	0.0194
NBS	.0270	.0074	.0063	.0199

TABLE V
PARAFFINS

$$H_3C-\underset{\underset{H_2}{|}}{C}-\underset{\underset{H_2}{|}}{C}-\underset{\underset{H_2}{|}}{C}-\underset{\underset{H_2}{|}}{C}-\underset{\underset{H_2}{|}}{C}-CH_3$$

n-HEPTANE

ISOOCTANE

COMPOUND	NO. CH$_3$/MOLE			NO. CH$_2$/MOLE		
	DET'D	TRUE	Δ	DET'D	TRUE	Δ
n-HEPTANE	2.0	2	0	5.4	5	0.4
n-HEXADECANE	2.2	2	.2	13.7	14	- .3
3-METHYL HEXANE	3.0	3	0	3.1	3	.1
ISOOCTANE	5.2	5	.2	.8	1	- .2
AVERAGE (21 PARAFFINS) MAXIMUM			0.24 .5			0.28 .6

TABLE VI

CYCLOPARAFFINS
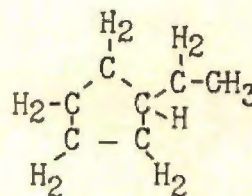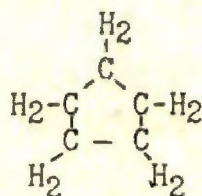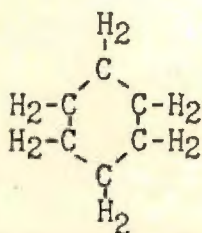
COMPOUND	NO. CH$_3$/MOLE			NO. CH$_2$/MOLE		
	DET'D	TRUE	Δ	DET'D	TRUE	Δ
CYCLOPENTANE	3.2	0	3.2	1.7	5	-3.3
METHYL CYCLOPENTANE	3.4	1	2.4	1.8	4	-2.2
ETHYL CYCLOPENTANE	3.1	1	2.1	2.9	5	-2.1
ISOPROPYL CYCLOPENTANE	3.8	2	1.8	2.0	4	-2.0
AVERAGE (12 CYCLOPAR.) MAXIMUM			1.90 3.2			-1.46 -3.3

TABLE VII
CYCLOPARAFFINS (CORRECTED)
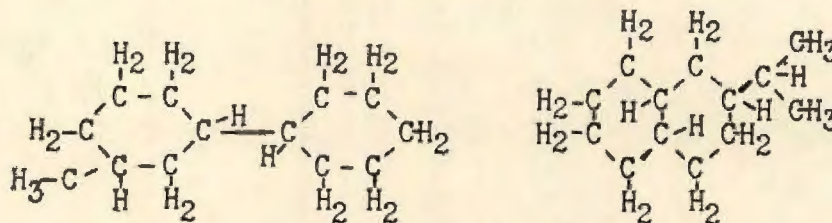
COMPOUND	NO. CH_3/MOLE			NO. CH_2/MOLE		
	DET'D	TRUE	Δ	DET'D	TRUE	Δ
METHYL CYCLOPENTANE	1.5	1	0.5	3.1	4	-0.9
METHYL CYCLOHEXANE	.6	1	-.4	5.5	5	.5
3-ME BICYCLOHEXYL	1.6	1	.6	8.8	9	- .2
ISOPROPYL DECALIN	1.4	2	-.6	8.0	7	1.0
AVERAGE (12 CYCLOPAR.)			0.56			0.86
MAXIMUM			-.9			1.5
AVERAGE (TYPE KNOWN)			0.08			0.16
MAXIMUM (TYPE KNOWN)			.2			.5

TABLE VIII
SINGLE RING AROMATICS
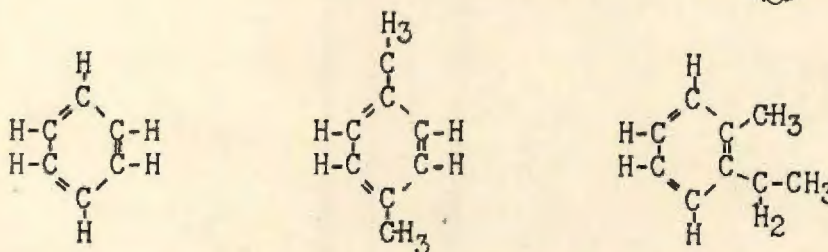
COMPOUND	NO. CH_3/MOLE			NO. CH_2/MOLE			NO. ARO CH/MOLE		
	DET'D	TRUE	Δ	DET'D	TRUE	Δ	DET'D	TRUE	Δ
BENZENE	0	0	0	0.1	0	.1	5.9	6	-0.1
p-XYLENE	2.3	2	.3	.1	0	.1	3.0	4	-1.0
o-ETHYL TOLUENE	1.9	2	-.1	.7	1	-.3	4.3	4	.3
n-BUTYL BENZENE	.9	1	-.1	3.2	3	.2	4.8	5	- .2
AVERAGE (15 ARO)			0.14			0.25			0.42
MAXIMUM			-.5			.9			-1.1

H-986

TABLE IX

TWO RING AROMATICS
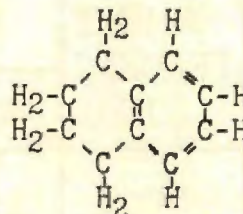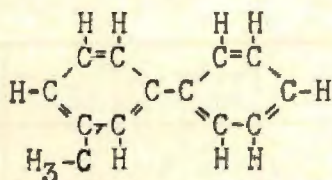
COMPOUND	NO. CH$_3$/MOLE			NO. CH$_2$/MOLE			NO. ARO CH/MOLE		
	DET'D	TRUE	Δ	DET'D	TRUE	Δ	DET'D	TRUE	Δ
3-ME BIPHENYL	1.3	1	0.3	-0.2	0	-0.2	8.7	9	-0.3
1,1-DIPHENYL PROPANE	.9	1	- .1	1.1	1	.1	10.2	10	.2
ISOPROPYL NAPHTHALENE	1.9	2	- .1	- .1	0	- .1	7.5	7	.5
TETRALIN	.1	0	.1	4.0	4	0	3.7	4	- .3
AVERAGE (9 ARO)			0.12			0.20			0.48
MAXIMUM			.3			.7			1.5

TABLE X

PARAFFIN BLENDS
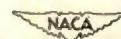
BLEND NO.	NO. CH$_3$/MOLE			NO. CH$_2$/MOLE		
	DET'D	TRUE	Δ	DET'D	TRUE	Δ
P-1	2.83	2.81	0.02	4.35	4.08	0.27
P-2	3.43	3.53	-.10	3.70	3.49	.21
P-3	3.44	3.34	.10	3.17	3.03	.14
P-4	3.66	3.81	-.15	2.15	2.15	0
P-5	4.10	4.15	-.05	1.72	1.76	-.04
AVERAGE			0.08			0.13

TABLE XI

CYCLOPARAFFIN BLENDS (CORRECTED)

BLEND NO.	WEIGHT PERCENT RING	NO. CH_3/MOLE			NO. CH_2/MOLE		
		DET'D	TRUE	Δ	DET'D	TRUE	Δ
N-1	77.4	1.06	1.02	0.04	4.19	4.63	-0.46
N-2	80.4	.30	.81	- .51	5.69	5.46	.23
N-3	82.8	.85	.76	.09	6.59	6.40	.19
N-4	84.7	.81	.91	- .10	4.92	4.97	- .05
N-5	88.7	.28	.53	- .25	10.36	9.59	.77
AVERAGE				0.20			0.37

TABLE XII
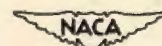
PARAFFIN - CYCLOPARAFFIN BLENDS (CORRECTED)

BLEND NO.	WEIGHT PERCENT RING	NO. CH_3/MOLE			NO. CH_2/MOLE		
		DET'D	TRUE	Δ	DET'D	TRUE	Δ
1	25.0	2.48	2.78	-0.30	3.44	3.52	-0.08
2	46.8	1.76	2.10	- .34	4.21	4.26	.03
3	62.9	1.05	1.16	- .11	4.96	5.27	- .31
AVERAGE				0.25			0.15

TABLE XIII

SINGLE RING AROMATIC BLENDS

BLEND NO.	NO. CH_3/MOLE			NO. CH_2/MOLE			NO. ARO CH/MOLE		
	DET'D	TRUE	Δ	DET'D	TRUE	Δ	DET'D	TRUE	Δ
A-1	1.02	0.99	0.03	0.35	0.33	0.02	5.09	5.16	-0.07
A-2	1.29	1.25	.04	.58	.65	-.07	4.99	4.85	.14
A-3	1.64	1.46	.18	.88	.98	-.10	4.76	4.70	.06
A-4	2.12	2.00	.12	.51	.69	-.18	4.23	4.29	- .06
A-5	1.66	1.58	.08	.83	.89	-.06	4.61	4.51	.10
AVERAGE			0.09			0.09			0.09

TABLE XIV

NACA
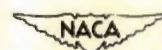
NEAR INFRARED ANALYSIS OF TWO REFINERY STREAMS

STREAM	TOTAL C MOLE	NO. CH_3 MOLE	NO. CH_2 MOLE	RATIO CH_3/CH_2
ALKYLATE	7.5	4.4	1.8	2.4:1
HOT-ACID OCTANE	8.1	4.6	.8	5.8:1
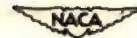
SOURCE   SAMPLE   ENTRANCE   PRISM   EXIT   THERMO-   AMPLI-   RECORDER
           IN   SLIT   SLIT   COUPLE   FIER
           CELL

ABSORPTION SPECTROMETER

Figure 1.
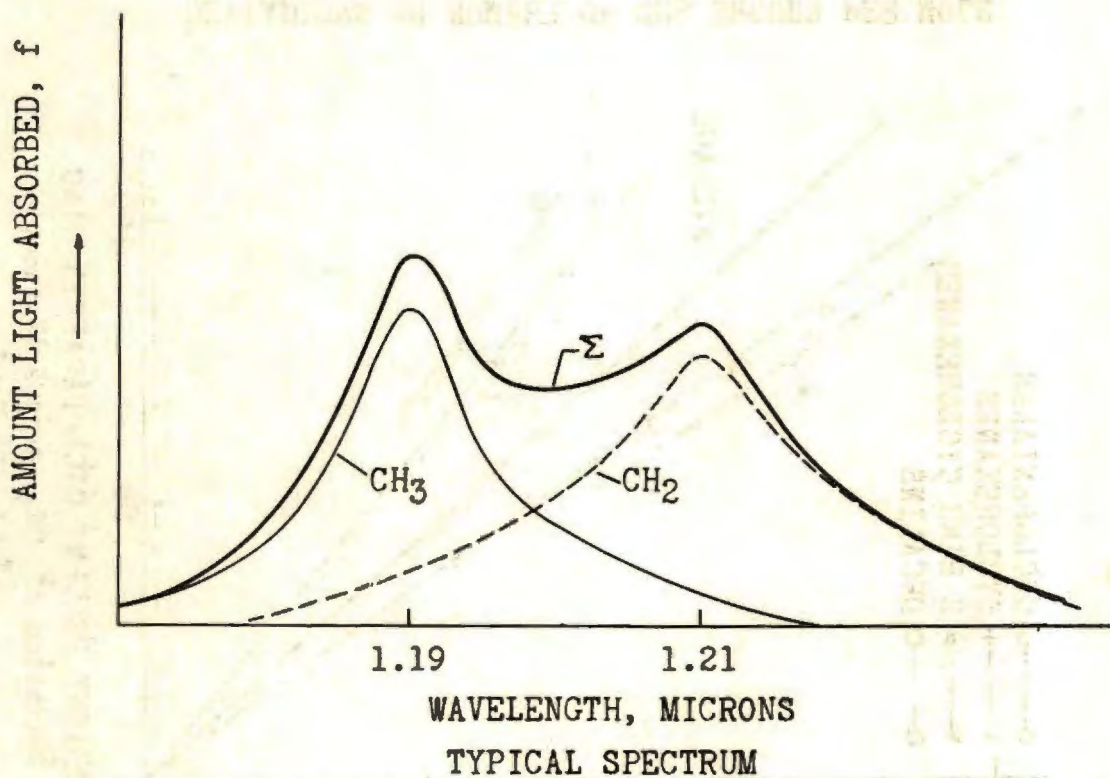
TYPICAL SPECTRUM

Figure 2.

Deviation of CH_3 groups as function
of percent ring

Figure 3.

Deviations of CH_2 groups as function
of percent ring

Figure 4.

THEORETICAL AND EXPERIMENTAL INVESTIGATION

OF DIBORANE AS A ROCKET FUEL

By John L. Sloop, Paul M. Ordin
and Vearl N. Huff

Flight Propulsion Research Laboratory

INTRODUCTION

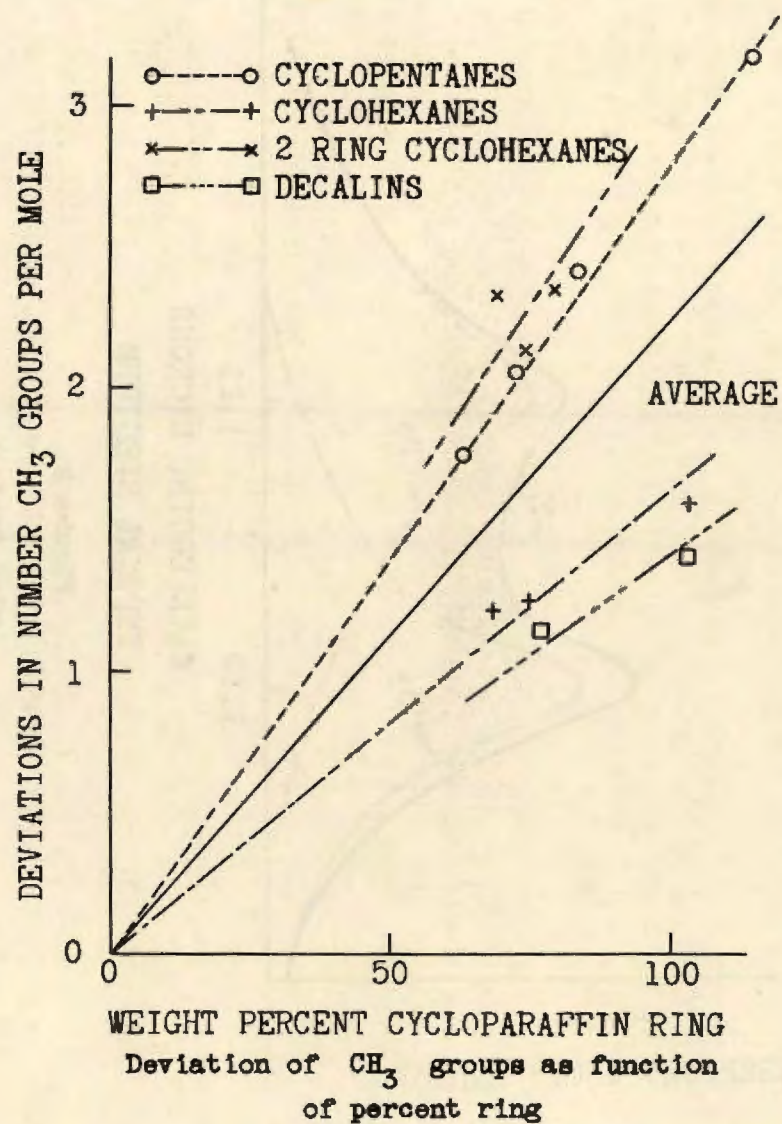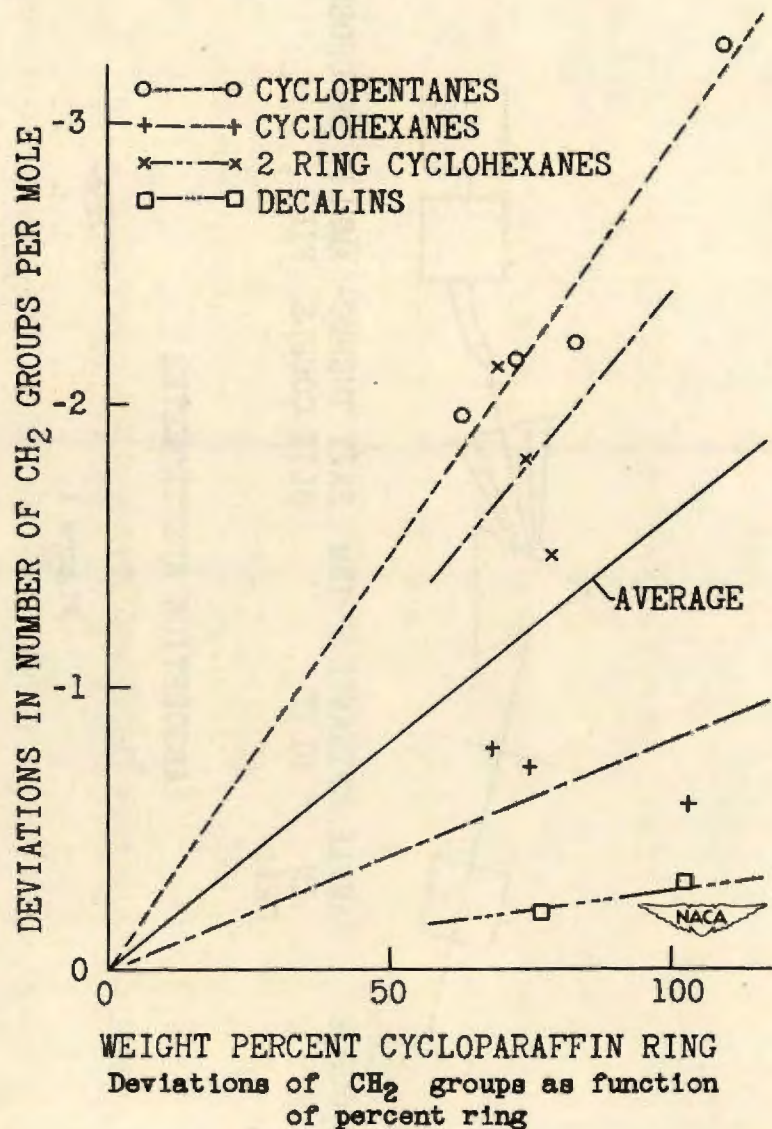The selection of a suitable liquid fuel for rocket engines requires the consideration of a number of complicated and often conflicting needs, involving the chemical and physical characteristics of the fuel.

The desirable propellant characteristics are:

1. High specific impulse, or a high amount of thrust per pound consumption of propellants, is one of the most important factors in considering a propellant combination. High specific impulse is approximately proportional to the square root of the reaction temperature divided by the mean molecular weight of the combustion products.

2. A high density reduces drag and increases the fuel loading factor (ratio of fuel weight to gross weight). Because high density has these effects on the drag and the fuel loading factor, which influence the range of the rocket-propelled vehicle, a high density is desirable.

3. Low reaction temperature is a characteristic that results in low heat transfer to the engine walls; however, in order to be most effective, low reaction temperature should be coupled with a low mean molecular weight of reaction products so that the ratio of reaction temperature to molecular weight of combustion products is high for high specific impulse.

4. High thermal stability and specific heat are desired in order to use the propellant as a coolant fluid before injection.

5. High reaction rates are advantageous in that they reduce the volume required for combustion and thereby reduce the amount of heat transferred to the engine walls.

6. A low vapor pressure is desired for utilization of the propellant as a coolant and also to reduce storage and handling problems.

7. An ideal propellant should have a low freezing point, be nontoxic, have high shock stability, and be nonself-igniting in air to facilitate handling, storage, and utilization with safety.

8. The propellant should be available in quantity or potentially available if large-scale operations are planned.

No one propellant has all of these desirable characteristics and a compromise is necessary. The direction of the compromise is dictated by the particular application under consideration.

 . The first step in a rocket fuel investigation is the calculation of theoretical performance of the fuel with several oxidants. If the performance appears promising, a program for the experimental evaluation of the better fuel-oxidant combinations can be initiated. The NACA Cleveland laboratory has a program in progress to evaluate theoretically and experimentally several high-energy chemical propellants for rocket propulsion; among these fuels are the boron hydrides. The boron hydrides have large heats of combustion; for example, approximately 6000 Btu per pound of diborane and oxygen as compared with approximately 4000 Btu per pound of gasoline and oxygen. Preliminary performance calculations indicated that diborane and pentaborane appear promising as rocket fuels. Inasmuch as diborane was the first boron hydride available, a detailed study of the theoretical performance of diborane with several oxidants was made. Through the cooperation of the Bureau of Aeronautics, Department of the Navy, a quantity of diborane was obtained and experimental performance data of diborane - hydrogen peroxide and diborane - oxygen were determined. The results of the theoretical and experimental work are presented herein.

THEORETICAL PERFORMANCE

Method. - The theoretical performance calculations require the determination of reaction-chamber gas composition, reaction temperature, nozzle-exit gas composition, and nozzle-exit temperature in order to obtain the specific impulse. The calculations were based on a chosen reaction pressure and exhaust pressure. The equilibrium composition of the gases and the corresponding chamber temperatures were determined by the usual thermodynamic methods. From the reaction temperature, reaction-chamber gas composition, and an isentropic expansion, the nozzle-exit temperature was determined (1) on the assumption of equilibrium composition during expansion and (2) on the assumption of constant composition during expansion.

The assumption of equilibrium expansion forms an upper limit for the energy available from the combustion products and frozen composition forms an approximate lower limit. However, lower values than those obtained with frozen composition will occur if sufficiently large specific heat lag is present.

An expansion with equilibrium composition gives a higher value of specific impulse than with frozen composition because of additional energy made available by the recombination of dissociated reaction products. The change in temperature and pressure during expansion is probably too rapid for a state of equilibrium to exist at every point in the expansion process but not so rapid that the reaction products remain entirely unchanged. The true state should lie between these two assumptions and its determination would involve consideration of the reaction kinetics for the particular reaction products involved. The enthalpy change from the reaction temperature to the nozzle-exit temperature was determined and assumed to be the available energy. The specific impulse was calculated from the available energy and the weight of a given quantity of propellants. Volume specific impulse or thrust per unit volume flow rate of propellants was obtained by multiplying the specific impulse by the density of the propellant mixture.

Results of calculations. - Performance calculations were made of diborane with hydrogen peroxide, oxygen, and fluorine at a combustion pressure of 300 pounds per square inch absolute and sealevel exhaust pressure (reference 1). The performance curves for the diborane - hydrogen peroxide B_2H_6-H_2O_2 propellant combination are shown in figure 1. The combustion temperature T_c, specific impulse I, and volume specific impulse I_d are plotted as a function of percent fuel by weight. The solid lines are performance parameters based on equilibrium composition expansion and the dotted curves are based on frozen composition during expansion. The maximum combustion temperature is 5850° R and occurs near stoichiometric on the fuel-rich side. The specific impulse increases in the fuel-rich region and at 35 percent fuel it reaches a maximum of 290 pound-seconds per pound for equilibrium expansion. The maximum specific impulse occurs in the fuel-rich region at a reaction temperature less than maximum as a result of a low mean molecular weight of reaction products in this region. The maximum volume specific impulse of 305 pound-seconds per cubic foot for equilibrium expansion occurs near stoichiometric because of the high specific gravity of hydrogen peroxide (1.436 at 77° F) as compared to the specific gravity of diborane (0.482 at -201° F).

The performance of the diborane - liquid oxygen B_2H_6-O_2 propellant system is shown in figure 2. The combustion temperature, specific impulse, and volume specific impulse are plotted as a function of percent fuel by weight. The maximum combustion temperature is $7239°$ R and occurs near stoichiometric in the fuel-rich region. The specific impulse increases in the fuel-rich region and at 36.6 percent fuel it reaches a maximum of 311 pound-seconds per pound for equilibrium expansion. The volume specific impulse remains fairly constant at a value of about 240 pound-seconds per cubic foot for a wide range of mixture rates and decreases at fuel-rich mixtures greater than 36 percent fuel.

The mole fraction of each product and the molecular weight of the reaction products plotted against percent by weight of diborane for the diborane - liquid oxygen combination are shown in figure 3. With increasing weight percentages of diborane, the amount of molecular hydrogen H_2 increases, whereas that of atomic hydrogen H increases and then drops sharply. This decreased dissociation in the rich region is due to the drop in combustion temperature. The amount of boron trioxide B_2O_3 increases slightly and that of water H_2O decreases with increasing amounts of fuel. The molecular weight of the reaction products M_c decreases with increasing amounts of diborane and this decrease causes the maximum specific impulse to occur in the fuel-rich region in spite of the lower combustion temperature.

The performance of the diborane - liquid fluorine B_2H_6-F_2 propellant system is shown in figure 4. The combustion temperature, specific impulse, and volume specific impulse are plotted as a function of percent fuel by weight. The reaction temperature reaches a maximum of approximately $9684°$ R in the stoichiometric region and decreases in the fuel-rich region. The specific impulse for equilibrium expansion reaches a maximum of 323 pound-seconds per pound at 13.6 percent fuel. The volume specific impulse reaches a maximum of 317 for equilibrium expansion near stoichiometric in the oxidant-rich region.

The mole fraction of each reaction product and the molecular weight of the reaction products plotted against percent diborane for the diborane - fluorine B_2H_6-F_2 combination are shown in figure 5. The mole fraction of boron trifluoride BF_3 remains practically constant, whereas the mole fraction of hydrogen fluoride HF decreases in the fuel-rich region. The molecular weight of the reaction products decreases with increasing percentages of fuel.

The values of maximum specific impulse and volume specific impulse for diborane with each of the three oxidants are given in the following table:

SUMMARY OF THEORETICAL PERFORMANCE

[Equilibrium expansion]

Fuel-oxidant	Fuel weight (percent)	Combustion temperature ($^{\circ}R$)	Equilibrium		Frozen	
			I	I_d	I	I_d
At maximum specific impulse						
B_2H_6-H_2O_2	35.2	5130	290	245	286	242
B_2H_6-O_2	36.6	6732	311	237	300	228
B_2H_6-F_2	12.7	9540	323	313	297	288
At maximum volume specific impulse						
B_2H_6-H_2O_2	11.9	5792	259	301	251	292
B_2H_6-O_2	25.7	7239	288	243	278	235
B_2H_6-F_2	9.85	9684	316	317	290	291

Comparison of diborane with other fuels. - After the theoretical performance values of diborane with the three oxidants, hydrogen peroxide, liquid oxygen, and liquid fluorine were obtained, these values were compared with those of other propellant combinations. Figure 6 shows a plot of specific impulse against volume specific impulse for comparison of diborane with a number of other rocket fuels. These data were obtained from calculations performed by the NACA Cleveland laboratory and other research organizations (references 1 to 4). The values plotted are for maximum specific impulse and were all based on frozen composition during expansion, except the pentaborane - liquid oxygen B_5H_9-O_2 propellant system for which only equilibrium composition values were available (references 2 and 5). The reaction-chamber temperatures in $^{\circ}R$ are shown in parentheses. In addition to the high-energy propellants, other fuel-oxidant combinations currently being used, such as ethyl alcohol - oxygen C_2H_5OH-O_2 and aniline - red fuming nitric acid $C_6H_5NH_2$-RFNA are shown on

this plot for comparison. The results show that combinations having high specific impulse values, such as hydrogen - oxygen H_2-O_2, have comparatively low volume specific impulse values and, conversely, combinations with high volume specific impulse, such as hydrazine - chlorine trifluoride N_2H_4-ClF_3, have comparatively low specific impulse values.

For some combinations it is possible to choose another mixture ratio and obtain a large gain in volume specific impulse at a small sacrifice of specific impulse (for example, hydrogen - fluorine H_2-F_2). It is desirable to have both specific impulse and volume specific impulse as high as possible and, in this respect, the boron hydrides are prominent. From computations made thus far, the propellant combinations with high specific impulse and high volume specific impulse are lithium - fluorine Li-F_2, pentaborane - oxygen B_5H_9-O_2, diborane - fluorine B_2H_6-F_2, diborane - oxygen B_2H_6-O_2, and hydrazine - fluorine N_2H_4-F_2.

Another consideration in the comparison of propellant combinations is the range obtained by a rocket-propelled missile using the various propellant combinations. A comparison of range involves additional variables and the choice of a set of conditions, which make a range comparison restrictive. A method of range comparison based on large rockets (reference 6) was used to compare several propellant combinations. The results are shown in figure 7.

With the ethyl alcohol - oxygen C_2H_5OH-O_2 altitude index taken as 1, the hydrogen - fluorine H_2-F_2 combination shows an altitude index of 2.14; lithium - fluorine Li-F_2, 1.87; hydrazine - fluorine N_2H_4-F_2, 1.73; diborane - fluorine B_2H_6-F_2, 1.64; diborane - oxygen B_2H_6-O_2, 1.53; diborane - hydrogen peroxide B_2H_6-H_2O_2, 1.42; hydrazine - oxygen N_2H_4-O_2, 1.31; hydrogen - oxygen H_2-O_2, 1.30; and aniline - red fuming nitric acid $C_6H_5NH_3$-HNO_3, 0.91. These values are for a fuel-oxidant ratio, which results in the greatest height for a rocket missile using this comparison method and may not necessarily be at the fuel-oxidant ratio resulting in the maximum specific impulse as shown in figure 6. Figure 7 indicates that diborane compares favorably with other high-energy fuels in a range consideration.

There are factors other than specific impulse, volume specific impulse, and range that must be considered in comparing rocket propellants; some of these propellant characteristics were enumerated in the INTRODUCTION. No attempt will be made to consider all of them at this time, but a few interesting points of comparison for several high-energy fuels are shown in the following table:

COMPARISON OF HIGH-ENERGY FUELS

Fuel	Specific gravity	Melting point (°F)	Boiling point (°F)	Performance with O_2[a]	
				Specific impulse (lb-sec/lb)	Combustion temperature (°R)
B_2H_6	$0.482^{-201°F}$	-266	-135	300	6732
B_5H_9	$0.61^{-32°F}$	- 52	118	[b]316	7880
N_2H_4	$1.002^{477°F}$	32	218	266	5690
H_2	$0.070^{-423°F}$	-434	-423	344	4510
Li	$0.534^{68°F}$	366	2928	[c]318	13500

[a]Frozen expansion except B_5H_9.
[b]References 2 and 5.
[c]Reference 7.

The fuels are diborane, pentaborane, hydrazine, hydrogen, and lithium. Their specific gravity, melting point, and boiling point are shown and specific impulse and combustion temperature with oxygen are given again for comparison.

Diborane is a gas in the normal state; as a liquid it has a comparatively low specific gravity of 0.482 at -201° F; it has a melting point of -260° F, and a boiling point of -135° F (reference 5). It is mildly toxic and at present is available only in small quantities.

Pentaborane has more desirable properties than diborane but is unavailable at the present time. It is a liquid in the normal state with a specific gravity of 0.61 at 32° F, a melting point of -52° F, and a boiling point of 118° F (reference 5). The melting point of pentaborane is low enough and its boiling point is high enough that

it can be stored and handled under many different climatic conditions
without the use of refrigeration or heavy storage cylinders. Complete
data on its properties are not yet available but it is probably no
more toxic than diborane. Pentaborane is apparently more stable than
diborane and should not be difficult to handle for rocket operations.
Pentaborane gives a high performance with oxygen and certainly should
with fluorine.

Hydrazine has the highest specific gravity, slightly over 1, of
the five fuels shown in the preceding table. It is a liquid in the
normal state with a melting point of 33° F and a boiling point of
218° F. The high melting point may involve logistic problems but
the high boiling point makes it appear promising as a regenerative
coolant. The specific impulse of hydrazine - oxygen is below that
of the boron hydrides.

Hydrogen gives the highest specific impulse of any fuel, but
it has the disadvantage of a very low specific gravity, 0.07, and
its very low boiling point of -423° F introduces many difficulties
in its use.

Lithium is a solid in the normal state and its melting point
of 366° F introduces practical difficulties in its use as a liquid.
It has a specific gravity of 0.534 at 66° F, which is comparatively
low. Its performance with oxygen is quite high (reference 7). The
reaction temperature of lithium with oxygen and fluorine are among
the highest known for chemical reactions.

The high combustion temperatures of the high performance pro-
pellant causes an especially difficult cooling problem. Most of
the temperatures are in the range of 4000° to $10,000^\circ$ F, which is
above the working temperature for available materials of construction.
Rocket engines that operate for very short periods of time can be
made of high temperature materials or metals of large heat capacity
so that no cooling is necessary. For longer periods of operation,
rocket engines with propellants having suitable characteristics can
use regenerative cooling. Most of the high-energy fuels are, how-
ever, unsuitable as coolants and for these a promising method of
cooling is internal-film cooling where a cool film is maintained on
the inner surfaces of the engine to shield the engine walls from
the hot combustion gases. Cooling is accomplished, however, at
some expense to performance and this must be considered in comparing
propellant combinations.

The NACA rocket fuels program includes an investigation of these
high-performance fuels. The order in which the work is done is deter-
mined by the availability of reliable thermodynamic data and by the

availability of the fuels. Diborane was the first of the boron
hydrides made available to the NACA for experimental evaluation
and was secured through the cooperation of the Bureau of Aeronautics,
Department of the Navy. The experimental investigation of diborane
was carried out in a 100-pound-thrust rocket engine first using
hydrogen peroxide as an oxidant (reference 8) and then liquid oxygen
(reference 9).

EXPERIMENTAL PERFORMANCE

A diagrammatic sketch of the 100-pound-thrust rocket unit
illustrating the propellant system, gas pressurizing system used
for pumping the propellants, and the counterbalanced propellant
weighing system for measuring the flow rate is shown in figure 8.
The oxygen was contained in a vacuum-jacketed stainless-steel
cylinder and a chrome-molybdenum steel tank was used to hold the
diborane. The fuel tank was equipped with a stainless-steel
bursting disk and high-pressure stainless-steel hand valves that
were packed with Teflon. The fuel lines and propellant valves
were refrigerated to maintain the diborane (boiling point, -134.5° F
at 1 atm.) in a liquid state up to the injector plate. The oxidant
and fuel tanks were each suspended from the lever arm of a counter-
balance and the unbalanced forces were transmitted to a sensitive
cantilever beam fitted with strain gages. The change in weight
during the run was recorded by having the strain gages connected
in a resistance bridge circuit of a modified, continuous-recording,
self-balancing potentiometer. The engine was mounted on a pivoted
stand, and thrust was measured by means of two strain gages mounted
on a cantilever beam subjected to bending by the engine thrust.
Charcoal-purified helium was used to pressurize the diborane and
liquid oxygen. Combustion and injection pressures were measured
by Bourdon-type pressure recorders. The flow diagram (fig. 8)
was for diborane - oxygen; for the diborane - hydrogen peroxide
experiments, the system was similar in most respects (reference 8).

The 100-pound-thrust rocket engine used in the diborane -
oxygen experiment is shown in figure 9. The engine comprises a
stainless-steel injector plate containing 8 solid jet injector
nozzles, a thick-walled copper combustion chamber with an inside
diameter of $2\frac{1}{4}$ inches and a length of 17 inches, and a convergent-
divergent copper exhaust nozzle designed to provide complete
expansion at a pressure ratio of 20.4. The diborane and liquid
oxygen injectors were located to permit the two streams to impinge.
The inner walls of the combustion chamber and exhaust nozzle were

chrome-plated to resist corrosion and erosion. The ratio of com-
bustion chamber volume to cross sectional area of exhaust nozzle
throat L* was 225 inches. The engine used for the diborane -
hydrogen peroxide experiment was essentially the same. The duration
of .the runs was approximately 6 seconds. The thrust, pressure, pro-
pellant flows, and several temperatures of the copper combustion .
chamber and nozzle were recorded continuously during the run.

The results of 1 run with diborane - hydrogen peroxide
B_2H_6-H_2O_2 and 11 runs with diborane - liquid oxygen B_2H_6-O_2
are shown in figure 10. Specific impulse in pound-second per pound
is plotted as a function of percent fuel by weight. Also shown
is the theoretical performance based on equilibrium expansion at an
assumed combustion chamber pressure of 300 pounds per square inch
absolute. The diborane - hydrogen peroxide run gave a specific
impulse of 211 pound-seconds per pound with a combustion chamber
pressure of 252 pounds per square inch absolute; this run gave
82 percent theoretical performance at the same pressure.

The runs with diborane - oxygen varied over a mixture range
of 22 to 42 percent fuel by weight. The specific impulse values
in the region of maximum performance varied from a low of 245 to
a high of 268 pound-seconds per pound. The maximum performance was
87 percent of theoretical on an equilibrium expansion basis and
90 percent of theoretical based on frozen equilibrium. Part of
the scatter of data is caused by flow weight uncertainties and part
can be attributed to variations of chamber pressure among the var-
ious runs; in the region of maximum specific impulse the pressure
ranged from 280 to 315 pounds per square inch absolute. The experi-
mental specific impulse values shown were obtained from measure-
ments taken during the run and were not corrected for the heat
transferred to the engine wall.

The amount of heat rejection to the walls, as measured by
the heat absorption of the copper was quite high - an average heat
rejection of approximately 3 Btu per square inch per second was
obtained for the chamber and approximately 6 Btu per square inch
per second for the nozzle. Considerable difficulty was experienced
with failure of equipment because of the high heat transfer.

An examination of the rocket engine after each run showed the
wall of the engine to be coated with a 1/32- to 1/16-inch gray to
dark brown layer of boron and boron oxide. The nature of the deposit
varied from the injector to the nozzle exit; at the injection end
the deposit was a thin, uniform light gray hard substance, which
changed to a thick, dark, irregular glazed deposit at the exit. The
deposit in the nozzle throat region was very thin.

SUMMARY

The theoretical performance of diborane with liquid oxygen, hydrogen peroxide, and liquid fluorine, and the comparison of specific impulse, volume specific impulse, and range for diborane - propellant combinations and for several other propellant combinations are presented. In addition, the paper presents the experimental performance of the diborane - liquid oxygen propellant combination in a 100-pound-thrust rocket engine.

REFERENCES

1. Huff, Vearl N., Calvert, Clyde S., and Erdmann, Virginia C.: Theoretical Performance of Diborane as a Rocket Fuel. NACA RM (to be pub.).

2. Anon: A Compilation of Computed Specific Impulse Values. Project RAND, RA-15049, Battelle Memorial Inst., Sept. 2, 1947. (Subcontract under AAF Contract No. W33-038-ac-14105 to Douglas Aircraft Co., Inc.)

3. Weymouth, F. R.: Hydrazine-Chlorine Trifluoride Combustion and Performance Calculations. Rep. No. 56-982-008, Proj. RASCAL, Bell Aircraft Corp., Nov. 1, 1947. (AAF Contract W33-038-ac-14169.)

4. Miller, Riley O., and Ordin, Paul M.: Theoretical Performance of Some Rocket Propellants Containing Hydrogen, Nitrogen, and Oxygen. NACA RM No. E8A30, 1948.

5. Clegg, J. W., and Moore, J. R.: Propellants for Supersonic Vehicles: Boron Compounds. Project RAND, RA-15042, Battelle Memorial Inst., Oct. 8, 1947. (Subcontract under AAF Contract No. W33-038-ac-14105 to Douglas Aircraft Co., Inc.)

6. Canright, R. B.: The Relative Importance of Specific Impulse and Propellant Density for Large Rockets. Rep. No. 4-29, Jet Prop. Lab., C. I. T., Jan. 7, 1947. (Ordcit Proj. Contract No. W-04-200-ORD-455.)

7. Parsons, J. W., Thompson, T. L., and Dixon, T. F.: A Survey of Liquid Rocket Propellants. Rep. No. NA-47-95, North American Aviation, Inc., April 1, 1947.

8. Rowe, William H., Ordin, Paul M., and Diehl, John M.: Investi-
    gation of the Diborane - Hydrogen Peroxide Propellant Combination.
    NACA RM No. E7K07, 1948.

9. Rowe, William H., Ordin, Paul M., and Diehl, John M.: Experi-
    mental Performance of Diborane - Oxygen in a 100-Pound-Thrust
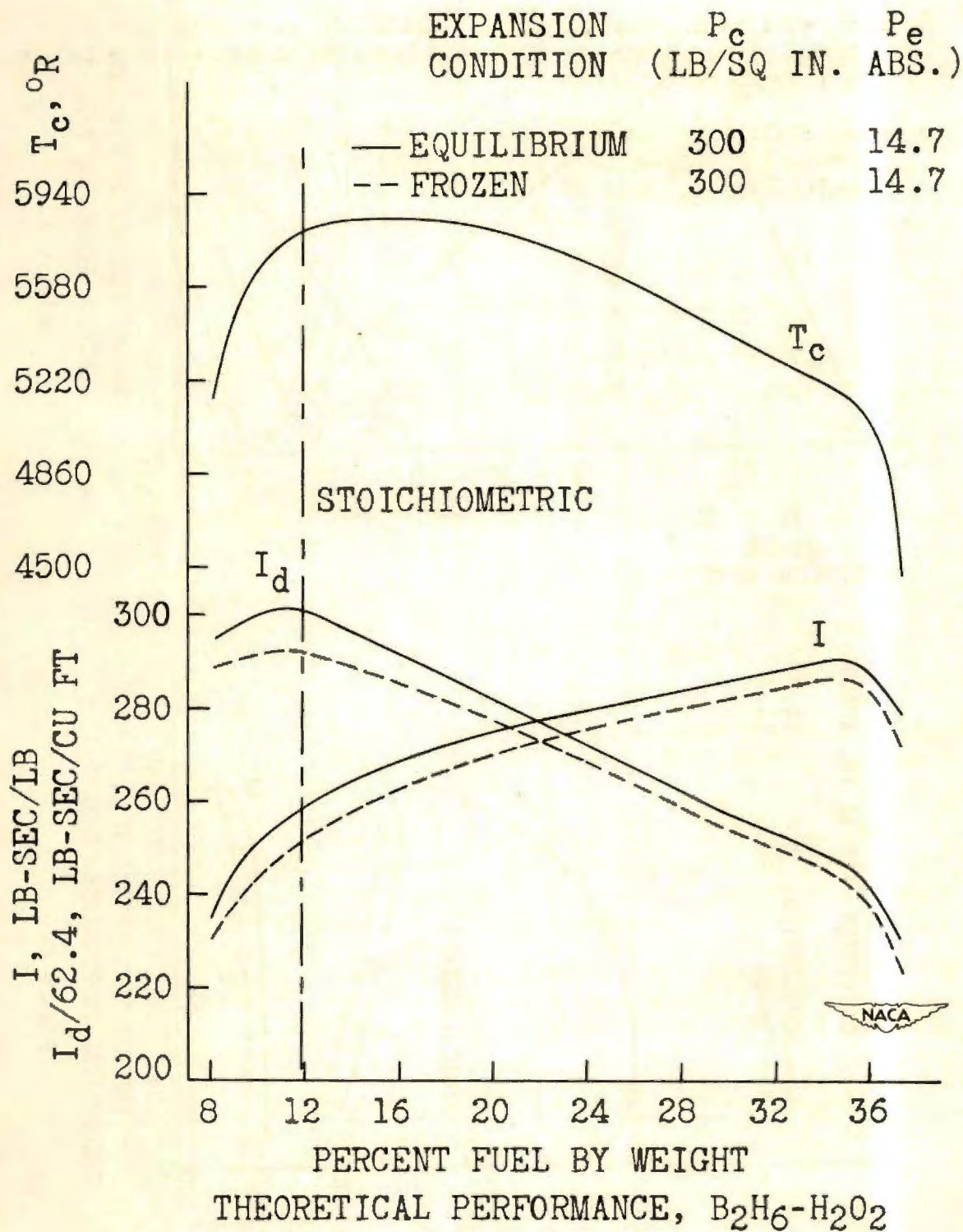   Rocket Engine. NACA RM (to be pub.).

THEORETICAL PERFORMANCE, $B_2H_6-H_2O_2$

Figure 1.

Figure 2.

Figure 3.

986-I

EXPANSION P_c P_e
CONDITION   (LB SQ IN. ABS.)

——— EQUILIBRIUM   300   14.7
- - - FROZEN   300   14.7

T_c, °R

I, LB-SEC/LB
I_d/62.4, LB-SEC CU/FT

PERCENT FUEL BY WEIGHT

THEORETICAL PERFORMANCE, B_2H_6-F_2

Figure 4.

MEAN MOLECULAR WEIGHT

MOLE FRACTION

STOICHIOMETRIC

WEIGHT PERCENT OF DIBORANE

REACTION PRODUCTS, B_2H_6-F_2
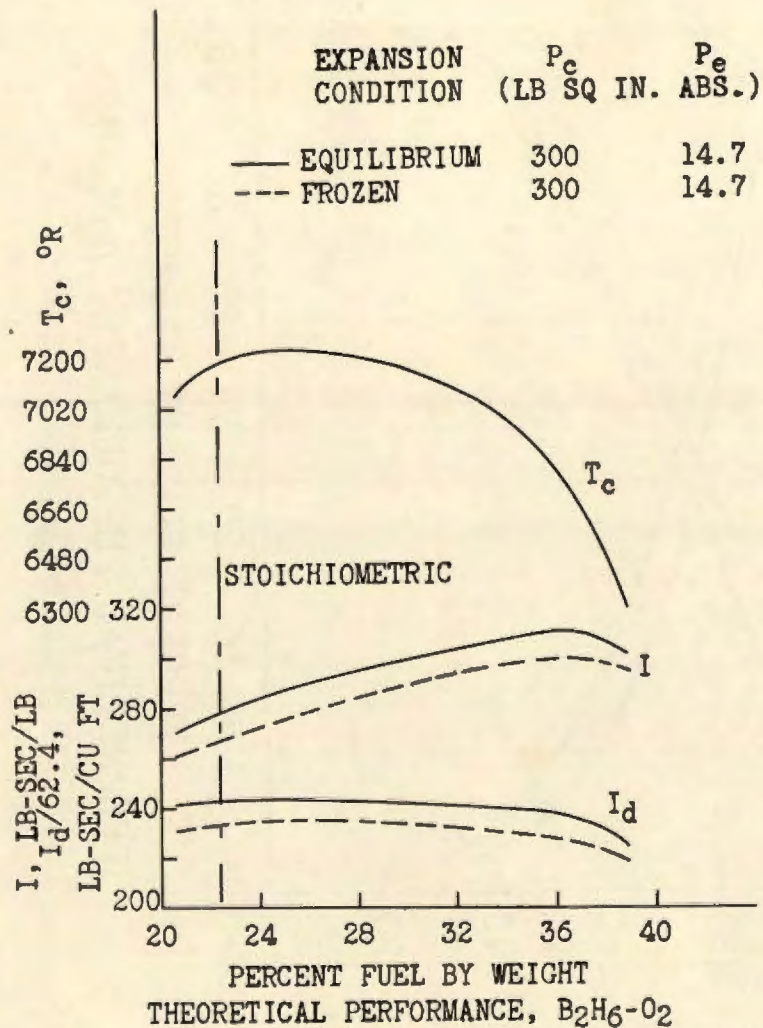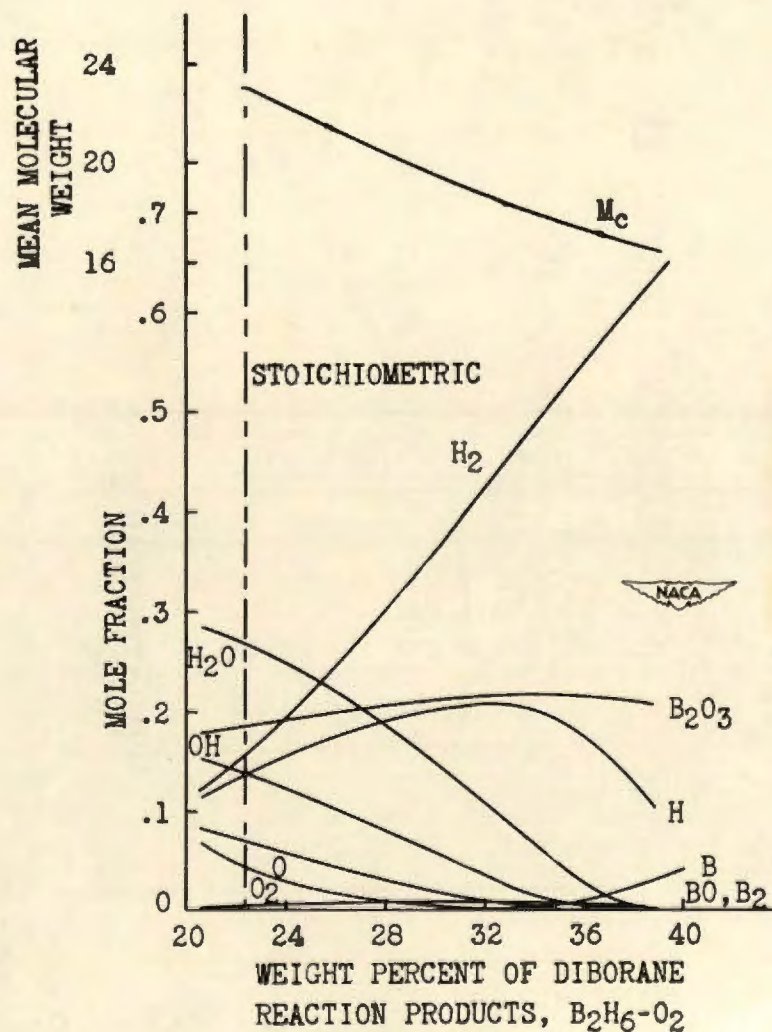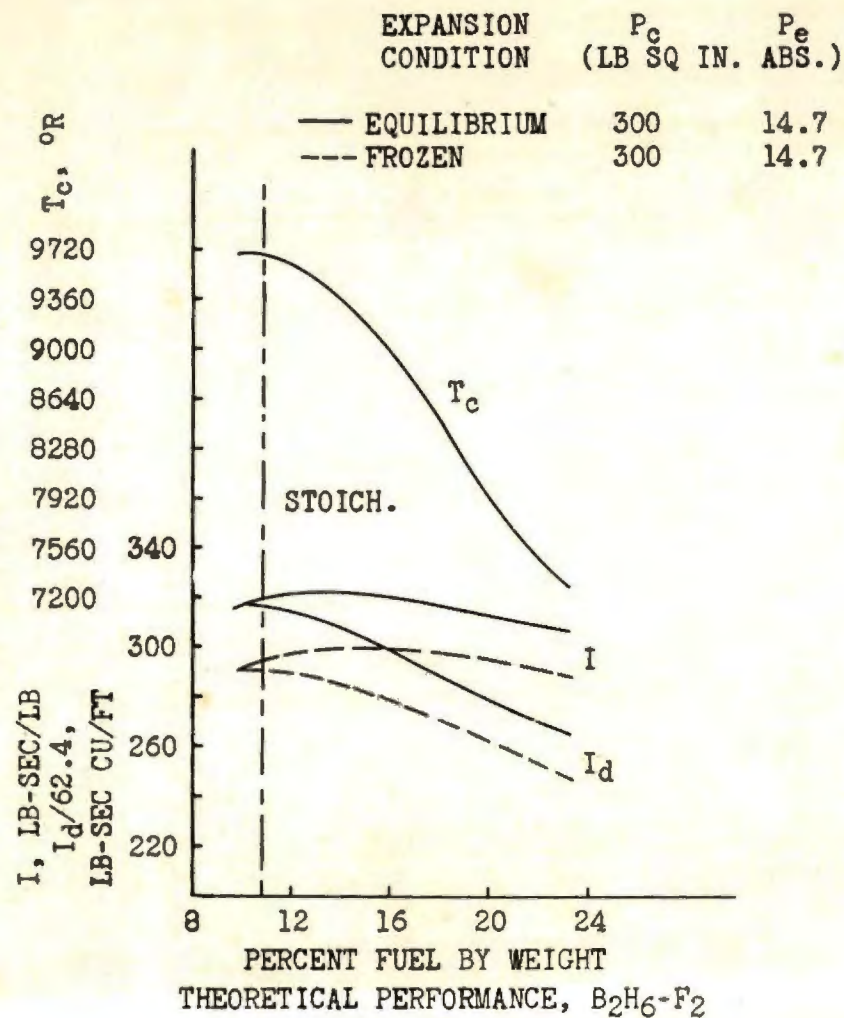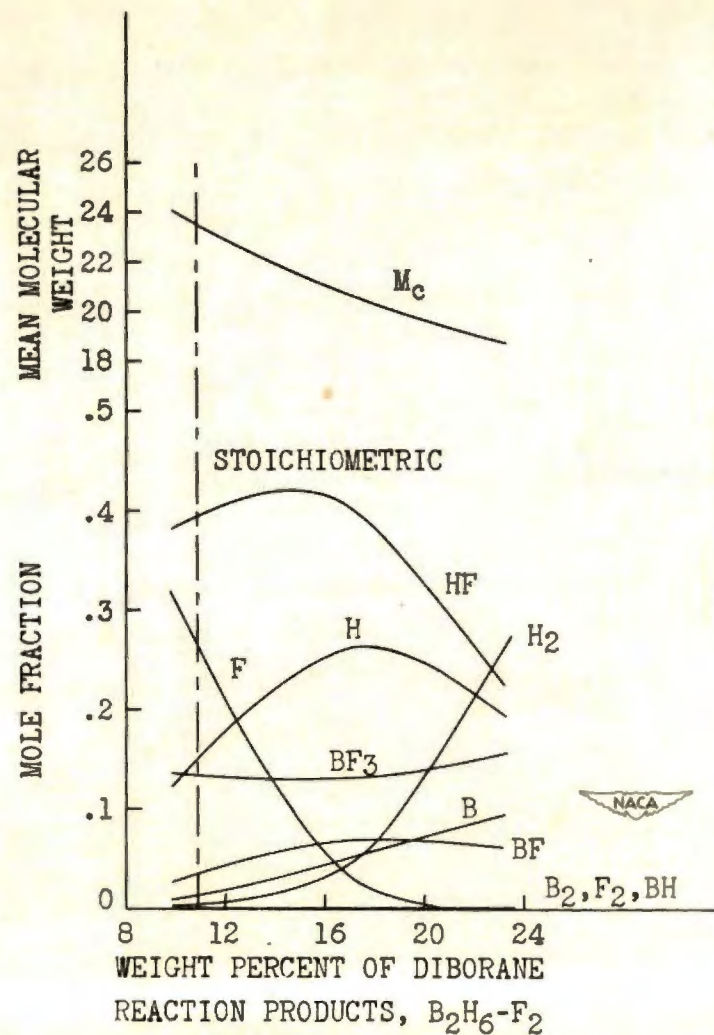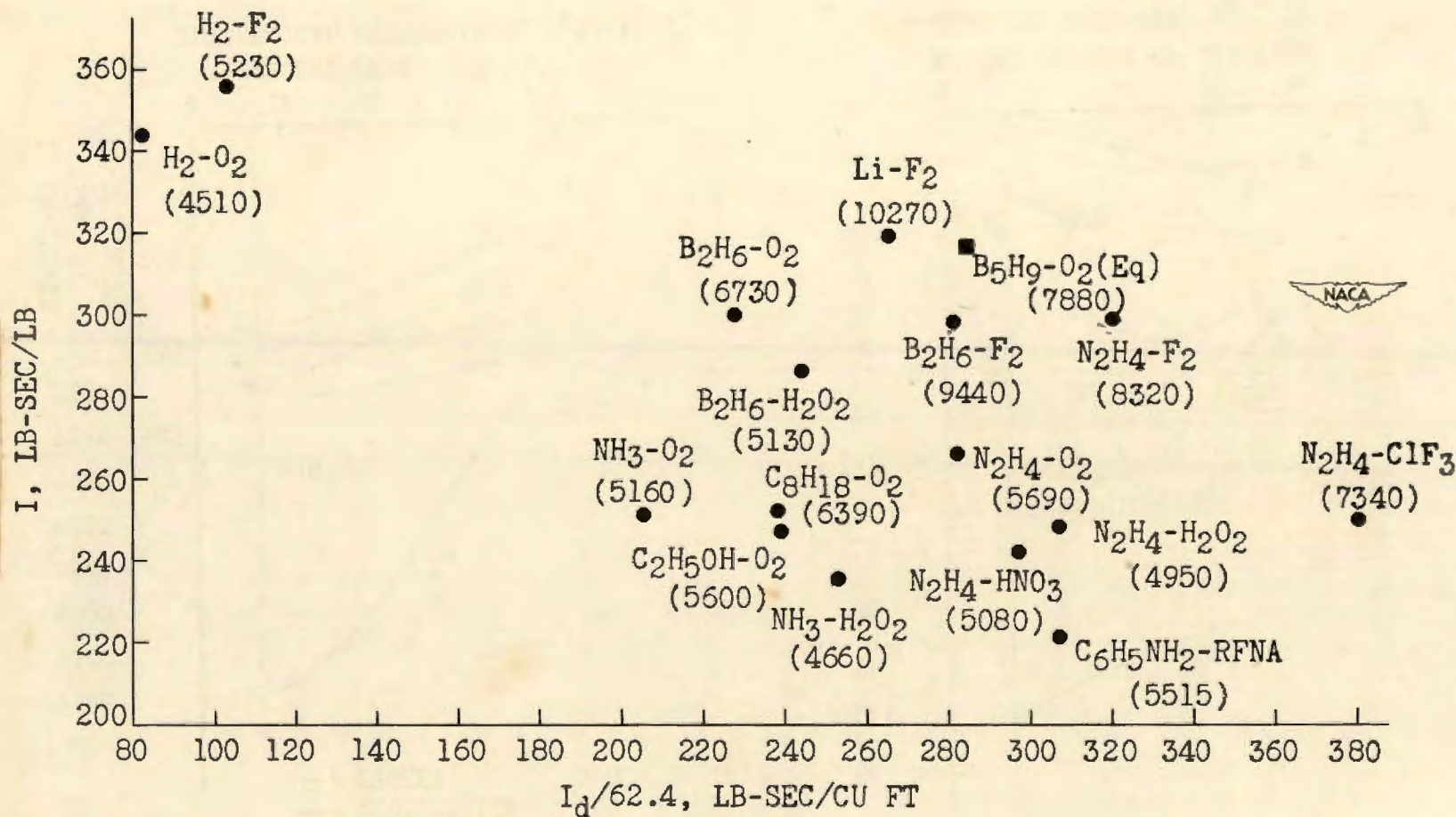
Figure 5.

COMPARISON OF PROPELLANTS

Figure 6.

986-I
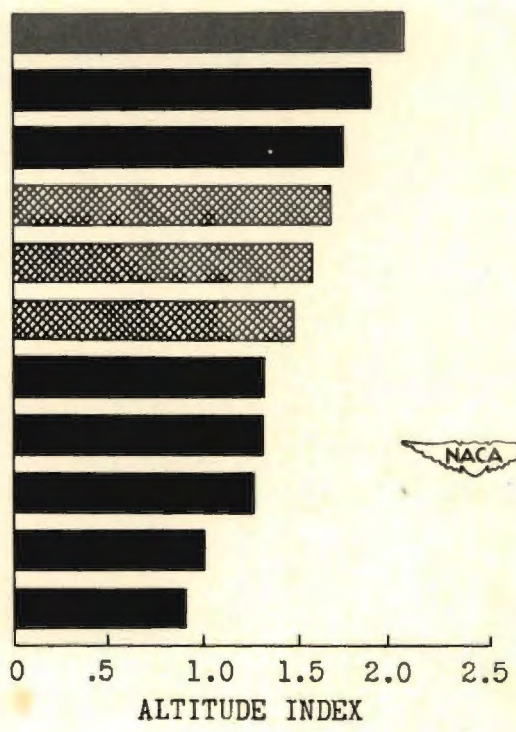
Figure 7.

Fig 5-2
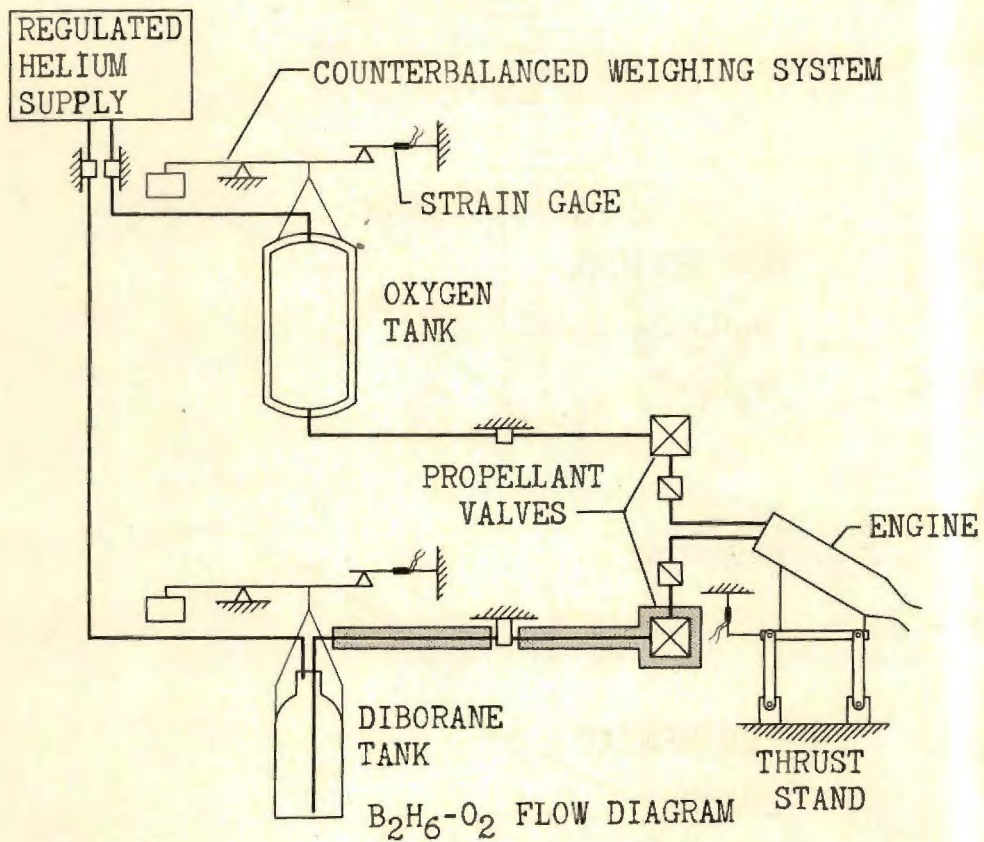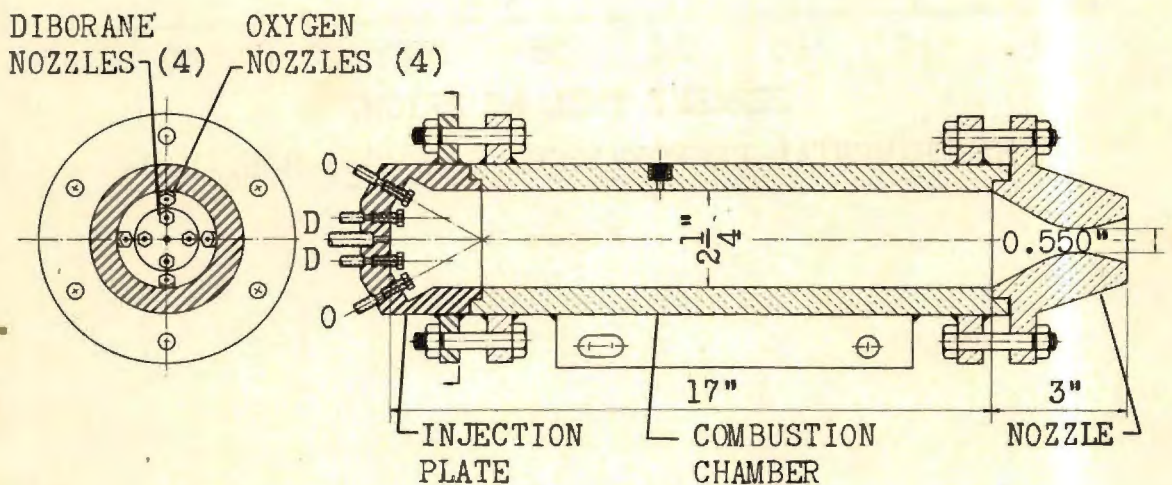
Figure 8.

$B_2H_6-O_2$ ENGINE

Figure 9.
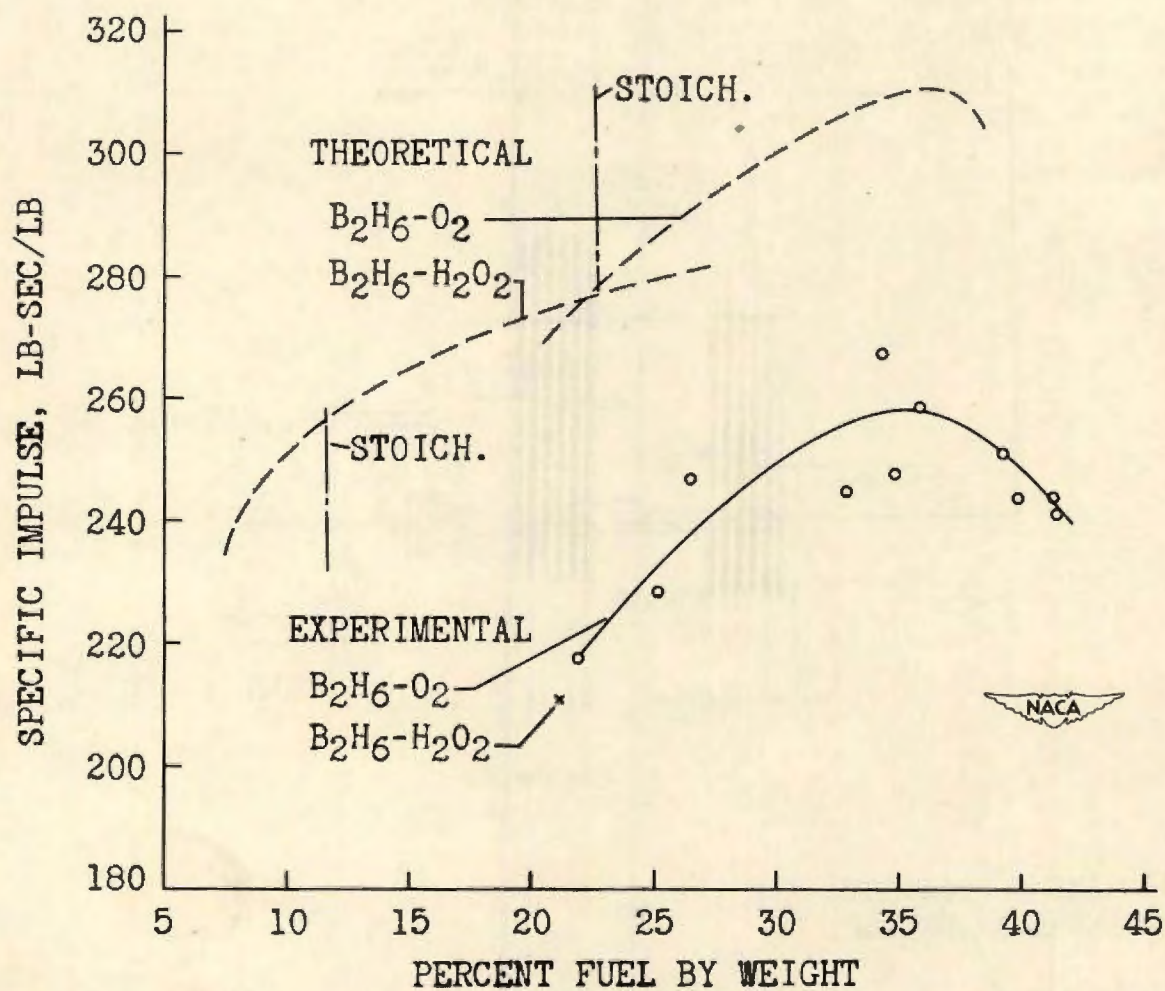
EXPERIMENTAL PERFORMANCE, $B_2H_6-O_2$, $B_2H_6-H_2O_2$

Figure 10.